A STUDY OF TRANSVERSE CRACKING IN OKLAHOMA FLEXIBLE HIGHWAY PAVEMENTS

By

MAGDY SALAH NOURELDIN

Bachelor of Science
Ain Shams University
Cairo, Egypt
1969

Master of Science
Ain Shams University
Cairo, Egypt
1973

Submitted to the Faculty of the Graduate College
of the Oklahoma State University
in partial fulfillment of the requirements
for the Degree of
DOCTOR OF PHILOSOPHY
May, 1977

A STUDY OF TRANSVERSE CRACKING IN OKLAHOMA

FLEXIBLE HIGHWAY PAVEMENTS

Thesis Approved:

Phillip G. Manbe
Thesis Adviser

Leroy Folks

R L Janes

Carol D. Oberlander

Norman N Durham
Dean of the Graduate College

ACKNOWLEDGMENTS

The author wishes to express his deep gratitude and sincere appreciation to his major adviser, Professor P. G. Manke, for his constant assistance and frequent advice throughout this study. Appreciation is also expressed to the other committee members, Professors R. L. Janes, J. L. Folks, and G. D. Oberlender, for their invaluable assistance and constructive guidance during this study.

A note of thanks is given to the School of Civil Engineering and the Oklahoma Department of Transportation for the financial support and assistance which contributed to the successful achievement of this research work. The author is also grateful to the Egyptian Government for the interest and financial support which made his advanced study in the United States possible.

Thanks are also extended to the Research and Development Division of the Oklahoma Department of Transportation for their excellent cooperation during field sampling. The author also wishes to express his deep gratitude to his classmate, Mr. Ismail M. Basha, for his sincere and invaluable help during the experimental phase of the research work. The helpful suggestions of Professor D. Holbert during the computer analysis of test results are also gratefully acknowledged.

The assistance of Miss Charlene Fries and Mrs. Brenda Morrison in preparing and typing the manuscript is gratefully acknowledged.

Special acknowledgment is also extended to the author's wife, Wafia, and parents for their unfailing encouragement and many sacrifices prior to and during his advanced study.

TABLE OF CONTENTS

LIST OF TABLES

LIST OF FIGURES

CHAPTER I

INTRODUCTION

The Problem and Its Nature

Cracking of the surface course of flexible pavements is generally considered to be a serious and extensive problem by highway agencies. Many factors, such as asphalt and aggregate properties, mix design, construction procedures, subgrade support, environmental conditions and traffic loading, influence the ability of a pavement to resist cracking (1, 2, 3).

Transverse cracking is a significant highway performance problem in Oklahoma, in many other states primarily in the northern and western sections of the United States (2, 4, 5, 6, 7) and in many provinces in Canada (3, 8, 9, 10, 11, 12). In some cases these cracks are limited in depth and affect only the bituminous surface while others penetrate through the whole pavement structure. At an early stage, these cracks are not particularly harmful, but very poor riding qualities can result as the cracks become progressively wider and deeper. Open cracks permit the ingress of surface water which can cause stripping in the asphalt-bound materials, softening of the subgrade and freeze-thaw damage. In extreme cases, depressions occur at these transverse cracks due to subgrade softening and/or pumping of fine materials and secondary cracks develop parallel to the main crack.

Pavement surfaces with this kind of cracking must be repaired to prevent further deterioration and to maintain the safe smooth riding quality desired by the motoring public. The surface crack conditions may become so bad that complete re-surfacing is required long before the "design life" of the pavement is reached. Frequently, this expensive solution is unsatisfactory since these cracks tend to reflect through the new surfacing in a short time if they have not been adequately sealed prior to overlaying.

Maintaining the riding quality of flexible pavements subjected to transverse cracking can be costly. It appears that modifying current design and construction procedures to reduce or eliminate this type of pavement distress is a more desirable and economical solution to this problem.

Method and Scope of Study

Previous field and laboratory studies have indicated that transverse cracking is most likely to occur due to thermal tensile stresses that are developed by pavement contraction at low temperatures. It seems that these cracks appear in the surface when the accumulated tensile stresses exceed the fracture strength of the asphalt concrete pavement. These studies also showed that the rheological properties of the asphalt binders largely affect the ability of asphalt concrete surfaces to resist these cracks (1, 3, 11).

The primary objective of this research was to determine the nature and extent of these cracks on Oklahoma flexible pavements and to investigate the possible causes of this form of distress. This research

dealt primarily with the bituminous components of the pavement and their influence or contributions to this type of cracking.

Initially, field inspection visits were made to pavement sections affected by transverse cracking in various areas of Oklahoma. Nine test sites with various degrees of cracking were selected from these sections for further comprehensive study. Original construction data on these sites were obtained from the Research Division of the Oklahoma Department of Transportation. Crack mapping and counting techniques were used to determine the severity of cracking at each test site. Six inch (15.24 cm) diameter cores of the pavement materials were recovered at various locations along newly developed cracks to study the nature and extent of these cracks in the pavement structure. Four inch (10.16 cm) diameter cores were taken at random locations in the vicinity of the cracks for further laboratory testing.

An indirect tensile-splitting apparatus was developed to evaluate the tensile properties of asphalt mixtures at any temperature in the laboratory. This method of testing involved loading cylindrical asphalt concrete specimens across a vertical diameter. The induced tensile stresses and strains could be calculated from recordings of load and horizontal deformation. This apparatus was employed to investigate the low-temperature tensile properties of the asphalt concrete specimens obtained from the test sites. In addition, asphalt surface course mixtures with various asphalt contents and asphalt viscosities were prepared and tested to determine the effects of asphalt content and viscosity on the tensile behavior of the mixtures at different temperatures.

The asphalt binder was recovered from the respective core specimens and tests were performed to evaluate the rheological properties of these recovered asphalt samples. Also, various 85-100 penetration grade asphalt cement samples (26 samples) were secured from different sources in Oklahoma and their rheological properties were studied. Use was made of the "stiffness modulus" concept (13, 14, 15) in characterizing the behavior of the asphalt cement samples and mixtures at low temperatures. The relation of this behavior to the problem of transverse cracking of flexible pavements in Oklahoma was investigated. The Statistical Analysis System (SAS) computer program (16) was used to analyze the test results and detect the correlations between these results and the actual field behavior.

CHAPTER II

REVIEW OF PREVIOUS RESEARCH WORK

Synopsis

The non-load associated cracking of flexible pavements was first recognized in the early to mid-1930s by Rader (17). However, the problem was not serious at that time because of the low paved mileage and the small traffic volumes and loads. After World War II, traffic volumes and construction increased rapidly. Higher pavement performance standards were required and transverse cracking started to be a serious and extensive problem. During the past fifteen years, various highway agencies and investigators have devoted a great deal of effort trying to find a practical solution to the problem. In 1965, the Canadian Good Roads Association (C.G.R.A.) indicated the severity of the problem and placed it in the first priority grouping of highway research needs (18). In 1966, the Association of Asphalt Paving Technologists (A.A.P.T.) published a symposium about the same subject (19). As a result, extensive field surveying and laboratory investigations were conducted in different parts of the United States and Canada (20, 21, 22, 23, 24). Most of these studies concluded that the problem of transverse cracking could be attributed to the thermal stresses that are developed due to temperature changes, in particular, changes in the low-temperature range. One of the most significant variables of the problem was found to be the consistency characteristics of the bitumen used in the surface layer.

In addition, factors of pavement age, subgrade type, and thickness of asphalt layer have been shown to be significant to the problem (1, 23, 25). In 1973, Haas presented a rather comprehensive summary of the major design approaches that have been used to analyze this low-temperature cracking (13).

Possible Causes and Major Factors

Transverse cracking can apparently occur from a variety of causes. Several studies have pointed out that this type of cracking is likely to occur when tensile stresses, either externally applied or internally developed, exceed the tensile strength of the material (19). These tensile stresses probably develop in several ways. For instance, in many locations having relatively cold climates, transverse cracking was developed as a result of the combination of low temperatures and the nature of the bituminous component of the pavement (1). Also, some types of subgrade soils can undergo significant shrinkage due to freezing and can exhibit deep cracks in the field (25). Where these cracks occur and extend through the pavement, it is likely that the nature of the subgrade is the major factor involved.

Haas et al. (1) have summarized some of the factors of possible significance in low-temperature cracking of flexible pavements. These have been subdivided into external and component factors as shown in Figure 1. It is important to realize that these different factors do not act independently but are coupled. For instance, the combination of traffic loads with a temperature drop in an asphalt concrete pavement would probably create a stress of sufficient magnitude to cause fracture.

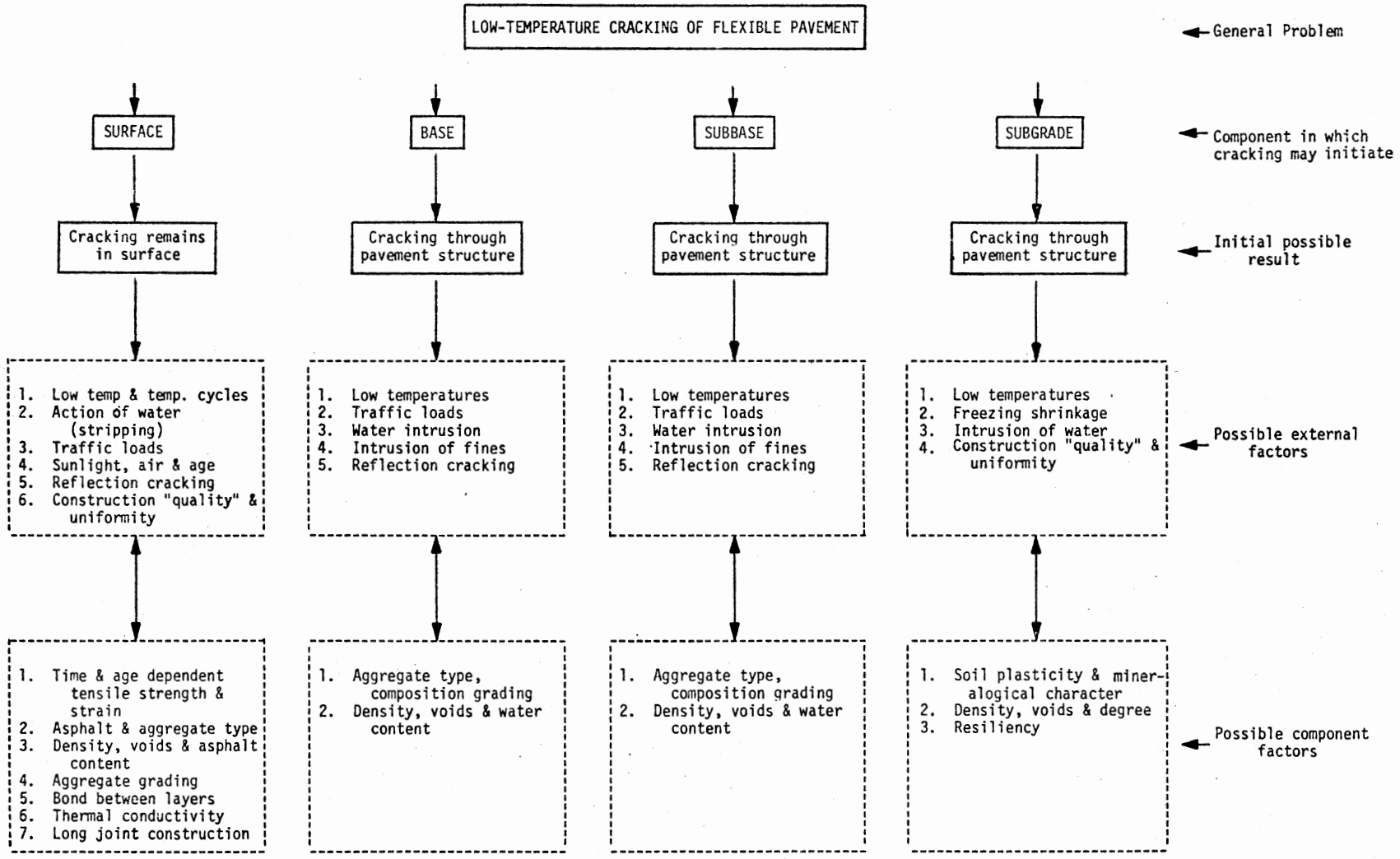

Figure 1. Factors of Possible Significance in Low-Temperature Cracking of Flexible Pavements (1)

Cracking Mechanism

Laboratory investigations conducted on asphalt cement and mixtures have shown that they lose some of their plasticity at low temperatures and behave essentially in an elastic manner. At the same time, the asphalt layer tends to contract but is partially or wholly restrained. It seems that this combination induces tensile stresses in the pavement material. The appearance of transverse cracks during rapid warming, following a prolonged cold period, indicated to some that fracture was being initiated during and as a result of this warming. However, actual field records indicated that fracture occurred when pavement surface temperatures reached a minimum (10, 26, 27, 28, 29). Instrumentation also revealed that most transverse cracks started at the surface but initially progressed to only a limited depth.

The previous findings partially substantiated the fracture mechanism hypothesis of Haas and Topper (30). This cracking hypothesis essentially postulated a two-stage phenomenon. At the first stage, a microcrack initiates at the surface of the asphalt layer when the induced thermal stresses exceed the tensile strength due to decreasing temperatures and this crack propagates only to some limited depth. At the second stage, the crack propagates to the full depth of the surface layer after one or more cycles of sudden warming. Because of pavement geometrics, the principal axis of contraction is in the longitudinal direction and, hence, the majority of these cracks are to be expected in the transverse direction.

Apparently, the relative influence of the subgrade properties and behavior on the cracking mechanism has not been quantitatively established in most of the experimental or theoretical approaches (1).

Field Investigations

Field investigations devoted to this problem can be divided into two broad approaches. The first was mainly oriented toward surveying, sampling, and testing the existing cracked pavements in order to document the extent of the problem and attempt to correlate certain factors with the frequency of cracking (1, 3). The second approach was primarily concerned with studying the effect of different materials and structural variables on the actual field performance of full-scale pavement sections (27, 29). Field testing programs included mapping the different cracking patterns and coring and sampling of base and subgrade materials. Cracking frequency diagrams were prepared to help in selecting specific areas for further detailed examination. This cracking survey also included the number of part, half, full and multiple transverse cracks occurring in each 500 ft interval of the pavement. Figure 2 represents a diagrammatic illustration of the previous four categories of cracks.

To develop a measure of cracking severity, a cracking index was developed by the Ontario Department of Transportation (22). This index is defined in the following equation:

$$C.I. = N_m + N_f + \frac{1}{2} N_h \qquad (2.1)$$

where

C.I. = cracking index.

N_m = number of multiple cracks
N_f = number of full cracks
N_h = number of half cracks

} per 500 ft of two-lane pavement.

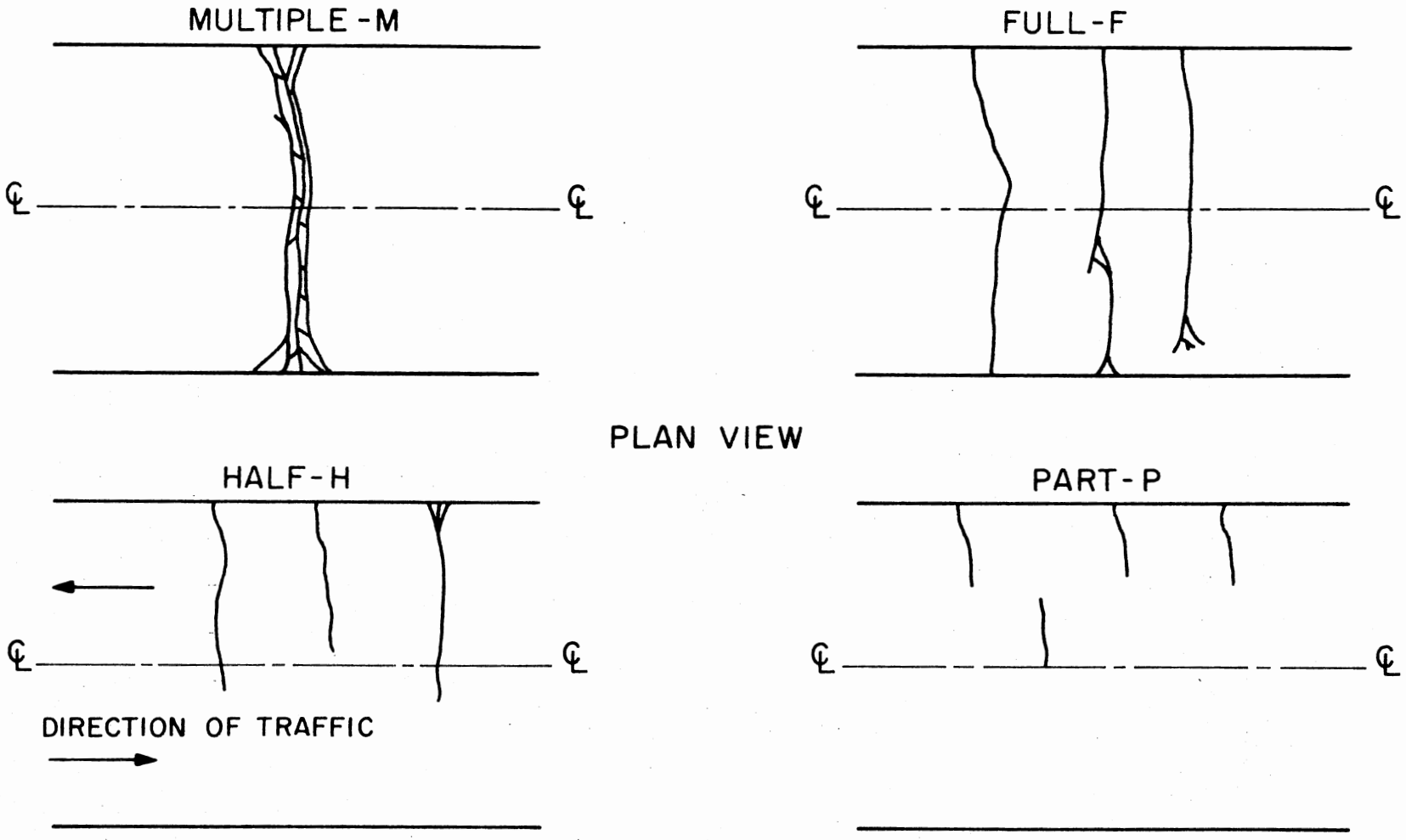

Figure 2. Different Types of Transverse Cracks (22)

It was felt that smaller transverse cracks usually occur subsequent to the formation of half or full cracks and, therefore, these smaller cracks were disregarded in the calculation of the cracking index (22).

Some initial field studies indicated that variables such as asphalt type, grade and source, as well as age and thickness of pavement, showed a significant correlation with the degree of cracking of pavement sections (9, 19, 31). Consequently, several full-scale experimental sections were constructed in various areas in Canada to evaluate the effect of these variables, particularly those concerning asphalt type and grade (28, 29, 32, 33). Air and subsurface temperatures were continuously recorded at these sections. Periodic crack surveys were made to detect crack initiation and to closely follow the propagation and development of these cracks. In addition, the structural capacity of these experimental sections was evaluated by field test procedures (10, 26, 27, 28). The analysis of the performance data on these sections again showed a significant correlation between the asphalt source, type and grade, and the observed degree of cracking. However, it was emphasized that low-temperature cracking appeared to be a complex phenomenon with many factors involved and that other variables could be highly important in certain situations (1).

Material Characterization

As previously concluded, the bituminous component of the pavement is a major variable in the low-temperature transverse cracking problem. This result was strong enough to guide the research efforts toward finding new methods of characterizing the behavior of asphalt cements and mixtures at low temperatures. Various investigations have pointed out

that one of the most satisfactory and applicable approaches is that of the stiffness concept (13, 14, 15). This concept was first introduced by Van der Poel (34) as follows:

$$s(t,T) = [\frac{\sigma}{\varepsilon}]_{t,T} \tag{2.2}$$

where

$s(t,T)$ = stiffness modulus, usually in terms of psi or kg/cm^2, of the material for a particular time of loading, t, and for a particular temperature, T.

σ = stress, ε = strain } at time "t" and temperature "T".

This modulus is an extension of Young's modulus of elasticity for a purely elastic solid, but specifies the time of loading and temperature and thereby recognizes the viscoelastic nature of the material. This stiffness modulus can be determined either by direct measurement or by indirect estimation methods. The direct approaches of measuring the stiffness include creep, relaxation, or constant-rate-of-strain testing in either tension or compression, or by dynamic or flexural testing methods (13). The stiffness modulus can indirectly be measured by the original Van der Poel method, or by the modification of this method as suggested by Heukelom (35) or Mcleod (36). These indirect methods were so termed because they provide an estimate of the stiffness modulus of the asphalt binder based on direct laboratory measurements. Routine test data is transformed into stiffness values using nomographs and/or charts.

Van der Poel's method of determining the stiffness of a bitumen was presented in 1954 (34), in the form of a nomograph. This nomograph

was derived from experimental data of two types of tests: (1) a constant-stress test (static creep test in tension), and (2) a dynamic test with an alternating stress of constant amplitude and frequency. Two routine tests of a bitumen were required to determine its stiffness modulus (S) from the nomograph. These tests were the penetration test, ASTM D-5 (37), and the ring-and-ball softening point test, ASTM D-36 (37). From the penetration value and the softening point temperature, the penetration index (P.I.) for the asphalt can be calculated. This index was first introduced by Pfeiffer and Van Doormaal (38) to indicate the temperature susceptibility of the penetration of the asphalt. This concept was based on the assumption that the penetration (100 gm, 5 sec) at the softening-point temperature is approximately 800. A nomograph for calculating the Pfeiffer and Van Doormaal P.I. is given in Figure 3. In general, the penetration index of most asphalts varies from -2.6 to +8.0 (34). The lower the P.I., the higher the temperature susceptibility.

The use of Van der Poel's nomograph to estimate asphalt stiffness can be summarized in the following steps:

1. Measure penetration at 77°F, 100 gm, 5 sec.
2. Measure softening point, $T_{R\&B}$.
3. Calculate penetration index, P.I., according to Pfeiffer and Van Doormaal (Figure 3).
4. Estimate stiffness, using the nomograph (Figure 4), from the following three parameters:
    a. Time of loading.
    b. Softening-point temperature minus test temperature.
    c. Penetration index of the asphalt.

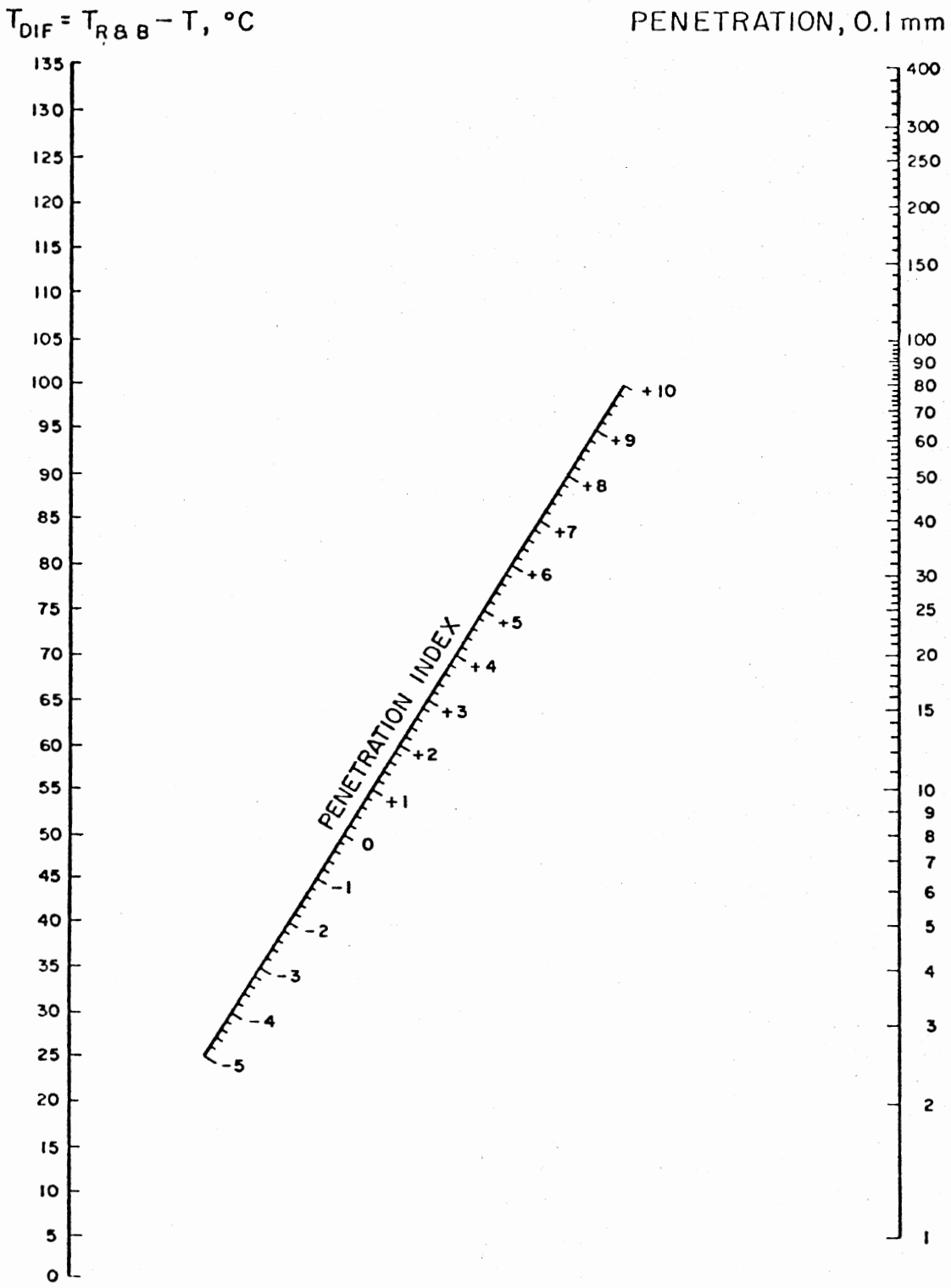

Figure 3. Nomograph for Determining Pfeiffer and Van Doormaal's Penetration Index (38)

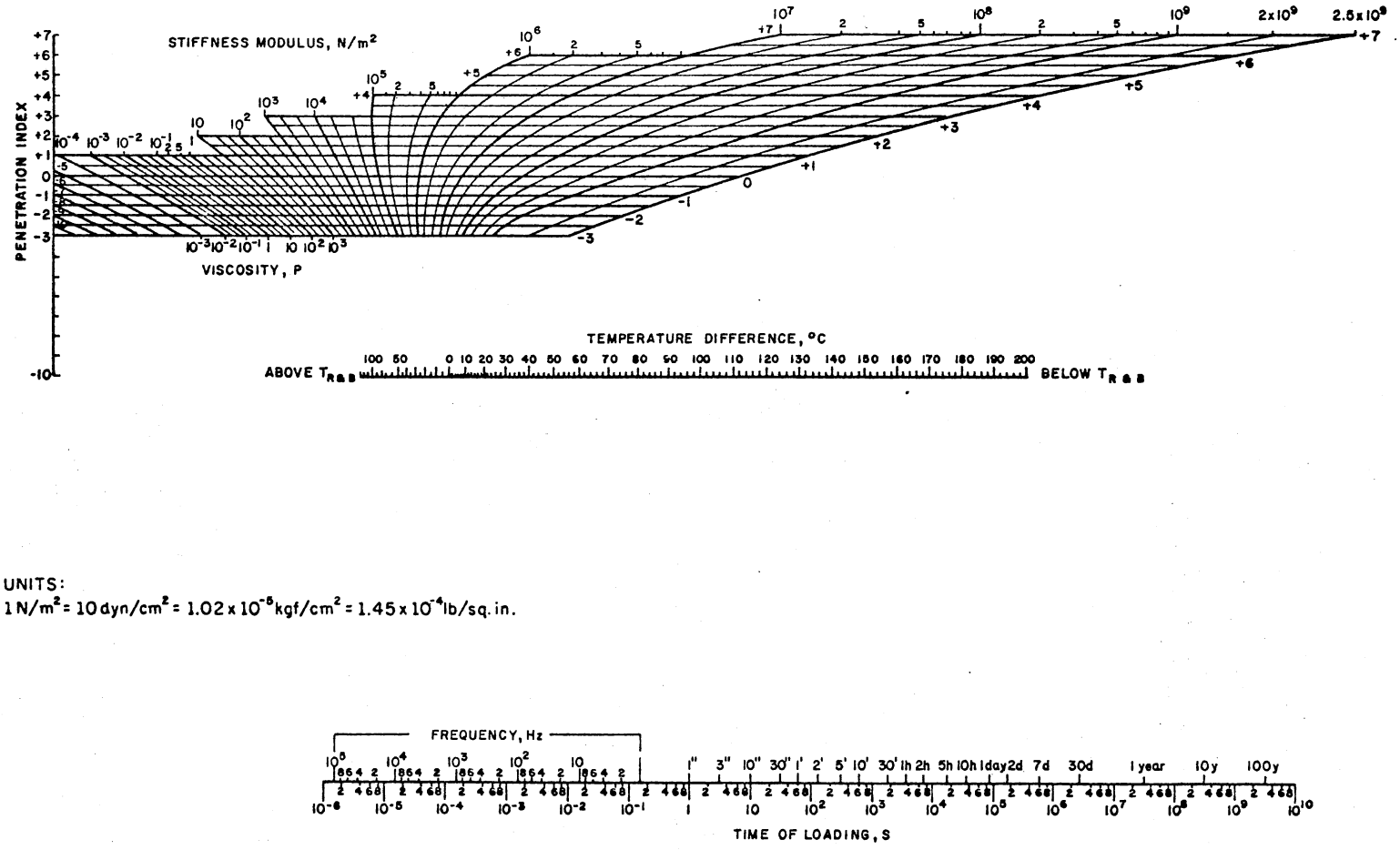

UNITS:
$1\ N/m^2 = 10\ dyn/cm^2 = 1.02 \times 10^{-5}\ kgf/cm^2 = 1.45 \times 10^{-4}\ lb/sq.in.$

Figure 4. Van Der Poel's Nomogram for Determining Stiffness Modulus of Bitumens (34)

Van der Poel checked the accuracy of his nomograph and concluded that the variation in measured stiffness values of an asphalt and the stiffness obtained from the nomograph seldom exceeded a factor of 2.0. However, Anderson et al. (14) indicated that Van der Poel's method could give erroneous stiffness values for a number of North American asphalts (blown asphalts and asphalts having considerable wax contents). As a result, Heukelom developed a Bitumen Test Data Chart (39) to relate the consistency of bitumens with temperature (Figure 5). The advantage of this chart is that it allows a "corrected" softening point to be determined for a waxy or blown asphalt. Heukelom suggested a modification of the Van der Poel method for estimating the stiffness modulus of asphalt cements. His modification can be summarized as follows:

1. Plot the viscosity and penetration values on the "Bitumen Test Data Chart".

2. A "corrected" ring-and-ball softening point, T_N, can be found by extending the penetration branch down. This T_N replaces $T_{R\&B}$.

3. The Pfeiffer and Van Doormaal P.I. is then replaced by Q, which can be calculated as follows:

$$Q = 20\,\frac{T_{2p} - T_N - 111}{T_{2p} - T_N + 222} \qquad (2.3)$$

where

T_{2p} = temperature at which the viscosity is equal to 2.0 poises. This temperature can be determined from the Bitumen Test Data Chart.

T_N = corrected softening point.

4. Use the Van der Poel nomograph to estimate the stiffness modulus for the particular time of loading and temperature.

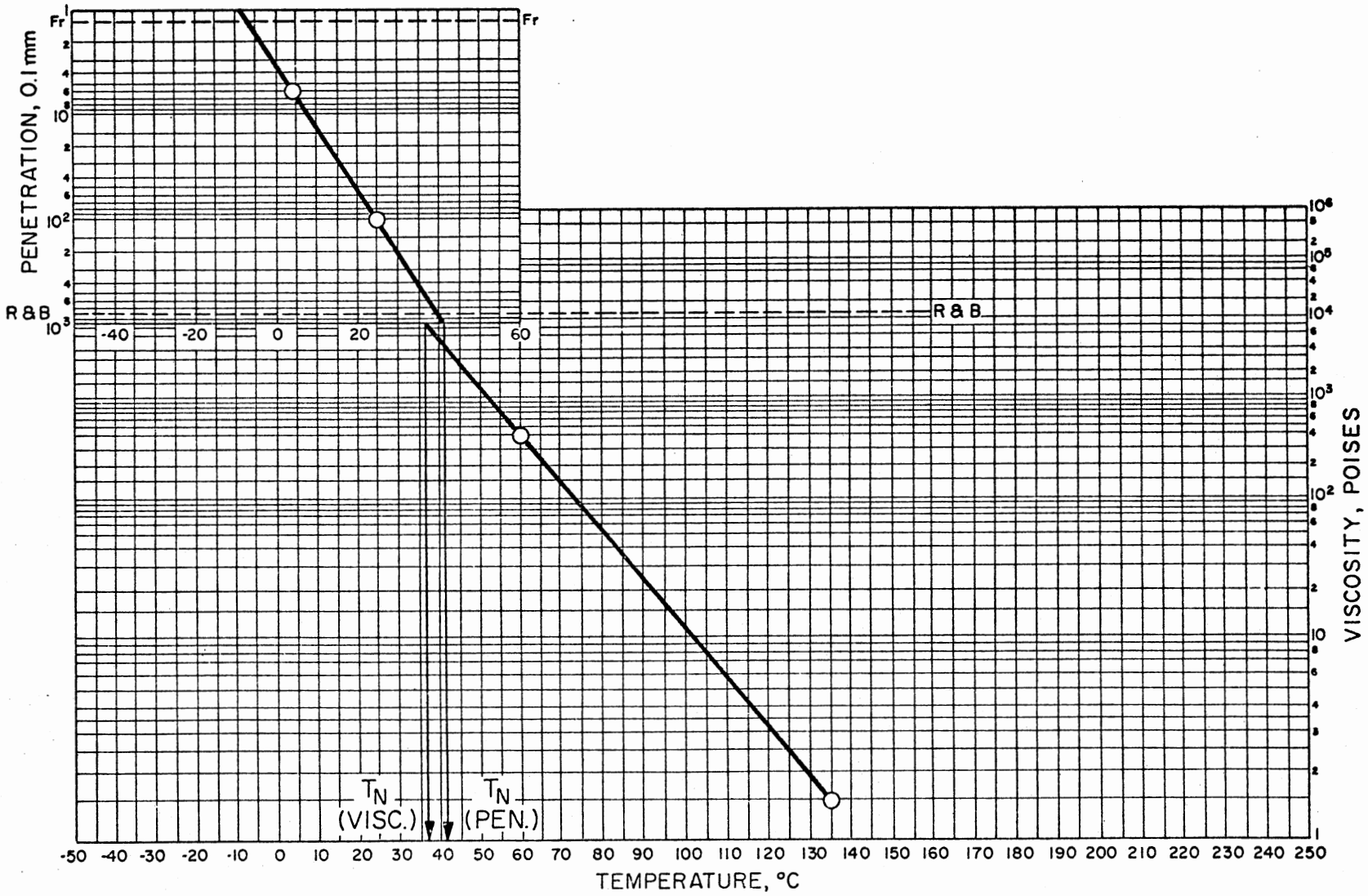

Figure 5. Heukelom's Bitumen Test Data Chart (39)

Mcleod (36) developed another method for estimating the stiffness modulus of asphalt cements. This method is based on the relationship between asphalt viscosity at 275°F (or at 140°F) and its penetration at 77°F. Mcleod believed that this relationship provided a very reasonable basis for expressing differences in temperature susceptibility of asphalt cements. He demonstrated that for asphalt cements of the same penetration at 77°F, there were remarkable differences in their viscosities at 275°F. As this approach for evaluating asphalt temperature susceptibility was different from those employed by Van der Poel and Heukelom, Mcleod used the term "Penetration-Viscosity Number" (PVN).

Mcleod's method for estimating the stiffness modulus of an asphalt cement may be summarized as follows:

1. The penetration-viscosity number (PVN) can be estimated from Figure 6 using the following equation:

$$PVN = \frac{\log L - \log x}{\log L - \log M}(-1.5) \qquad (2.4)$$

where

x = viscosity in centistokes at 275°F for the asphalt cement for which PVN is to be determined.

L = viscosity in centistokes at 275°F for a PVN of 0.0, determined from Figure 6 for the penetration at 77°F of the given asphalt cement.

M = viscosity in centistokes at 275°F for PVN of -1.5, determined from Figure 6 for the penetration at 77°F of the given asphalt cement.

2. The ring-and-ball softening point temperature ($T_{R\&B}$) is called the "base temperature" by Mcleod and is determined from the nomograph shown in Figure 7, rather than by actual testing.

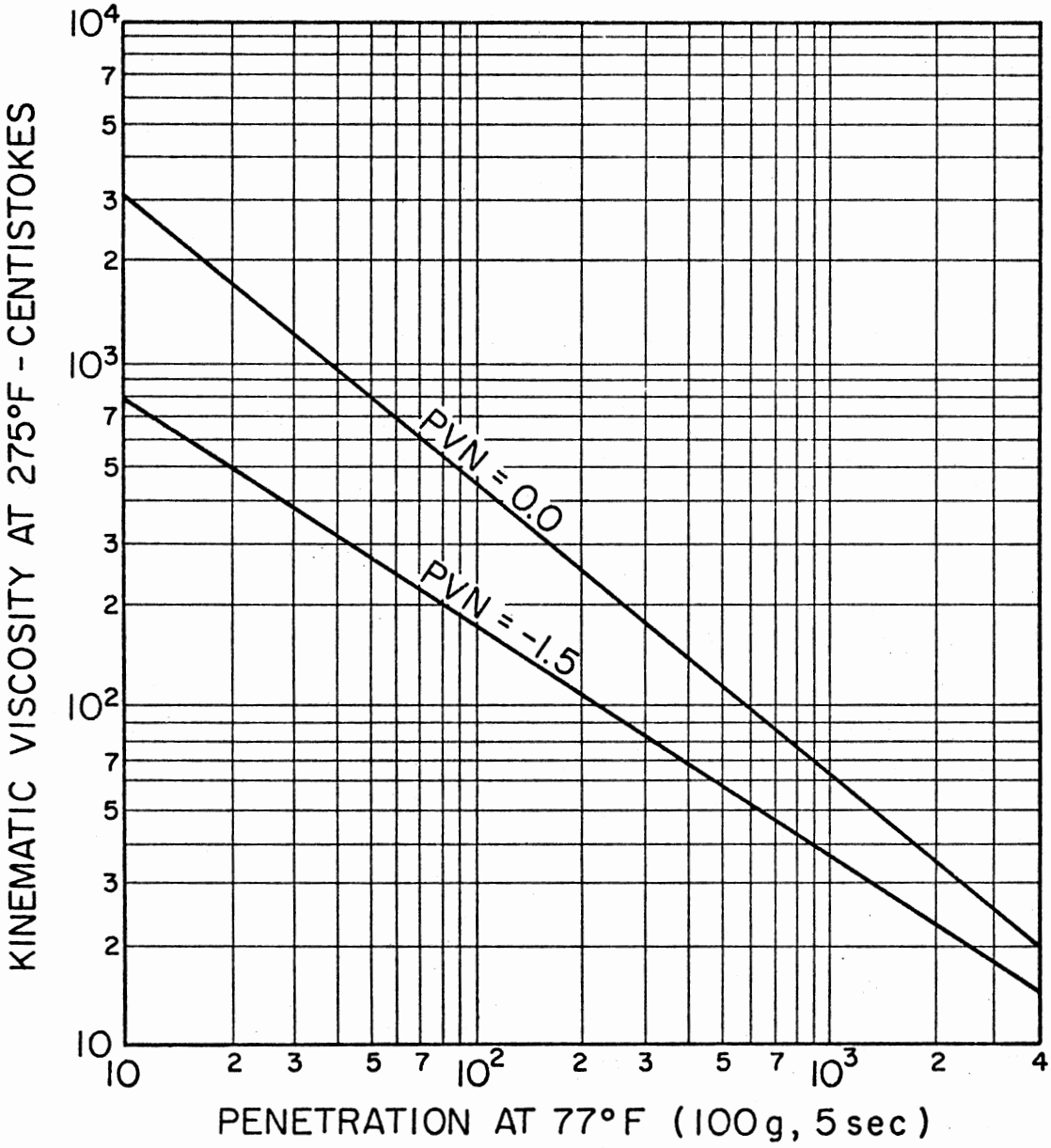

Figure 6. McLeod's Chart for Estimating the PVN of an Asphalt Cement (36)

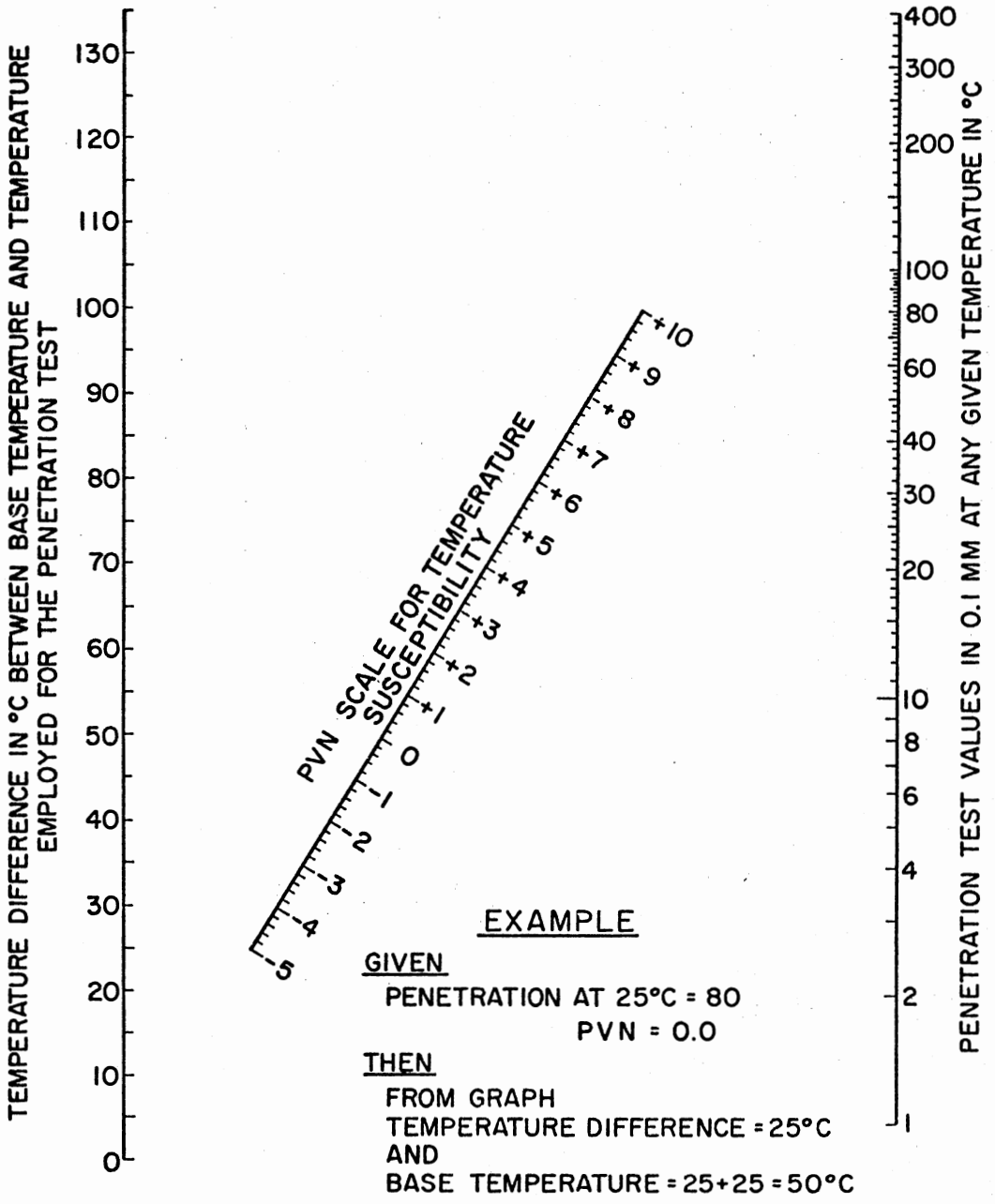

Figure 7. Suggested Modification of Heukelom's Version of Pfeiffer's and Van Doormaal's Nomograph for Relationship Between Penetration, Penetration Viscosity Number and Base Temperature (36)

3. The modulus of stiffness of the asphalt is then determined using Mcleod's modification of Heukelom's and Klomp's nomograph (40) as shown in Figure 8.

Based on the stiffness modulus of the asphalt cement, the stiffness modulus of the asphalt concrete mixture can be determined by the following relationship, which was first developed by Van der Poel and later modified by Heukelom and Klomp (40):

$$S_{mix} = S_{ac} \left[1.0 + \left(\frac{2.5}{n}\right) \left(\frac{C_v}{1.0 - C_v}\right)\right]^n \qquad (2.5)$$

where

S_{mix} = stiffness of asphalt concrete mixture, kg/cm^2.

S_{ac} = stiffness of asphalt cement, kg/cm^2.

$n = 0.83 \log_{10} \frac{4 \times 10^5}{S_{ac}}$.

C_v = volume concentration of the aggregate in the mixture, defined as follows:

$$\frac{\text{Volume of compacted aggregate}}{\text{Volume of (asphalt + aggregate)}} = \frac{100 - \%\ \text{VMA}}{100 - \%\ \text{air voids}},$$

where VMA = voids in mineral aggregate.

When dealing with asphalt concrete cores cut from a pavement or a compacted laboratory sample, the previous equation for C_v can be replaced by an equivalent equation as follows:

$$C_v = \frac{1}{1 + c} \qquad (2.6)$$

where

$$c = \frac{W_s}{W_g} \cdot \frac{G_g}{G_s} = \frac{\%\ \text{of asphalt by weight of aggregate}}{100.0} \left[\frac{G_g}{G_s}\right].$$

where

W_s = weight of asphalt.

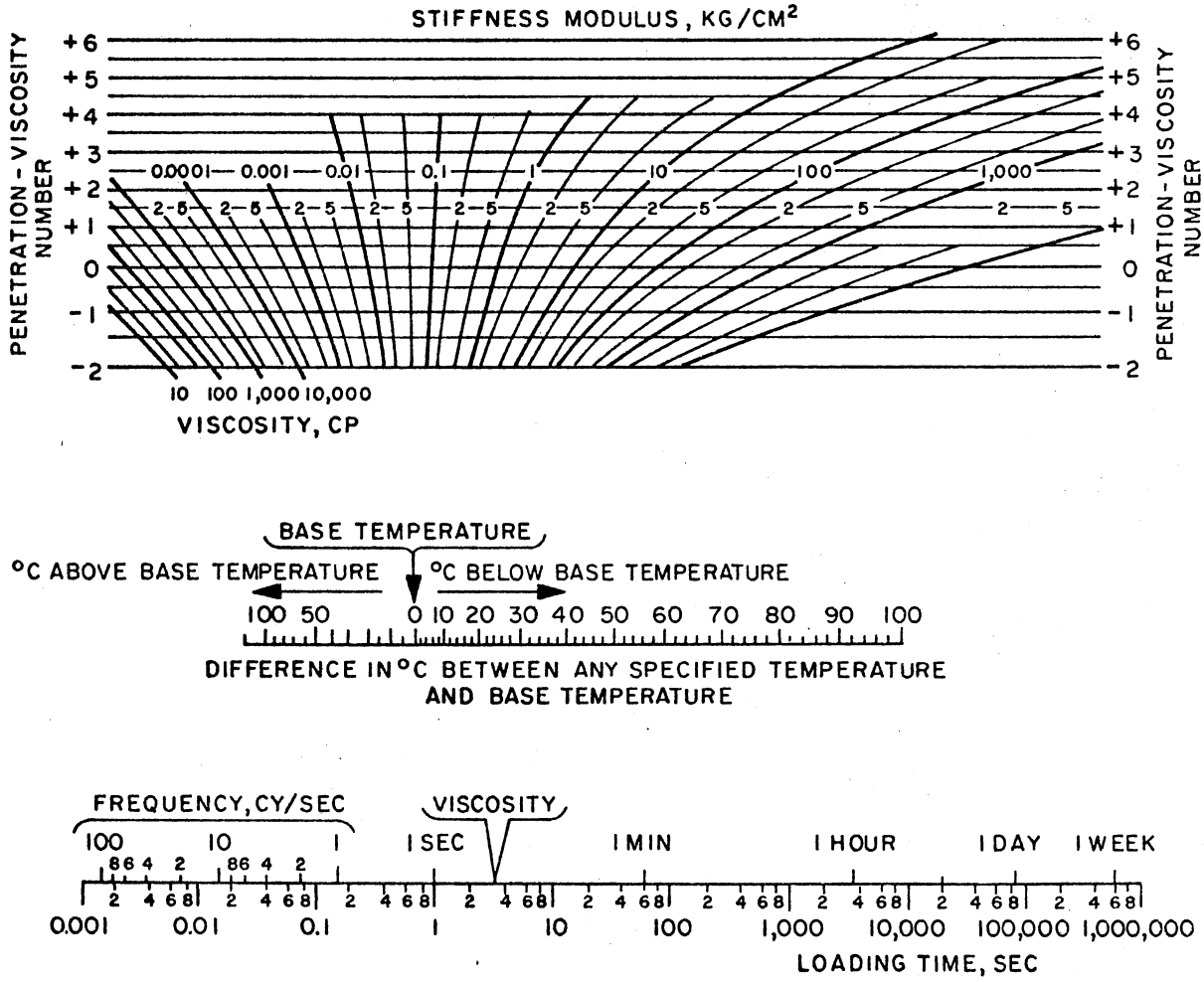

Figure 8. Suggested Modification of Heukelom's and Klomp's Version of Van Der Poel's Nomograph for Determining Modulus of Stiffness of Asphalt Cements (36)

W_g = weight of aggregate.

G_s = specific gravity of asphalt.

G_g = specific gravity of aggregate.

A chart for solving the equation of S_{mix}, for a range of C_v values from 0.6 to 0.94, is presented in Figure 9. Heukelom and Klomp stated that the relation of S_{mix} is applicable to well-compacted mixtures with about 3 percent air voids and C_v values between about 0.7 and 0.9. For mixtures with air voids greater than 3.0 percent, Draat and Sommer (41) derived a correction to be applied to the C_v value. The corrected C_v value (C_v') is determined as follows:

$$C_v' = \frac{C_v}{1 + H} \tag{2.7}$$

where

H = actual percent air voids - 3.0%.

Haas (13) discussed the use of indirect methods in estimating stiffness modulus of asphalt cements and mixtures. He indicated some limitations, in both their use and in the application of the results, that should be kept in mind. However, he concluded that these methods are quick, easy to use, and most useful for initial estimates of stiffness modulus.

Some research studies recommended the use of the tensile splitting test to evaluate the low-temperature tensile fracture strengths and strains of asphalt concrete materials, either secured from the field or freshly prepared (42, 43, 44). Another important parameter in previous analysis and design approaches was the coefficient of thermal contraction of the paving mixture. Several investigations have been performed to determine this coefficient, some of which indicated that the coefficient

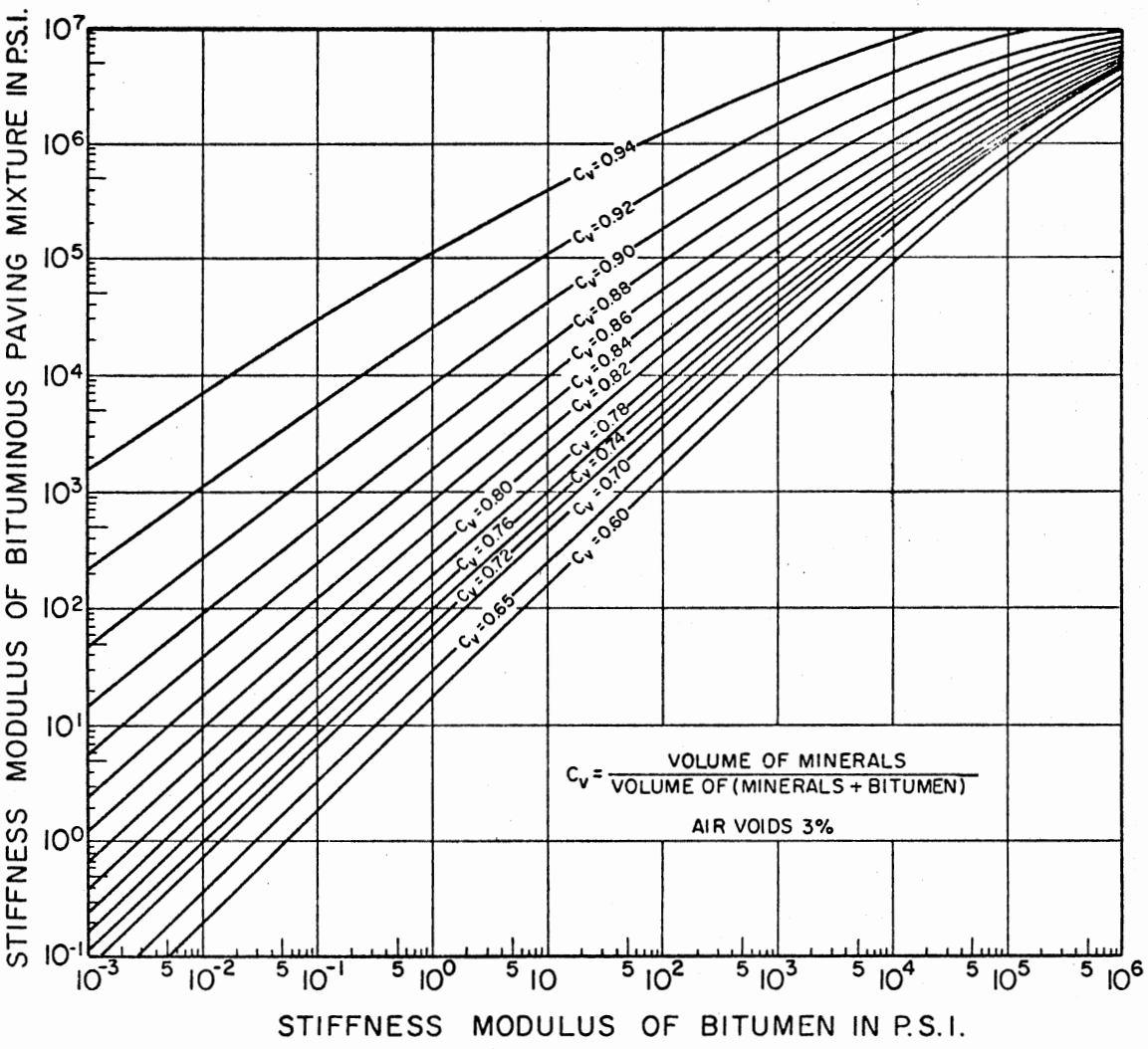

Figure 9. Relationships Between Moduli of Stiffness of Asphalt Cements and of Paving Mixtures Containing the Same Asphalt Cements (40)

is not linear over the entire low-temperature range. Phang (45) has conducted a comprehensive set of tests to evaluate the contraction coefficient and he reported values for field samples ranging between $0.95 \times 10^{-5}/F°$ and $1.81 \times 10^{-5}/F°$, with an average value of $1.5 \times 10^{-5}/F°$ in the temperature range -20°F to +30°F.

Available Design Approaches

According to Haas (13), several major alternative design approaches to low-temperature shrinkage cracking have been developed. However, he indicated that some of these approaches are highly empirical and do not make provisions for estimates of error. Haas also pointed out that these approaches can be temporarily used until the more fundamental procedures have been fully developed and validated. These approaches may be grouped into four categories:

1. Specification adjustment.
2. Limiting stiffness.
3. Fracture temperature prediction.
4. Statistical correlations to observed cracking.

Specification Adjustment

The behavior of asphalt concrete mixtures at relatively high temperatures has been the main interest of the paving technologists for many years. Thus, specifications for controlling asphaltic paving mixtures were only concerned with stability at 140°F and density and voids at 77°F and little interest was evidenced in controlling the behavior of asphaltic mixtures at low temperatures. Unfortunately, the importance of stability at high temperature may have been overemphasized.

In many cases, high stability has been attained at the expense of plasticity by using low-penetration asphalt cements and, as a result, these mixtures were more susceptible to cracking at low temperature. This has suggested a new approach for design criteria. Several agencies have adjusted their specifications to require softer (higher penetration) grades of asphalt, while others retained their penetration grades but have specified a fairly high minimum viscosity requirement at either 140° or 275°F (1).

It seems that some progress has been achieved in some cold regions with using only softer grades of asphalt cement (1, 11, 23). However, Haas (1, 13) has stated that if softer asphalts are used, there can be long-term effects on other aspects of pavement performance, such as rutting and fatigue, that should be evaluated.

Limiting Stiffness

Several studies have indicated that the stiffness modulus of the asphalt concrete mixture at low winter temperatures was the major factor governing transverse cracking. All these studies agreed that mixtures of lower stiffness modulus should be used to eliminate or decrease transverse cracking during a pavement's service life. Consequently, a design approach was developed to specify limiting or critical stiffness values for various low service temperatures.

Mcleod (36) examined a variety of data from Canadian test roads, and he concluded that cracking would occur if the stiffness of a mix in service falls within the range of 1×10^6 to 2×10^6 psi (7×10^4 to 1.4×10^5 kg/cm^2) at the minimum temperature encountered at a depth of 2.0 in. This stiffness value was suggested for a dense, well-graded

mix (C_v = 0.88) at 2 x 10^4 seconds loading time. As a result, he prepared a tentative design guide for maximum moduli of stiffness for various temperatures, as shown in Table I. The table includes the levels of stiffness at which cracking is expected and the levels at which cracking should be eliminated. The latter is a design guide which essentially incorporates a "safety factor" of 2.0 to account for hardening in service. Mcleod has translated this criteria into an asphalt cement selection guide, as shown in Figure 10, for various levels of penetration index. The diagram shows, for example, that to avoid cracking for a minimum temperature of -40°F, an asphalt cement of P.I. = 0.0 should not be harder than 300 penetration at 77°F.

In Ontario, Fromm and Phang (46) have performed a series of calculations similar in concept to those of Mcleod for specifying the grade of asphalt that should be used for a given temperature. They assumed a critical stiffness of 1.38 x 10^8 N/m^2 (2 x 10^4 psi) with a loading time of 2.8 hrs (10,000 sec). Phang has also suggested, as have others, that the minimum expected temperature should be chosen on a probabilistic basis.

In the Ste. Anne Test Road, observations of cracking frequency and analysis of the rheological properties of the bitumens using Van der Poel's nomograph were carried out. Burgess et al. (21) concluded that the critical stiffness of the bitumen was 2.4 x 10^8 N/m^2 (2500 kg/cm^2 or 35,550 psi) for 0.5 hr loading time at a temperature of -40°F. This 0.5 hr loading time corresponds to a cooling rate of 10°C per hour.

Haas (21) examined the stiffness implications of a variety of asphalt cement specifications in Canada and the United States together with some values from previous investigations. He compared the results

TABLE I

MAXIMUM MIX STIFFNESS FOR SELECTING
ASPHALT CEMENT GRADE (23)

Minimum Temp. at a Pavement Depth of 2.0 in., F°	Stiffness Modulus, psi	
	Cracking Expected	Cracking Eliminated
-40	1,000,000	500,000
-25	700,000	300,000
-10	400,000	200,000
+10	100,000	50,000

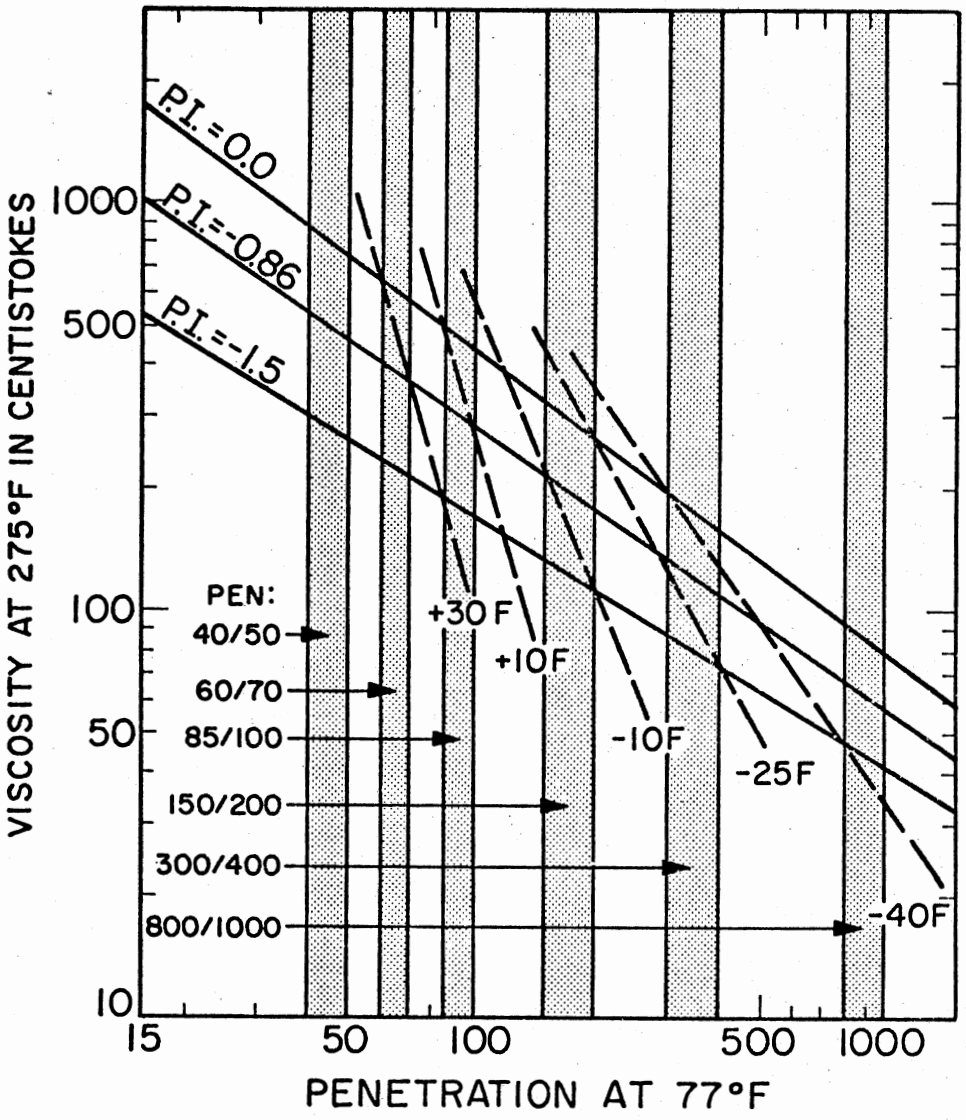

Figure 10. Selection of Asphalt Cement Grade for Various Design Temperatures (23)

of his study with Mcleod's limits and concluded that these limits are satisfactory. Also, Lefebvre (47) and Hajek and Haas (48) indicated that Mcleod's procedure of estimating the stiffness modulus of asphalt cements was apparently the best indirect method.

In summary, the foregoing discussion shows that a design approach using a limiting stiffness modulus is reasonable and provides some very useful quantitative guidelines. Also, Mcleod's method of determining stiffness modulus and his proposed design stiffness criteria appear to be satisfactory and can be correlated with actual field performance of asphalt concrete mixtures.

Fracture Temperature Prediction

It has been pointed out that the postulated mechanism of cracking was primarily based on the concept of having induced thermal stresses that exceeded the tensile fracture strength of the pavement. The estimate of fracture temperature depends on calculating these stresses due to a drop in temperature and comparing them with the tensile strength of a given layer. When the tensile strength is exceeded by the accumulated stresses, fracture should occur as shown in Figure 11.

The thermal stresses can be calculated in either a rigorous or an approximate manner. The approximate method was originally proposed by Hills and Brien (49) to calculate the thermal stresses in a long completely restrained strip using the following equation:

$$\sigma_x(T) = \alpha \sum_{T_o}^{T_f} S(\Delta T) \cdot \Delta T \qquad (2.8)$$

where

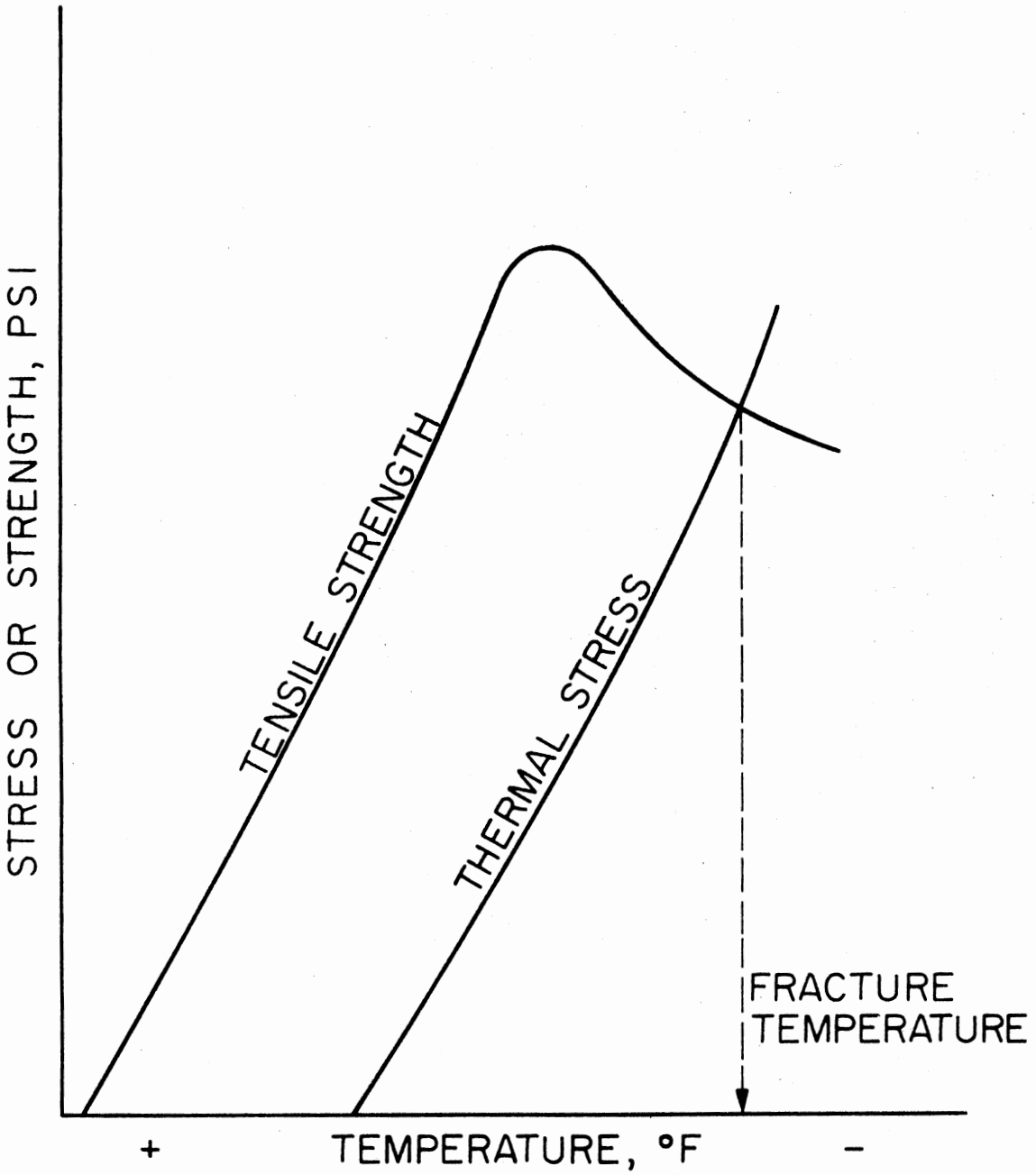

Figure 11. Schematic Diagram of the Fracture Temperature Concept

$\sigma_x(T)$ = accumulated thermal stress for a particular cooling rate, T.

α = average thermal contraction coefficient over the temperature drop, $T_o - T_f$.

T_o, T_f = initial and final temperatures.

$S(\Delta T)$ = stiffness at the midpoint of discrete temperature intervals ΔT over the range of T_o to T_f, using a loading time corresponding to the time interval for the ΔT change.

Haas and Topper (30) have extended this approach to include both temperature and stiffness gradients through the depth of the asphalt layer. The method they developed was used to calculate thermally induced stresses in several previous efforts (21, 33, 50) and to predict the probable fracture temperature.

The rigorous approach for calculating thermally induced stresses has been generally postulated by Humphreys and Martin (51) and was later applied to asphalt pavements by Monismith et al. (52). According to this approach, the pavement layer was considered as a linearly viscoelastic plate of infinite lateral extent which was completely restrained. The stresses calculated by this method were, apparently, unrealistically high. This was due to the assumption of infinite lateral extent of the layer (1, 30). Extensive analysis of Ste. Anne Test Road data and comparison with the field observations of fracture showed that the approximate approach of calculating thermal stresses could yield reasonable results (24, 53).

Haas (13) pointed out that some limitations should be considered while using the fracture-temperature prediction approach, and Shahin (54) had indicated that a single fracture temperature cannot be

considered a satisfactory criterion for design purposes because of the great variation of the asphalt concrete properties over the entire road length.

Statistical Correlations to Observed Cracking

Observations and data collected from various research studies have indicated that certain variables were significantly related to the observed degree of cracking. These variables have been used by several investigators in developing mathematical models to estimate the low-temperature shrinkage cracking frequency of future pavements, on the basis of past experience. Fromm and Phang (22) have developed equations for a cracking index for Ontario conditions based upon a stepwise and linear multiple regression techniques. Likewise, Hajek and Haas (48) have constructed a predictive model which estimates the cracking frequency in terms of a cracking index for various ages in the life of the pavement. This model may be defined as follows:

$$C.I. = f(s, t, a, m, d) \tag{2.9}$$

where

C.I. = cracking index.

s = stiffness (kg/cm^2) of the original asphalt cement, determined by Mcleod's method (36) for a loading time of 20,000 seconds and at a winter design temperature m.

t = combined thickness of the asphalt layers (in.).

a = age of pavement (yrs).

m = winter design temperature (C°).

d = subgrade type code, dimensionless (d = 5 (sand); d = 3 (loam); d = 2 (clay)).

A nomographic solution for this model has been developed and is shown in Figure 12. Haas (13) showed that the model was evaluated in terms of its statistical significance, rational behavior, and relation to the observed data. The results suggested that the model could be used for initial design purposes with a considerable degree of confidence.

Modifying Temperature-Sensitivity of Asphalt Binders

In recent years, considerable efforts have been directed toward investigating the advantages of using additives, such as natural rubber, synthetic polymers, and asbestos fibers, to modify or improve the temperature-sensitivity of asphalt cements and/or mixtures. Thompson (55) presented the results of a full-scale road experiment that employed natural rubber as an asphalt modifier. These results indicated that the addition of rubber had a marked effect on the viscosity and temperature-sensitivity of the asphalt binder. Apparently, viscosity was increased at high temperatures and decreased at low temperatures. As a result, stability and resistance to cracking could both be attained.

Fabb (56) conducted a laboratory investigation to study the temperature consistency characteristics of asphalt cements modified by certain kinds of synthetic polymers. Results of this study showed that certain polymers can improve the thermal cracking resistance of asphalt cements. However, Fabb indicated that the use of these polymers for this purpose should be economically studied.

Hignell et al. (57) investigated the asbestos fiber modification of asphalt paving mixtures. Their findings revealed that asbestos fiber

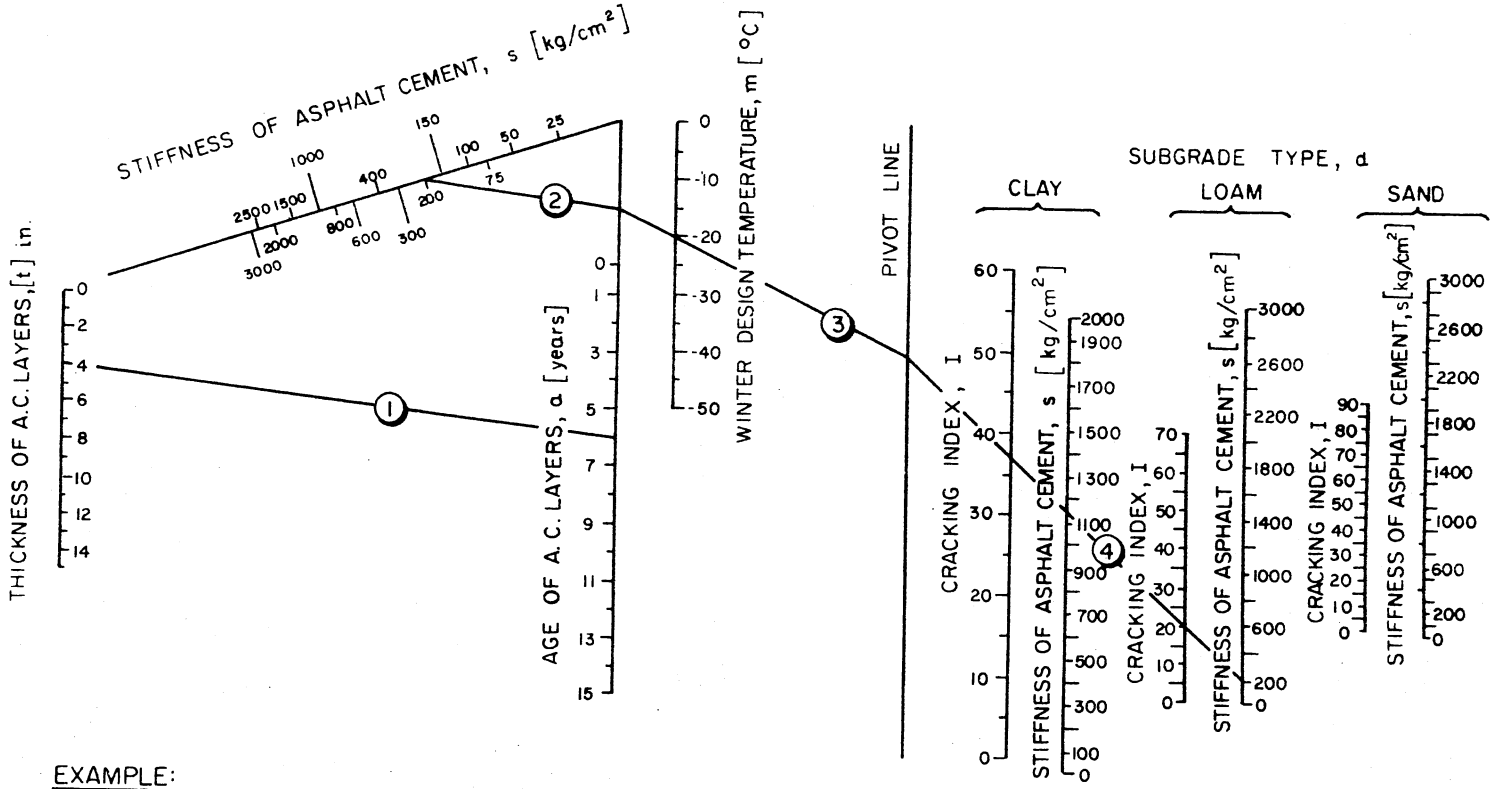

EXAMPLE:

thickness = 4 inches
age = 6 years
stiffness of original asphalt cement = 200 kg/cm²*
winter design temperature = -20 °C
subgrade type = loam

*for temp. = m and time = 20000 sec.

NOTE:

A) lines (1) and (2) are parallels
B) in step (4) select scales for the appropriate subgrade type

RESULT: cracking index = 20 at 6 years

Figure 12. Nomograph for Predicting Low-Temperature Cracking Frequency of Asphalt Pavements (13)

can improve the temperature susceptibilities of dense-graded asphalt mixtures. Also, they indicated that asbestos fibers may be very useful where a softer asphalt is to be used for low-temperature cracking considerations. Their use, in this case, served to increase medium to high service temperature stiffness so that the desired resistance to fatigue and pavement deformation could be achieved.

Treating Existing Cracked Pavements

The foregoing design appraoches provide some guidelines for avoiding or reducing transverse cracking in newly constructed pavements. However, a large problem remains with existing cracked pavements. For a number of years, transverse cracking in flexible highway pavements has been treated as a maintenance problem and several efforts were made to fill and patch the existing cracks. Various crack sealing procedures and materials have been investigated to determine the optimum method for treating cracked pavements. For example, Wolters (58) conducted a field study to evaluate various joint preparation and material application procedures for sealing transverse cracks in Minnesota flexible pavements. This study has indicated that adhesion failure was the major type of distress that occurred in sealed cracks. Wolters recommended that surface brushing and blowing out with air should be performed prior to sealing the cracks. He also indicated that all cracks sealed in flexible pavements should be slightly overfilled to assure longer service life.

Some other research studies indicated that satisfactory serviceability of cracked pavements could not be achieved by maintenance alone and resurfacing appeared to be the only answer (1). Unfortunately, existing cracks reflected up through the resurfacing in a very short

time, thereby significantly reducing the normal service life of these overlays. However, a field study performed at Alberta, Canada (1) has indicated that satisfactory pavement performance was achieved when the overlay had been placed during the period of maximum crack heaving.

In summary, a significant amount of additional work is apparently still required to determine the most economical, efficient and practical technique of treating existing cracked pavements.

CHAPTER III

EXPERIMENTAL DESIGN

The design of an experiment can generally be defined as a complete sequence of steps taken to insure that appropriate data will be obtained for objective analysis (59). This concept was utilized in planning and conducting the experimental field and laboratory programs to provide a maximum amount of information relevant to the transverse cracking problem.

The objective of the field testing program was to investigate the possible causes of cracking and the factors that caused contrasting degrees of cracking to occur in particular highway pavements. Various highway sections exhibiting different types of transverse cracking were visited. Some of these sections were suggested by the Research and Development Division of Oklahoma Department of Transportation and others were located by research personnel during field trips to different locations in Oklahoma. Preliminary surveys of these sections were made to: (1) check the sight distance available to on-coming traffic, (2) visually examine the degree, nature and extent of existing cracks, (3) locate recently developed cracks for further study, (4) make a general rating of pavement surface condition, and (5) study the geometric design characteristics of the pavement sections.

A great deal of consideration was given to the vertical and horizontal alignment at these sections to assure that the safety of research personnel could be maintained during further field operations. Tentative selection of possible test sites depended mainly on available safe sight distances. Any site on a horizontal or vertical curve was disregarded and, where possible, another location on a tangent section in the same vicinity was selected. Suitable field locations were marked and identified as possible test sites for the experimental field study.

Selection of the test sites was based on both the results of the initial field survey and the planned time schedule. Consideration was given to the selection of test sites where a relatively wide variation in degrees of cracking had occurred in order to possibly identify and contrast the contributing factors existent at these sites. Also, transverse cracking was observed at pavement sections on both the high-quality interstate and lower quality state highway systems, and test sites from both types of facilities were included in the study. In order to investigate the effect of aging on the observed degree of cracking, pavements of various ages were considered in the final selection of the test sites.

To keep the amount of experimental work within practical time limits, a total of nine test sites was finally selected for detailed investigation. Permanent identification of these sites was made by attaching a 10.0 in. x 11.0 in. (25.4 cm x 27.94 cm) red painted metal sheet to the right of way fence at each test site. These markers were located at a measured odometer distance from the nearest intersec-

tion, bridge, or the boundary line of the county in which the test sites were located. At each test site, a 500 ft length of pavement which satisfied the safe sight distance requirements was chosen for detailed crack surveying, counting and coring. A Rolatape (Model 200) was used to measure the 500 ft length of the pavement and the beginning and ending points were marked with a yellow paint stripe along the shoulders.

The selected test sites included four sections on State Highway Number 177 where various degrees of cracking were observed. The other five sites were on sections of Interstate 35 and Interstate 40. Two of these interstate sites had almost no cracking and were chosen for comparison. Table XIV in Appendix A shows the exact locations and the construction and maintenance dates for these sites.

Field Testing Program

The field study started with mapping and counting the cracking patterns within the chosen 500 ft lengths of pavement. These data were used to develop a cracking index for the sections as a measure of cracking severity. In addition, newly developed cracks, i.e., extremely narrow transverse cracks that did not extend the full width of the pavement, were selected at various sites during the crack survey. Pavement cores spanning these narrow cracks were obtained in an attempt to ascertain the mechanism of transverse cracking.

Another part of the field study consisted of securing pavement core samples for further laboratory testing. A previous study (60) showed that traffic loads tended to densify the asphalt concrete paving

materials. Consequently, it was decided that any evaluation of the pavement core samples should consider their location with respect to traffic wheel paths and the field cores were classified as "wheelpath" and "non-wheelpath" samples. It was also planned to evaluate the tensile properties of the field samples at three low temperatures. To accomplish this, eighteen field core specimens were required at each test site. As test sites where almost no cracking was observed, core specimens were taken from nine wheelpath and nine non-wheelpath locations within the chosen 500 ft length of pavement. At other test sites, randomization principles were used to choose three full cracks from those previously counted during crack surveying of the individual test sites. At appropriate offset distances from the edges of these cracks, six core specimens were obtained as illustrated in Figure 13. These cores were also identified as wheelpath and non-wheelpath samples.

Laboratory Testing Program

The laboratory testing program was designed largely on the basis of the results of the study of the preliminary pavement cores. As previously mentioned, these were obtained by coring across very narrow transverse cracks. Examination revealed that in a majority of cases these "beginning" cracks did not extend through the pavement matrix. Apparently, the cracks had originated at the surface and had propagated or extended to a limited depth in the underlying layers (Figure 14a). In a few core specimens, these narrow cracks extended completely through the asphalt paving layers (Figure 14b). It is

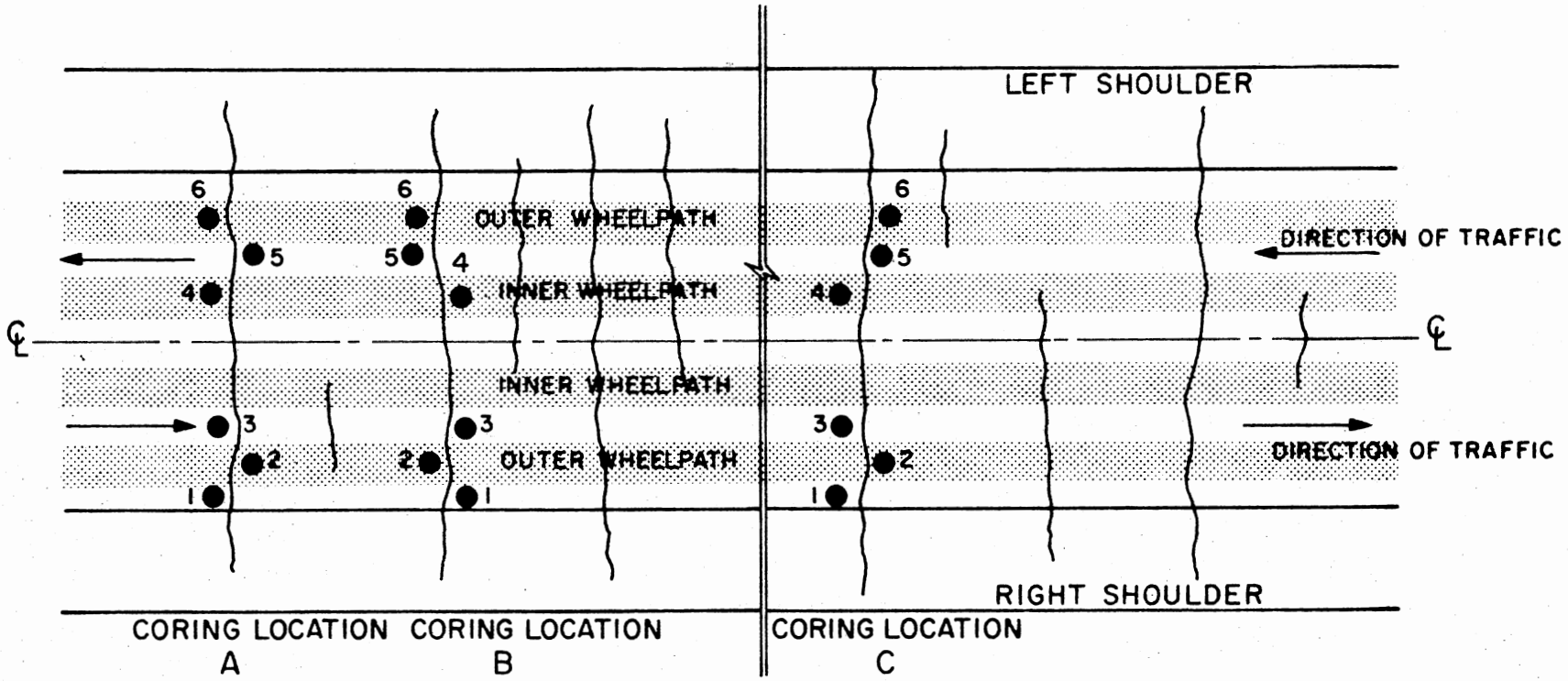

Figure 13. A General Layout of Coring Plan for a 2-Lane Test Site

(a)

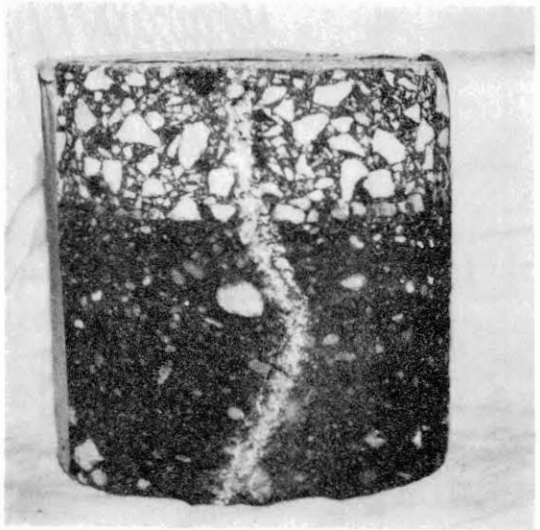

(b)

Figure 14. Extension of Transverse Cracks in the Pavement Matrix

possible that these full-depth cracks are also due to thermally induced stresses in the pavement and have had the neccessary time and ambient conditions to propagate the full pavement depth. However, there is an alternate possibility that these cracks first occurred at the pavement-subgrade interface and resulted from load induced stresses and/or subgrade soil aberrations.

Based on the hypothesis that the transverse cracks are caused by tensile forces developed in the pavement surface and that these forces are due to the low-temperature response of the asphalt paving mix, the research approach was directed towards evaluating the low-temperature behavior of the asphalt materials and mixtures and correlating this behavior with the actual field performance data, i.e., the cracking index of the pavement section.

Evaluation of Field Samples

The first part of the laboratory testing program was an evaluation of the properties of the asphalt concrete surface course of each test site. The upper layer of each core specimen was cut and the thickness and diameter were measured. Bulk specific gravity values of the wheelpath and non-wheelpath paving mixtures were determined by averaging the values for three representative samples. To evaluate the tensile properties of field samples over a low-temperature range, three temperatures, 0^{o}, -5^{o}, and 10^{o}C, were chosen for the tests. A relatively simple and practical tensile splitting apparatus (Chapter IV) was used to determine the tensile properties of these field specimens at the various temperature levels.

The design of the experiment can be defined as a "split-plot design" (61) where field samples represented experimental units obtained from nine test sites (blocks). Experimental units secured from each test site were divided according to their location into two "main plots", wheelpath and non-wheelpath. Each main plot was subdivided into three subplots to which the aforementioned temperature levels were randomly applied. To increase the precision of the experiment, each temperature level (subplot treatment) was applied to three samples (replicates).

A modified Rice's specific gravity test was used to determine the maximum specific gravity of the field samples. These test samples were those previously chosen for bulk specific gravity determinations and the test results were used to calculate the percent density and air void content of the wheelpath and non-wheelpath materials.

The asphalt cement binders were extracted from the pavement materials and the average asphalt content of each surface mix was determined. These asphalt binders were recovered from the extraction solutions for further laboratory testing. Three recovered asphalt samples from each test site were tested to determine their rheological properties. These properties were used in calculating the stiffness moduli of the various asphalt materials and mixtures, according to McLeod's approach. These stiffness moduli were calculated at a service temperature of $-10^{o}F$ ($-23.3^{o}C$). The choice of this temperature was based upon the climatological data of Oklahoma and the pavement temperature data reported in another research study (27).

The laboratory test results and the calculated stiffness values were correlated with the actual field performance data of individual test sites as measured by their cracking indices. However, it is important to note that the chosen test sites had not been sampled just at the point of incipient cracking. Apparently, some had cracked years before and considerable aging of the asphalt binders had taken place since the initial cracking. Other pavements had few cracks and their properties were still some distance from the critical point. Thus, the best that could be hoped for was a considerable scattering of values when correlated with the amount of cracking that had occurred.

Evaluation of Laboratory Materials and Mixtures

The experimental approach of characterizing the behavior of asphalt materials and mixtures at low temperatures was extended to investigate and/or predict the performance of fresh asphalt materials and mixtures. Eighty-one compacted specimens of a Type C surface course mixture (45) containing various asphalt contents and different penetration grades of asphalt cement were prepared and tested using the tensile splitting apparatus. This was done to study the effect of three factors, temperature, asphalt content, and asphalt penetration grade, on the tensile properties of the asphalt concrete mixtures. Three levels of each factor were employed in this study to allow for useful comparisons. These levels were as follows:

1. Temperature: $+20^{o}$, 0^{o}, and -10^{o}C.
2. Asphalt content: 4.5, 5.0, and 5.5 percent by total weight.
3. Asphalt grade: 91, 124, and 160 penetration.

Based on the statistical definition of "design of experiment", this was considered as a "3 x 3 x 3 factorial experiment" where treatments were the various possible combinations of factors and factor levels. Three specimens (replicates) per each treatment were tested to increase the precision of treatment comparisons.

The stiffness moduli of the above asphalt binders and mixtures were calculated at various low temperatures (0^{o}, -10^{o}, -20^{o}, -30^{o}, and $-40^{o}C$) according to McLeod's method. Also, the stiffness moduli of 26 asphalt cement samples secured from different sources in Oklahoma were determined at the expected lowest service temperature ($-10^{o}F$, or $-23.3^{o}C$). The calculated stiffness values were compared to the limiting stiffness moduli reported in the literature for the same conditions of temperature and rate of loading. The results of these comparisons were used as a quantitative measure or an indication of the ability of the respective surface layer mixtures to resist cracking at Oklahoma's lowest service temperature.

CHAPTER IV

DEVELOPMENT OF THE TENSILE SPLITTING TEST EQUIPMENT

The tensile splitting test was originally developed to evaluate the tensile strength of concrete and mortar materials (63, 64). In recent years, the use of this test was extended to include cement-treated gravel, lime-soil mixtures and asphalt-stabilized materials (24, 42, 65, 66). This test involves loading a cylindrical specimen with a compressive load distributed along two opposite generators. This results in a failure that usually occurs by splitting along the diameteral plane as shown in Figure 15.

The tensile splitting test used in the experimental phase of the study provided a relatively simple means for determining the tensile properties of asphalt concrete specimens at low temperature. It was hoped that this test procedure would be useful in investigating the ability of the common asphalt paving materials in Oklahoma to resist shrinkage cracking at low temperatures.

Theory of the Test

The theoretical concept of the tensile splitting test is based on the theory of elasticity. Assuming plane stress and considering a circular disk subjected to concentrated loads on the diameter as shown in Figure 16, the general equations that express the tensile, compressive

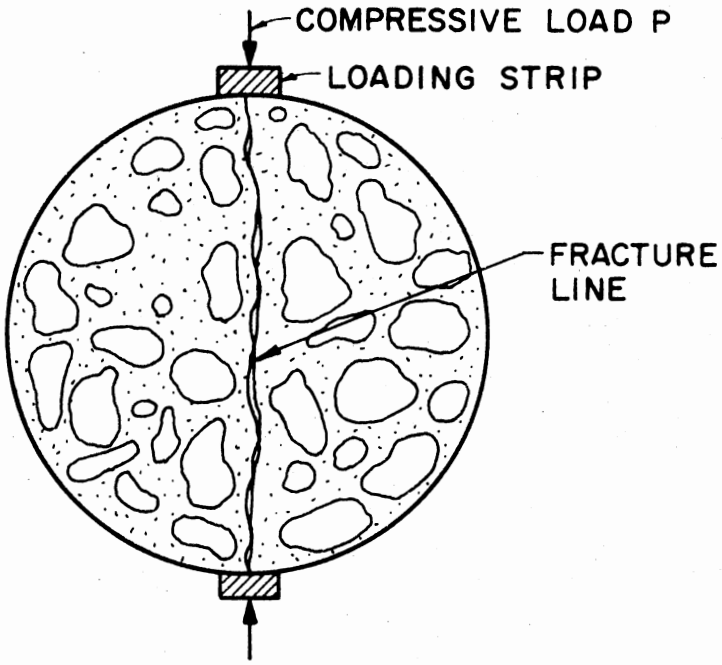

Figure 15. The Indirect Tensile Splitting Test

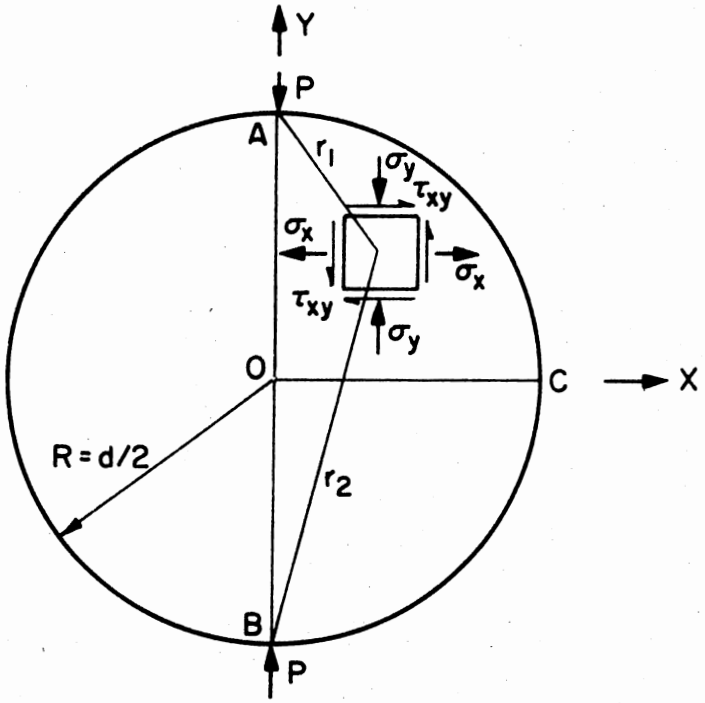

Figure 16. Diagram Showing the Loading Disk and the Resultant Stress Conditions (63)

and shear stress on an element within the disk, are as follows (63):

$$\sigma_x = \frac{-2p}{\pi t}\left[\frac{(R - y)x^2}{r_1^4} + \frac{(R + Y)x^2}{r_2^4} - \frac{1}{d}\right] \tag{4.1}$$

$$\sigma_y = \frac{-2p}{\pi t}\left[\frac{(R - y)^3}{r_1^4} + \frac{(R + y)^3}{r_2^4} - \frac{1}{d}\right] \tag{4.2}$$

$$\tau_{xy} = \frac{2p}{\pi t}\left[\frac{(R - y)^2 x}{r_1^4} - \frac{(R + y)^2}{r_2^4}\right] \tag{4.3}$$

where

σ_x, σ_y, τ_{xy} = stress components with respect to rectangular co-ordinates.

x, y = rectangular co-ordinates.

p = load applied to specimen.

t = thickness of cylindrical specimen.

d = diameter of cylindrical specimen.

R = Radius of cylindrical specimen.

r_1, r_2 = location co-ordinates.

Considering points between O and C on the horizontal x-axis where $y = 0$ and $r_1 = r_2 = \sqrt{x^2 + R^2}$, both σ_x and σ_y vanish at the circumference and reach maximum values at the center. These maximum stresses can be written as follows:

$$\sigma_x = \frac{2P}{\pi t d} \tag{4.4}$$

$$\sigma_y = \frac{-6P}{\pi t d} \tag{4.5}$$

This indicates that the material tested should have a compressive strength at least three times its tensile strength to assure a tensile failure.

Along the y-axis, where $x = 0$, $r_1 = R - y$, and $r_2 = R + y$, the stress equations reduce to:

$$\sigma_x = \frac{2P}{\pi td} \tag{4.6}$$

$$\sigma_y = \frac{-2P}{\pi t}\left[\frac{2}{d-2y} + \frac{2}{d+2y} - \frac{1}{d}\right] \tag{4.7}$$

$$\tau_{xy} = 0 \tag{4.8}$$

The distribution of stresses along a horizontal and vertical diameter, as calculated from the previous equations, are shown in Figure 17 and Figure 18.

As can be seen in Figure 18, the horizontal tensile stress, σ_x, along the vertical plane has a constant value of $2P/\pi td$ and the vertical compressive stress, σ_y, has a minimum of $-6P/\pi td$ at the center and a maximum value of infinity at the load points. With a line load, it seems that the specimen is likely to fail near the load points due to the high compressive stresses. However, photoelastic studies (63) have shown that these compressive stresses can be greatly reduced by using a distributed load applied through a short loading strip. These loading strips were found to be sufficient to retard the compressive failure at the load points so that the specimen fails due to the tensile stress at the center (64).

The total tensile strain at failure for a 4.0 in. (10.16 cm) diameter specimen with a 0.5 in. (1.27 cm) curved loading strip can be determined as follows (67):

$$\varepsilon_{TF} = X_{TF}\left[\frac{0.1185\nu + 0.03896}{0.2494\nu + 0.06730}\right] \tag{4.9}$$

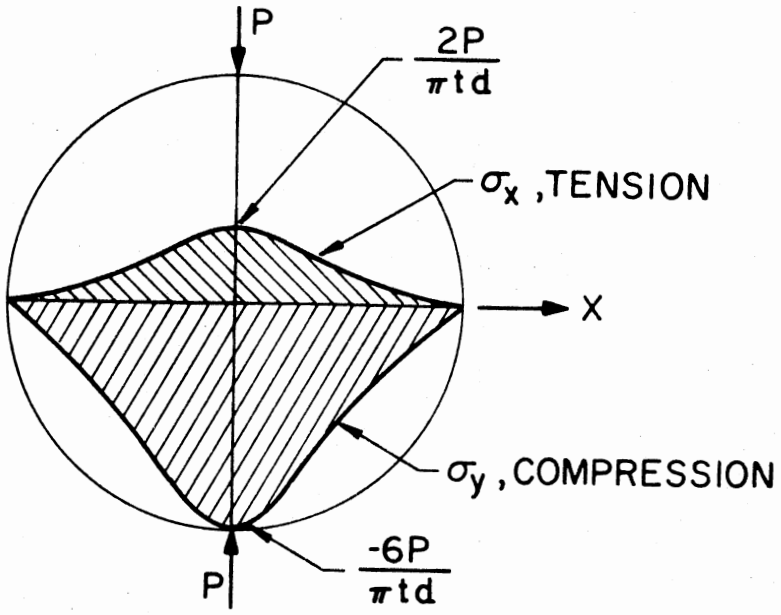

Figure 17. Stress Distribution on X-Axis (66)

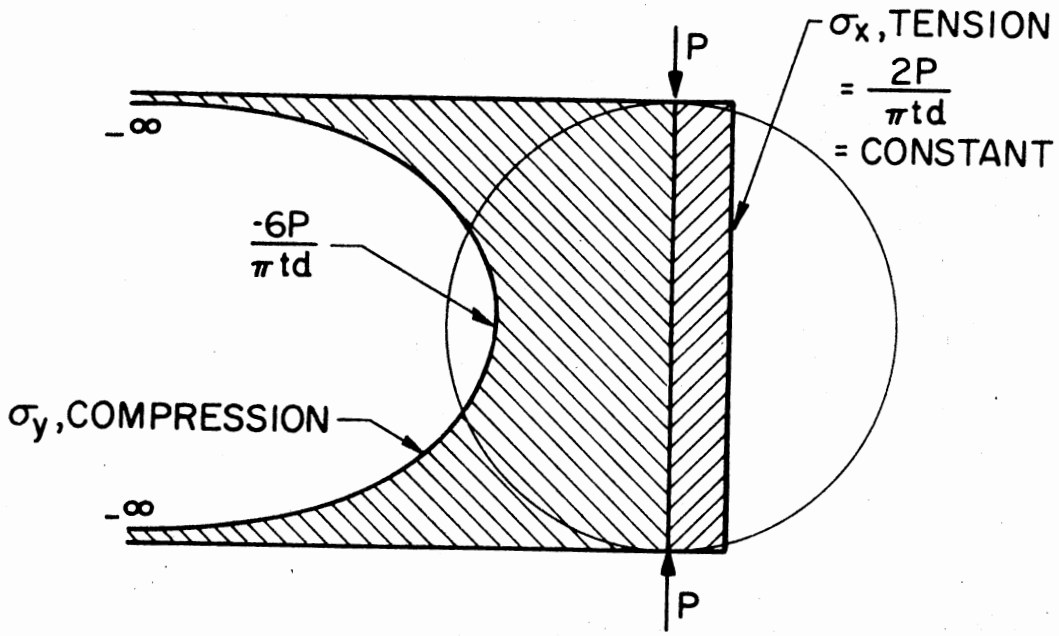

Figure 18. Stress Distribution on Y-Axis (66)

where

ε_{TF} = total tensile strain at failure, in./in.

X_{TF} = total horizontal deformation at failure, in.

ν = Poisson's ratio of asphalt concrete material.

Previous studies have shown that Poisson's ratio of asphalt concrete materials varies between 0.25 and 0.35 with an average of 0.3 (67). Substituting this value in equation 4.9, the total strain at failure can be expressed as:

$$\varepsilon_{TF} = 0.524\ X_{TF} \tag{4.10}$$

Deviations of Test From Ideal Conditions

The previous theoretical analysis was based on an idealized case of an elastic, isotropic and homogeneous material. Actually, the test deviates from the assumed ideal condition. However, some of these deviations were thought to have a minor effect on the results obtained from the test (68). For instance, it was indicated that the random distribution of aggregate particles in an asphalt concrete specimen tends to minimize the effect of heterogeneity. Also, the assumption of plane stress was considered to be valid for the 2.0 in. (5.08 cm) thick specimens, since they are relatively thin. Also, the behavior of asphalt concrete materials at low temperature is essentially elastic in nature, therefore, the assumption of elasticity of the material may be reasonable under this condition.

One of the main test deviations is the loading method. Actually, the line load is distributed over an area because of the practice of

applying the load through a loading strip. Studies concerning the effects of a loading strip on stress distribution have shown that the magnitude of the vertical compressive stresses is considerably reduced and that the magnitude of the horizontal tensile stresses is generally unchanged near the center of the specimen. However, the tensile stress changed to compression directly beneath the loading strips (64). Therefore, it may be concluded that the effect of the loading stip is quite localized and that the specimen will ordinarily fail in the central portion due to tensile stress.

Test Method

The indirect tensile splitting test used in the experimental portion of this study involved applying compressive loads at a rate of 0.06 in./min (0.152 cm/min) (42) across a marked diameter of the cylindrical asphalt concrete specimens. The apparatus for this test is shown in Figure 19, the load was distributed by using 0.5 in. (1.27 cm) wide loading strips that were curved at the interface with the specimen and had a radius of curvature equal to that of the specimen (2 in. or 5.08cm). A load cell placed on the upper loading plate was used to continuously measure the applied compressive load. The horizontal deformation of the specimen was determined during the test by series-connected linear variable differential transducers attached to the opposite faces of the specimen. Output signals from both the load cell and the differential transducers were continuously fed to an X-Y recorder. Load response was transmitted to the y-axis and horizontal deformation response to the x-axis. This resulted in a load deformation trace on the recorder paper as shown in Figure 20. From this graph, the maximum load causing

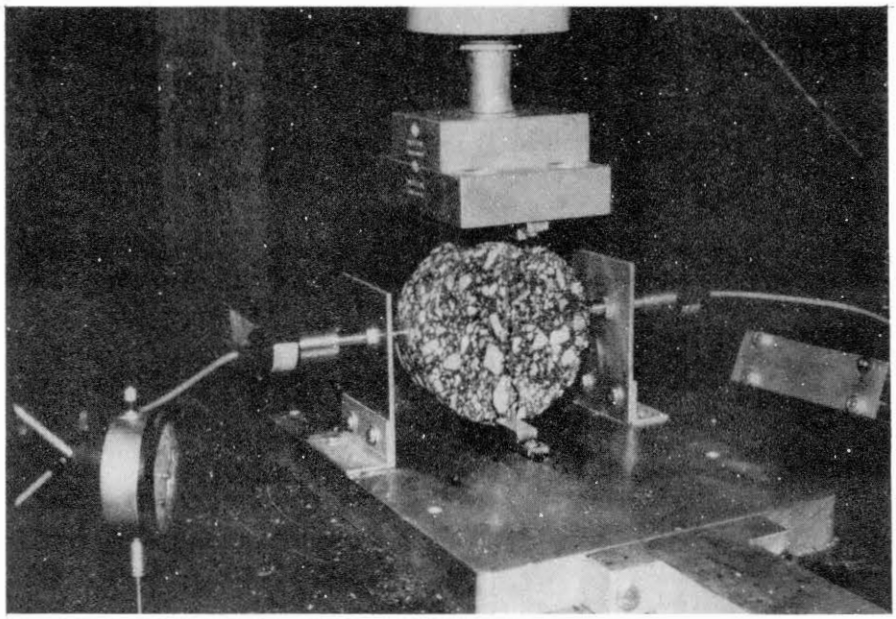

Figure 19. The Modified Tensile Splitting Test Equipment

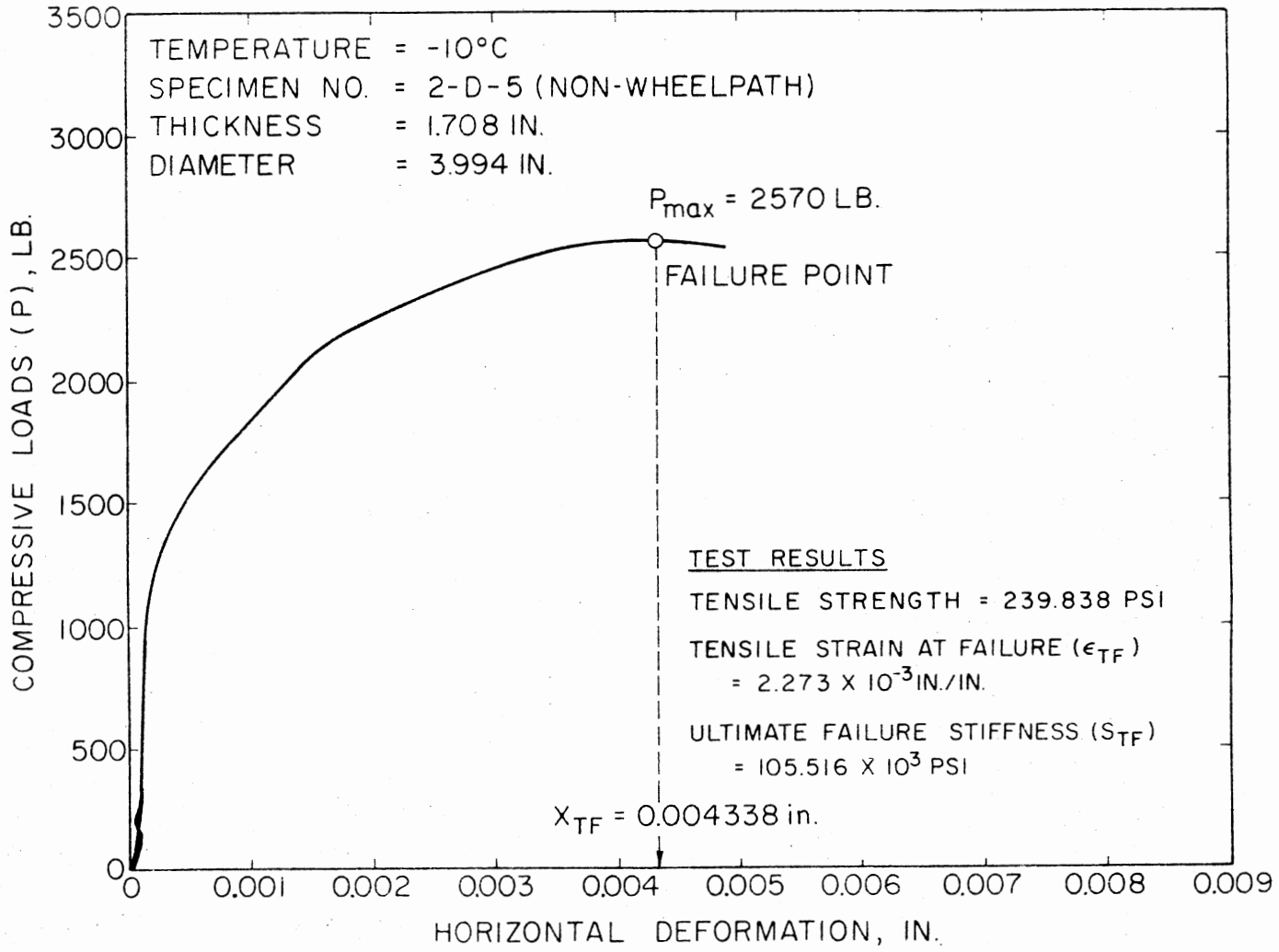

Figure 20. A Typical Load-Deformation Graph from the Indirect Tensile Splitting Test

failure (P_{max}) and the corresponding total horizontal deformation (X_{TF}) were determined. The tensile fracture stress and the total tensile strain at failure were calculated from equations 4.6 and 4.10, respectively. The ultimate stiffness was also computed as follows:

$$S_{TF} = \frac{\sigma_{TF}}{\varepsilon_{TF}} \tag{4.11}$$

where

S_{TF} = ultimate failure stiffness (psi).

σ_{TF} = tensile strength (psi).

ε_{TF} = tensile strain at failure (in./in.).

It was felt that this failure stiffness value might be a better indicator of the low temperature behavior of the material since it combines both the tensile strength and failure strain responses.

The initial apparatus for measuring the horizontal deformations employed a pair of cantilever arms with attached strain gages (Figure 21). This type of deformation transducer system was adopted from a Texas research study (69). During testing, it was found that the specimens tended to shift slightly, leaving one of the cantilever arms. To prevent this shift, it was necessary to pretension the cantilever arms so that the sides of the specimen would be in continuous contact with each of the arms during the test. It was very difficult to maintain the required pretension while measuring the relatively large horizontal deformations and, subsequently, a different measurement system was employed. Trial tests using linear variable differential transducers to measure the horizontal deformation showed that this system was easier to use and had greater sensitivity and accuracy. Even with this improved measurement

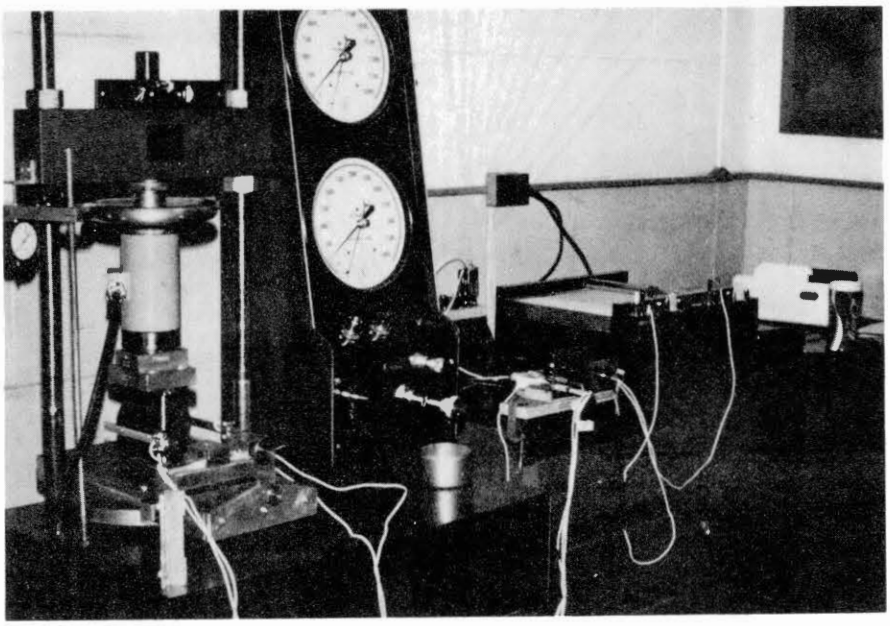

Figure 21. The Original Tensile Splitting Test Equipment

system, it was still neccessary to make slight corrections on some of the load-deformation traces. These corrections were simply extrapolations of the initial portions of the traces to eliminate the effects of seating and minor slippage of the specimen at the beginning of the test. Figure 22 illustrates the required correction on a typical trace.

Apparatus Used

The special apparatus used to determine the tensile properties of asphalt concrete specimens can be summarized as follows:

1. Loading Machine - a hydraulic universal testing machine of a 60,000 lb (27,216 kg) capacity was used to apply compressive loads at a rate of 0.06 in./min (0.152 cm/min).

2. Upper and lower adaptor plates - special aluminum plates were attached to the universal testing machine to position the loading strips and the differential transducers.

3. Loading strips - a pair of curved-face loading strips made from aluminum were attached to the upper and lower adaptor plates.

4. Aluminum angles - a pair of aluminum angles were used to position and hold the differential transducers.

5. Load cell - a load cell, type U-1 Baldwin Lime Hamilton Corporation, of 10,000 lb (4535 kg) capacity was used to measure the applied load.

6. Deformation measuring device - a pair of Trans-Tek series 350, linear variable differential transducers were used to measure horizontal deformations.

7. Direct current power supplies - three Micronta variable DC

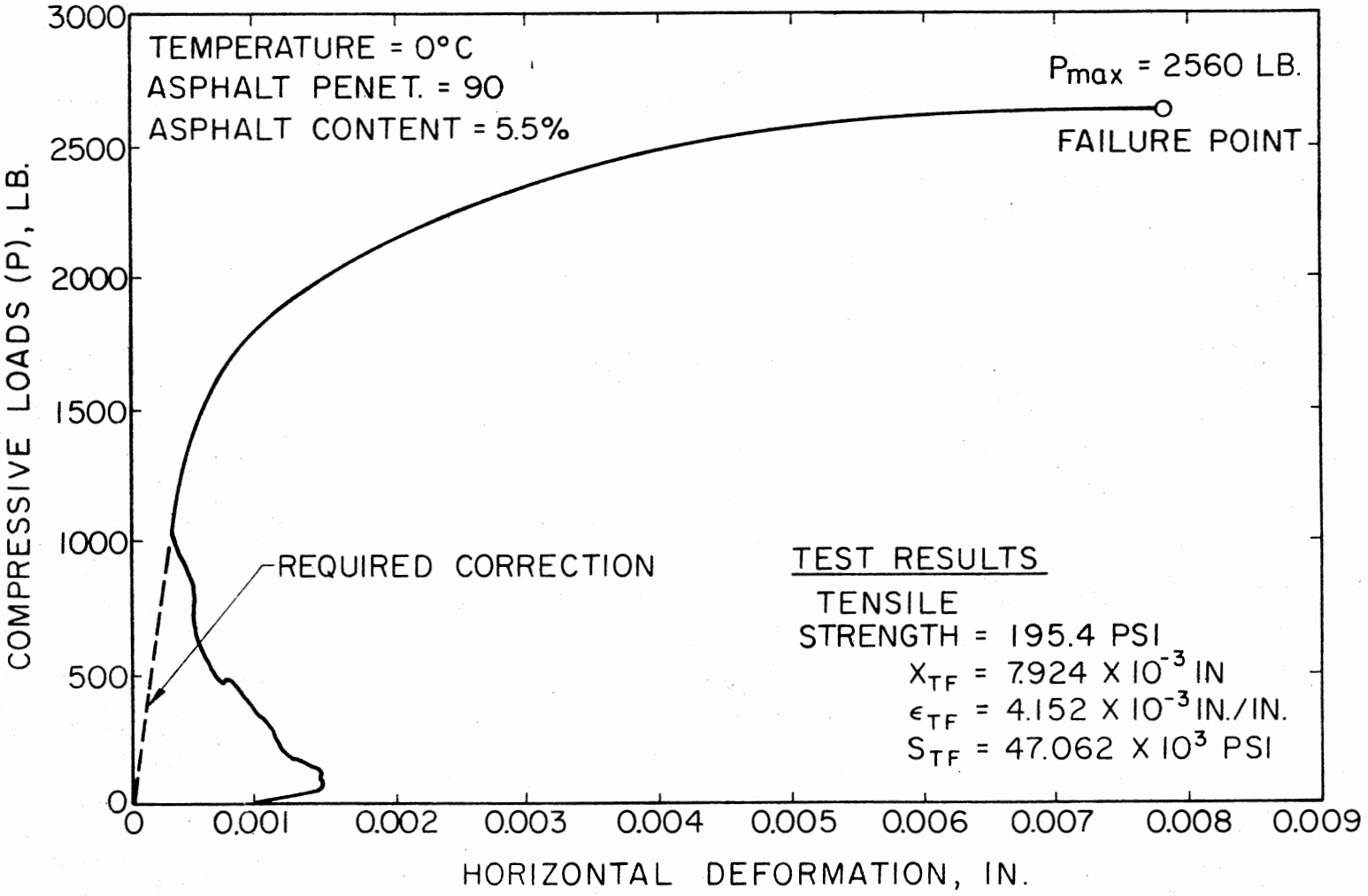

Figure 22. Required Correction of A Typical Load-Horizontal Deformation Curve

power supplies (Catalogue Number 22-126) were used to power the load cell and the differential transducers.

8. Voltage indicator - a digital voltmeter, Data Precision Model 245, was used to set the various input and output voltage requirements.

9. Recorder - a Houston Instrument, Model Omnigraphic 2000, X-Y recorder plotter was used to plot the load-deformation curves.

10. Calibration device - a simple calibration device was used along with the digital voltmeter to calibrate the differential transducers.

Figure 23 shows a detailed drawing of the tensile splitting test apparatus and Figure 24 shows the electrical installation diagram for the apparatus. The transducer calibration device is shown in Figure 25.

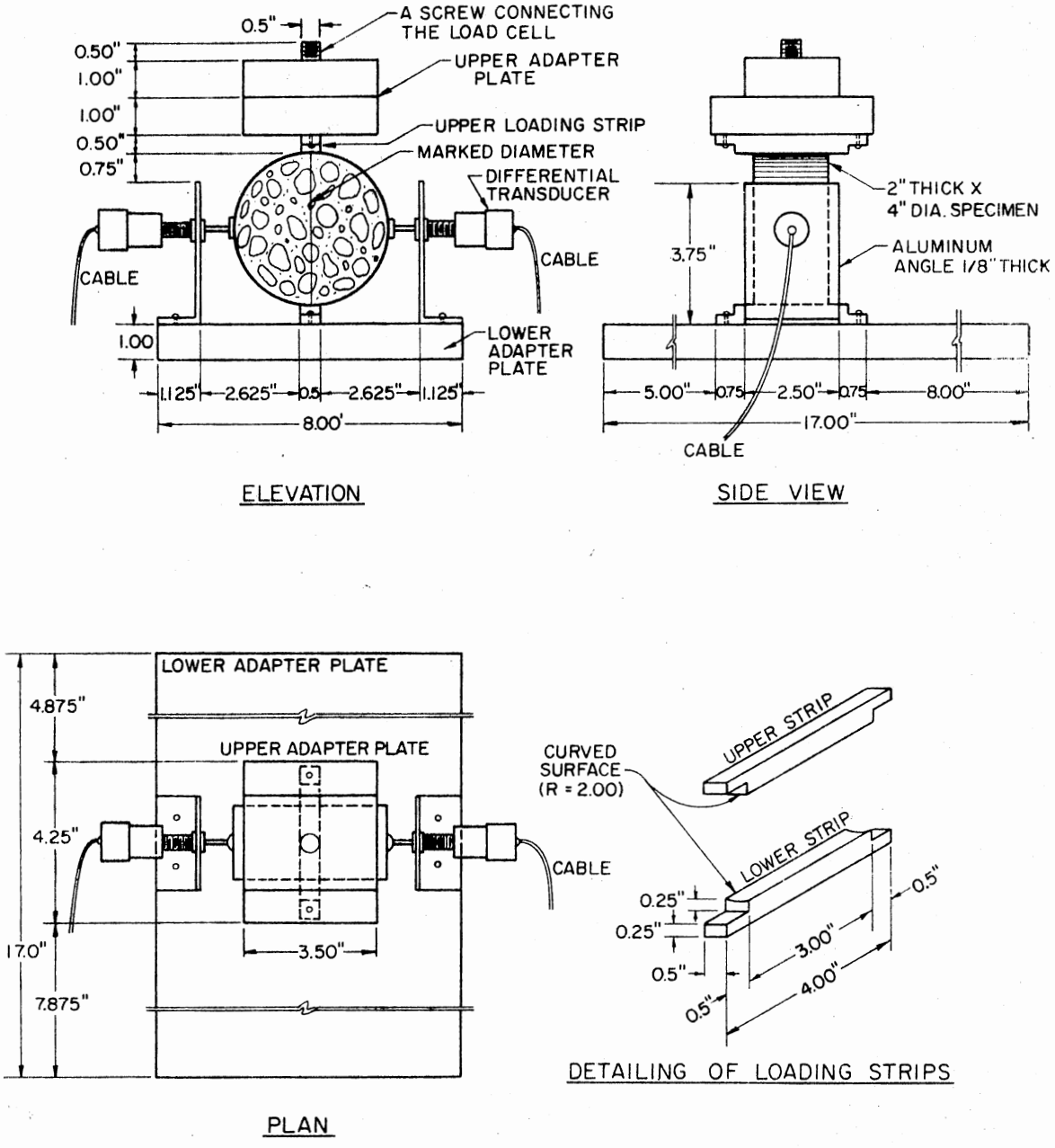

Figure 23. Detailed Drawing of the Tensile Splitting Test Apparatus

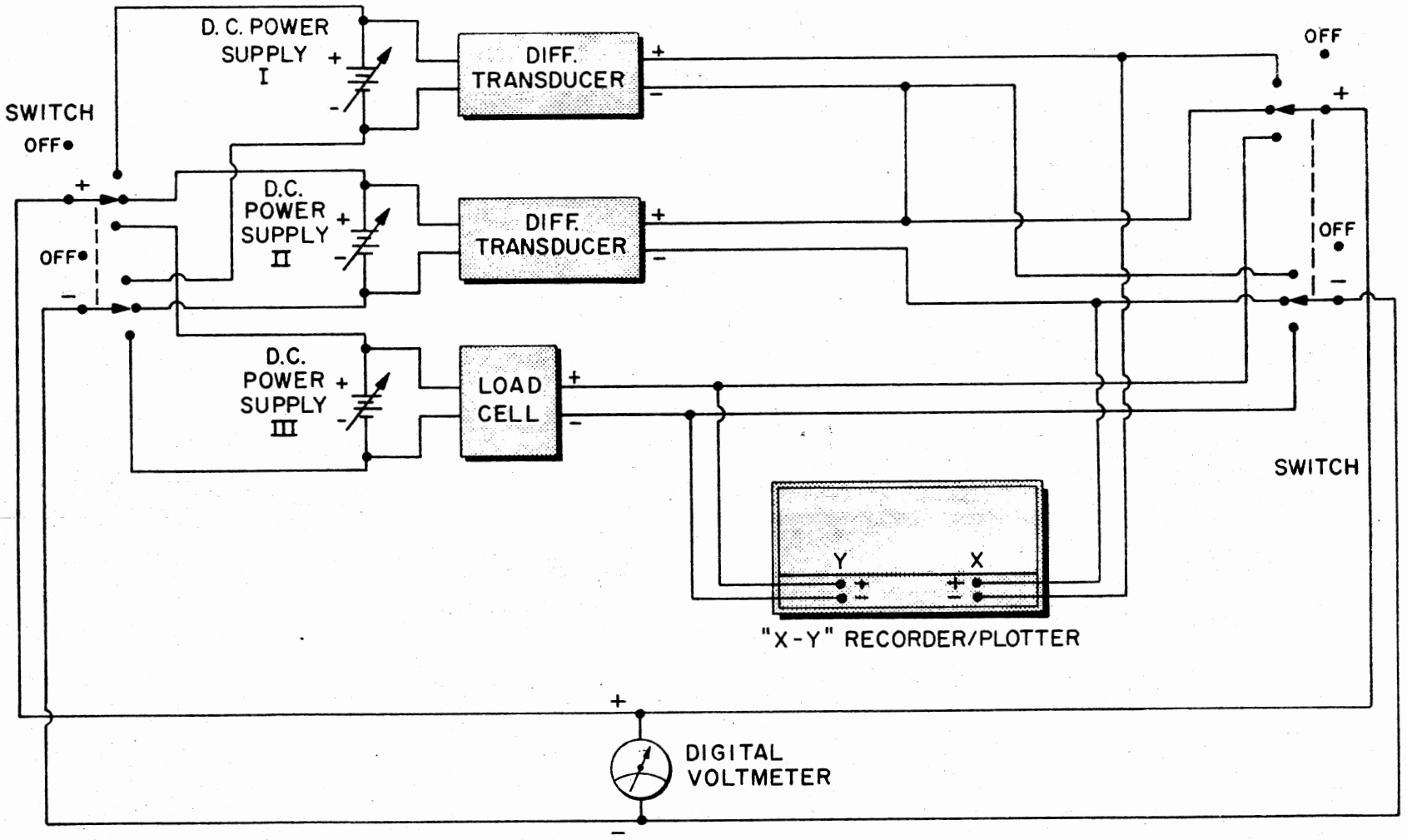

Figure 24. Electrical Installation Diagram

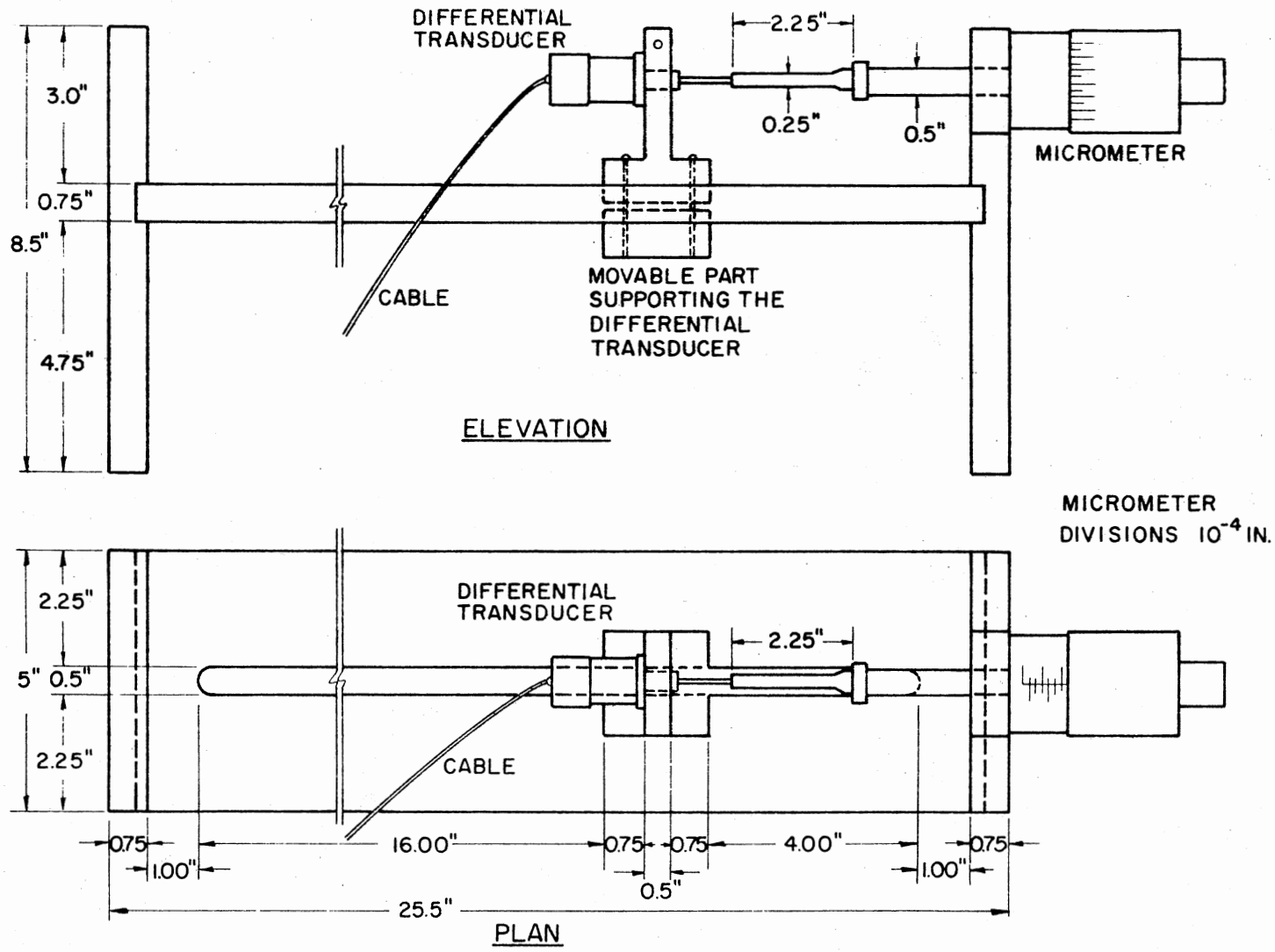

Figure 25. Calibration Device for the Differential Transducers

CHAPTER V

TEST PROCEDURES

The experimental program of this research was divided into two main phases relative to test procedures followed in surveying and core sampling at the field test sites and those employed in the laboratory to evaluate the desired properties of both field core samples and laboratory mixtures.

Field Test Procedures

Safety

The conduct of all field work on the State and Interstate highways was regulated to a great extent by the safety requirements for the research personnel. All field work was terminated whenever there was any form of bad weather conditions at the test site. No traffic control was required during the crack mapping and counting. However, research personnel wore high visibility safety vests and hats during the conduct of their work. Also, all the crack surveying work was carried out from the highway shoulders at the test sites. Special safety precautions were required during the coring operations at the test sites. One lane of the highway was kept open to traffic while the other was blocked for the core drill operations. At all the interstate test sites, appropriate warning signs were placed at least 880 yards (800 meters) in advance of the work area. This was followed by

directional signals, flagmen and finally a physical barrier to close the lane being cored to traffic. The advanced warning signs were not required on the state highway test sites and the small traffic volumes were satisfactorily controlled by directional signals and flagmen. After completing the coring operations in the first lane, directional markers and barriers were switched to permit work in the other lane. All signing, signaling, blocking and flagging were carried out by personnel provided by the Research and other respective Divisions of the Oklahoma Department of Transportation.

Crack Survey

The crack survey included mapping and counting all the cracking patterns encountered in a 500 ft length chosen for study. Two research personnel working together were required to conduct this crack surveying. The first rolled a distance measuring device as he walked along one of the shoulders while the other carried a field data sheet similar to that shown in Figure 26. Crack patterns were sketched on this sheet and classified according to type (multiple, full, half and part) as those previously indicated in Figure 2. Each of these four types and the corresponding distance measured from the starting point of the 500 ft length were recorded in the appropriate columns of the field data sheet. At the end of each survey, the total number of multiple, full and half cracks were determined so that a cracking index for the particular site could be established. At every test site, some of the relatively new cracks were inspected and suitable ones were marked with yellow paint along the highway shoulder for further study. To show the severity and extent of some particular cracks,

School of Civil Engineering
Oklahoma State University

TRANSVERSE CRACKING IN FLEXIBLE PAVEMENTS

Field Data

Date:_____ By:_____ Highway Number:_____ Highway Type:_____

Survey Direction:_____ Site Number:_____ Site Description:_____

Dist., ft.	Cracking Data		General Rating of Surface Condition	Remarks
	Pattern	Class		
0 10 20 30 40 50 60 70 80 90 100	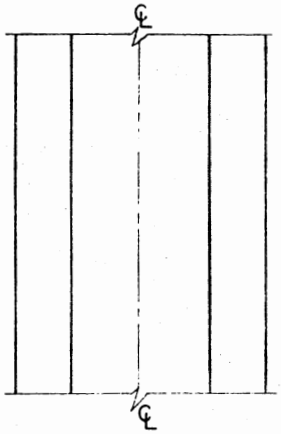			

Figure 26. Field Data Sheet for Crack Surveying and Mapping

photographs were taken and the corresponding cracks were identified in the field data sheet.

Core Drill Operations

All the core drill operations were scheduled in advance with the Research and Development Division of the Oklahoma Department of Transportaion. For the preliminary crack study, a 6.0 in. (15.24 cm) diameter core drill was used to obtain core specimens at the end and/or middle of some particular part cracks at each test site. The angular speed and the rate of penetration of the core barrel were adjusted to minimize any disturbance of the pavement layers. To obtain laboratory test specimens, a 4.0 in. (10.16 cm) diameter core drill was used to cut 18 full-thickness cores at the selected wheelpath and non-wheelpath locations. At full cracks, these core locations were marked on the pavement surface about 8.0 in. (20.32 cm) away from the crack, as previously indicated in Figure 13. After coring, each specimen was immediately wrapped in a plastic bag, appropriately identified and carefully stored for transporting to the laboratory.

Laboratory Test Procedures

Cutting Field Core Specimens

The pavement specimens used in the tensile splitting tests were obtained by cutting the surface layer, approximately 2.0 in. (5.08 cm) thick, from the 4.0 in. (10.16 cm) diameter cores with a diamond edged concrete saw. The cut face of these specimens was trimmed to remove any surface irregularities. These specimens were then dried and stored prior to testing.

Preparation of Laboratory Specimens

Laboratory specimens used in this study were prepared from locally available materials. The aggregates consisted of 1/2 in. (1.27 cm) top size crushed limestone, limestone screenings and coarse and fine river sands. The source of the limestone aggregates was the Quapaw Company's quarry in Drumwright while the coarse and fine river sands were obtained from borrow pits in Kay and Payne counties, respectively. The sieve analysis, specific gravity and water absorption test results of these aggregates are given in Appendix B. These aggregates were combined to meet the gradation limits stipulated by the Oklahoma Transportation Department - Type C surface course specifications. The combined grading and the specification limits are shown in Figure 42 in Appendix B. Three asphalt cements having 91, 124, and 160 penetrations were used in this study. The 124 and 160 penetration grades were produced by blending a 85-100 penetration asphalt cement with a non-volatile oil flux. Both the asphalt cement and flux were secured from the Allied Materials Corporation in Stroud. The rheological properties of the three asphalt cement binders are shown in Table XVII in Appendix B.

The laboratory test specimens were prepared by mixing the combined aggregate blend with 4.5, 5.0 and 5.5 percent asphalt by total weight. The Hveem-Gyratory method of compaction (70) was employed to compact the test specimens and Hveem stability tests were performed to determine the optimum asphalt content of each mixture. A summary of these test results is given in Appendix B.

Bulk Specific Gravity

The bulk specific gravity of the laboratory test specimens was determined by weighing a specimen in air, weighing it in water, and computing its bulk specific gravity. Previous research conducted at Oklahoma State University (60) concluded that the bulk specific gravity values of field core samples were appreciably affected by water absorption. Based on this finding, the bulk specific gravity of field core specimens were determined with the samples coated with paraffin in compliance with ASTM method of test D-1188 (37). Tests were performed on at least three samples and an average value was computed.

Tensile Splitting Test

1. Thickness and Diameter Measurements: The thickness of each test specimen was measured at five points, at the center and at the ends of two arbitrarily perpendicular diameters, and the average value was recorded as the specimen thickness. The diameter of the specimen was also determined as the average value of three measurements taken at approximately equal intervals along the specimen thickness. All the thickness and diameter measurements were made to the nearest 0.001 in. (0.0254 mm). In order to easily position the test specimen on the loading strips, chalk was used to mark a diametral loading line on one face of the specimen.

2. Cooling: A Lab-Line low-temperature cabinet or freezer was used to cool the test specimens to the desired temperature. A remote sensing temperature monitoring device (Scanning Tele-Therometer,

YSI Model 47) was used to detect the temperature of the freezing cabinet, the test room, and the test specimens. To monitor the temperature of the test specimens, four thermisters of the monitoring device were embedded at various points inside a dummy specimen similar in size and composition to the actual test specimens.

An approximate time of four minutes was required to take a test specimen from the freezing cabinet, position it, and run the test. A pilot study employing various low temperatures was performed to determine the rate of temperature increase at the different points of the dummy specimen. The results of this study indicated that an average rate of temperature increase of 1^{o} C/min could be assumed for the selected low temperature range of the test, i.e., 0^{o} to -10^{o}C. Therefore, the initial cooling temperature of specimens tested at this range was adjusted to four degrees less than the corresponding actual test temperature.

Test specimens were placed together with the dummy specimen in the freezing cabinet and the desired temperature was set on the cabinet controls. The temperature monitoring device was used to frequently check the temperature inside the cabinet and at the different sensor locations of the dummy specimen. The cabinet temperature was regulated, when necessary, and approximately four hours were required to achieve the desired testing temperature.

3. Testing: After making the necessary electrical connections on the load cell, the transducers, and the recorders, the power supplies were set to input the previously calibrated voltages of the load cell and the differential transducers. The appropriate horizontal and vertical scales of the X-Y recorder plotter were chosen and a

10.0 in. (25.4 cm) by 15.0 in. (38.1 cm) sheet of graph paper was attached to the recorder.

The universal testing machine was warmed up for approximately 30 minutes before adjusting the deformation rate. By using a dial gage attached to the lower platen of the loading machine and a stop watch, the rate of deformation was regulated till a rate of 0.06 in./min (0.152 cm/min) was achieved.

After starting a stop watch, the specimen was removed from the freezer and carefully centered on the lower loading stip of the test apparatus. The upper loading head was slowly moved down until light contact was made with the test specimen. Position of the specimen was checked to make sure that the marked loading line was in a vertical plane passing through the center of the loading strips. The starting point of the load-deformation trace was marked by the recorder pen on the graph paper. When the elapsed time reached four minutes, load was applied to the test specimen until failure. The point at which the slope of the load-deformation trace reached zero was marked and the maximum load causing failure was recorded on the graph paper.

Rice's Specific Gravity

The maximum specific gravity of the test specimen mixtures was determined using the ASTM method of test D-2041 (37). This test procedure was slightly modified so available equipment in the Oklahoma State University Civil Engineering Asphalt Laboratory could be used. These modifications were listed in a previous research study (60).

Asphalt Extraction

Asphalt binders were extracted from pavement core samples in accordance with ASTM method of test D-2172 (37). Before processing, an asphalt content of six percent by total weight was assumed and the approximate weight of pavement material required to secure about 200 gm of recovered asphalt cement was calculated and used in the extraction. This quantity of asphalt was sufficient for at least four penetration samples of the asphalt binders at each test site. Test specimens were randomly chosen from the field cores so that representative asphalt cement samples would be obtained.

Asphalt Recovery

Asphalt was recovered from the extraction solution by a slightly modified Abson test method. Previous tests performed at the Asphalt Laboratory of the Oklahoma Department of Transportation using the ASTM method of test D-1856 (37) indicated that asphalt hardening occurred during the course of the recovery procedure. This asphalt hardening was considered to be primarily due to the combined effect of high temperature and the time during which this temperature was maintained (160^{o}C and 15 minutes, respectively). To investigate this effect, trials were made employing three different penetration grades of asphalt cement (40-50, 85-100 and 120-150). The original penetration of each asphalt cement was determined in accordance with ASTM method of test D-5. Each asphalt cement was mixed with a sufficient quantity of a solvent (1,1,1-trichloroethane) so a solution similar to that obtained from the extraction test could be made. Abson recovery

tests were performed on the prepared solutions and all possible combinations of three temperature levels (150, 155 and 160^{o}C) and three time periods (5, 10 and 15 minutes) were tried. After each test, the penetration of the recovered asphalt was determined and compared with that of the original asphalt.

The results of this investigation substantiated the previous findings of the Oklahoma Department of Transportation research personnel. The amount of hardening was found to be a function of both the test temperature and time. Also, the observed amount of hardening of the relatively soft asphalt grades was greater than that of the harder asphalts. This finding can be attributed to the higher content of resins and oils of the soft asphalt cement as compared to those of the harder grades. For the expected penetration values of field asphalts, linear interpolation of the test results indicated that hardening of the field asphalts during the test procedure could be either eliminated or minimized by reducing the temperature to about 155^{o}C and the time to 6 minutes.

An International (Size 2, Model V) centrifuge was used to process the extraction solutions prior to the asphalt recovery procedure. The angular speed of this centrifuge was regulated to produce the centrifugal force specified in the ASTM standard test.

Asphalt Properties

The asphalt cements recovered from the test sites and those used in the laboratory investigation were evaluated in terms of their rheological properties. The following tests were performed at the Oklahoma Department of Transportation Asphalt Laboratory:

1. Penetration test, ASTM D-5.
2. Kinematic viscosity test, ASTM D-2170.
3. Absolute viscosity test, ASTM D-2171.

The softening point of the asphalt cements was determined at the Oklahoma State University Civil Engineering Asphalt Laboratory by the ring-and-ball procedure conforming to ASTM method of test D-36.

CHAPTER VI

TEST RESULTS AND DISCUSSION

Field Core Samples

Tensile Properties at Low Temperatures

The tensile splitting test results (Appendix C) were used as input data for a statistical analysis of variance. Tests for evidence of real differences in the observed values and an estimation of the magnitude of such differences were conducted using the Statistical Analysis System (SAS) computer program (16). The results of these tests indicated the Observed Significance Level and acceptance or rejection of the null-hypothesis (no differences) was based on a reasonable significance level. For this study, a value of 0.05 was considered as the significance criterion for the rejection or acceptance of the hypothesis of no differences. The results of this analysis and of the correlation studies with the observed degrees of cracking (Appendix A) are discussed for the three tensile properties investigated.

Tensile Strength: The average tensile strength values are given in Table II and illustrated in Figure 27. Analysis of variance of all test results indicated a strong evidence of location (wheelpath and non-wheelpath) differences in the tensile strength values and the observed significance level was 0.0014. Figure 27 shows that the

TABLE II

AVERAGE TENSILE STRENGTH OF FIELD CORE SPECIMENS

Site No.	Average Tensile Strength (σ_{TF}), psi					
	Wheelpath			Non-Wheelpath		
	-10°C	-5°C	0°C	-10°C	-5°C	0°C
1	346.493	262.400	247.659	336.119	239.109	223.114
2	307.558	266.903	233.484	252.685	247.629	215.526
3	344.593	339.630	217.713	340.220	308.527	227.333
4	266.994	252.431	252.263	266.432	235.613	218.533
5	366.904	347.032	323.727	385.208	328.192	299.024
6	393.775	338.680	290.535	418.583	329.180	251.143
7	406.310	286.475	248.348	345.847	277.801	272.088
8	412.611	353.420	305.426	366.612	357.580	304.768
9	355.571	332.091	230.342	384.394	259.606	266.930

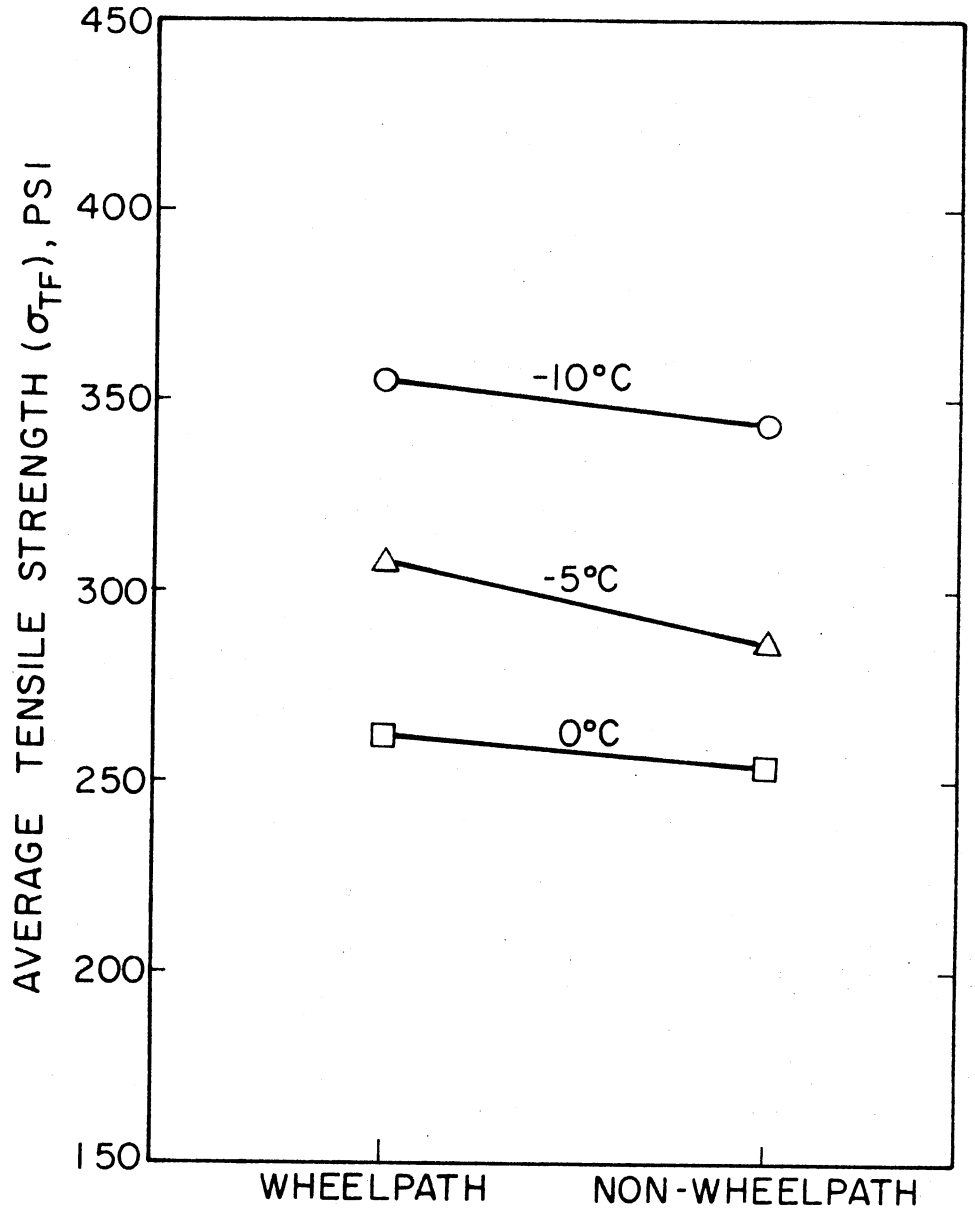

Figure 27. Average Tensile Strength of Wheelpath and Non-Wheelpath Specimens at Various Low Temperatures

tensile strength of wheelpath specimens were considerably greater than those of the non-wheelpath specimens. The high tensile strengths associated with wheelpath specimens can be attributed to the relatively high pavement densities developed under traffic wheel loads.

Test temperature had a very significant effect on the tensile strength values. Average tensile strengths at $-10^{o}C$ were noticeably higher than those at -5^{o} and $0^{o}C$, respectively. The observed significance level was 0.0001. These results indicated the general behavior of the asphalt concrete mixtures at low temperatures, i.e., as temperature decreased, the mixture became increasingly rigid, lost some of its plasticity and behaved in an elastic manner. Consequently, an increase in the average tensile stress at failure could be expected.

The analysis of variance showed that the greater variation in the tensile stength values was attributed to difference in properties of the test sites (blocks) and the observed significance level was 0.0001. In general, higher tensile strengths were observed for the interstate sites (Sites 5 to 9). This may indicate the importance of the quality and adequacy of pavement design and construction procedures on the service behavior at low temperatures.

A correlation study was made to investigate the general trend of the tensile strength-cracking index relationship. To minimize the effect of variation in material properties, this correlation study was performed for wheelpath and non-wheelpath specimens separately. Data was fed into a Hewlett-Packard Calculator Plotter (Model 9862 A) and the coefficients of correlation and determination (r and R^2) were computed for the first and second degree polynominals, respectively, by the corresponding SAS computer program. The regression lines, correlation coefficients (r) and corresponding observed significance levels (α) are illustrated in

Figures 28 and 29 for wheelpath and non-wheelpath specimens, respectively.

In general, test sites with a high degree of cracking showed lower tensile strength values. However, a considerable scattering of tensile strength values was observed. A significant part of the scatter involved is probably due to the natural non-homogenity of the materials which, in turn, reduced the observed correlation coefficients.

The results of this analysis indicate that pavement surface mixtures with high tensile strengths will generally be more resistant to fracture at low temperatures. However, tensile strength should not be the only variable considered since the pavement can crack due to excessive tensile strains.

Tensile Strain at Failure: Table III and Figure 30 shows the average values of tensile strain at failure for wheelpath and non-wheelpath specimens. As can be seen in Figure 30, tensile strains of wheelpath specimens were considerably higher than those of the non-wheelpath specimens. Analysis of variance of test results showed that the observed significance level associated with location differences was 0.0042. With the exception of the average tensile strain value of wheelpath specimens at $-10^{o}C$, average tensile strain at failure significantly decreased as temperature increased. The observed significance level was 0.034. This substantiated the effect of service temperature on the behavior of the asphalt concrete mixtures. As discussed earlier, lower tensile failure strains at relatively low temperatures can be related to the elastic rather than the viscoelastic response of the asphalt mixture. No significant interaction was found between temperature and location ($\hat{\alpha} = 0.6$).

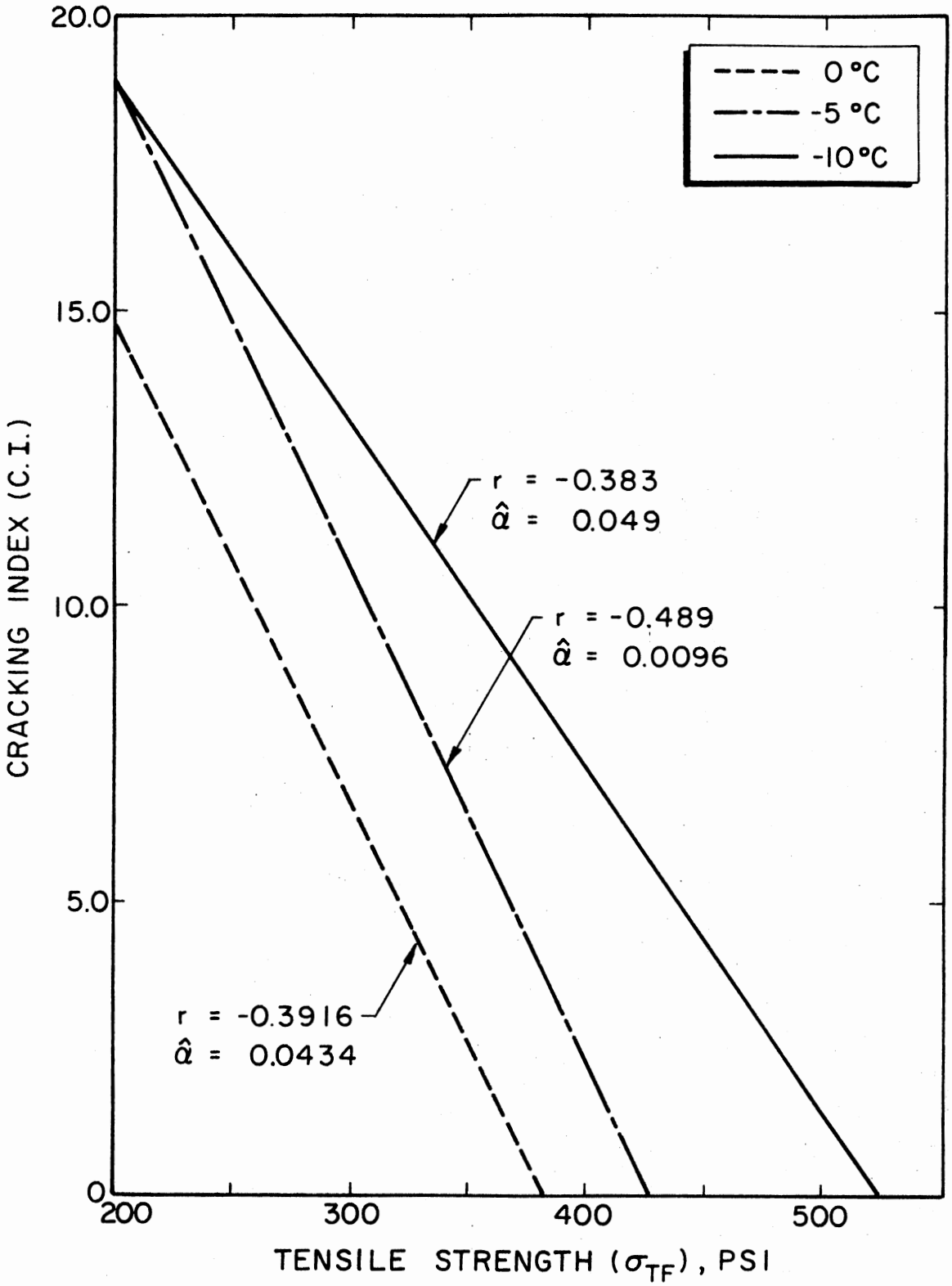

Figure 28. Relationship Between Tensile Strength of Wheelpath Specimens and Cracking Index

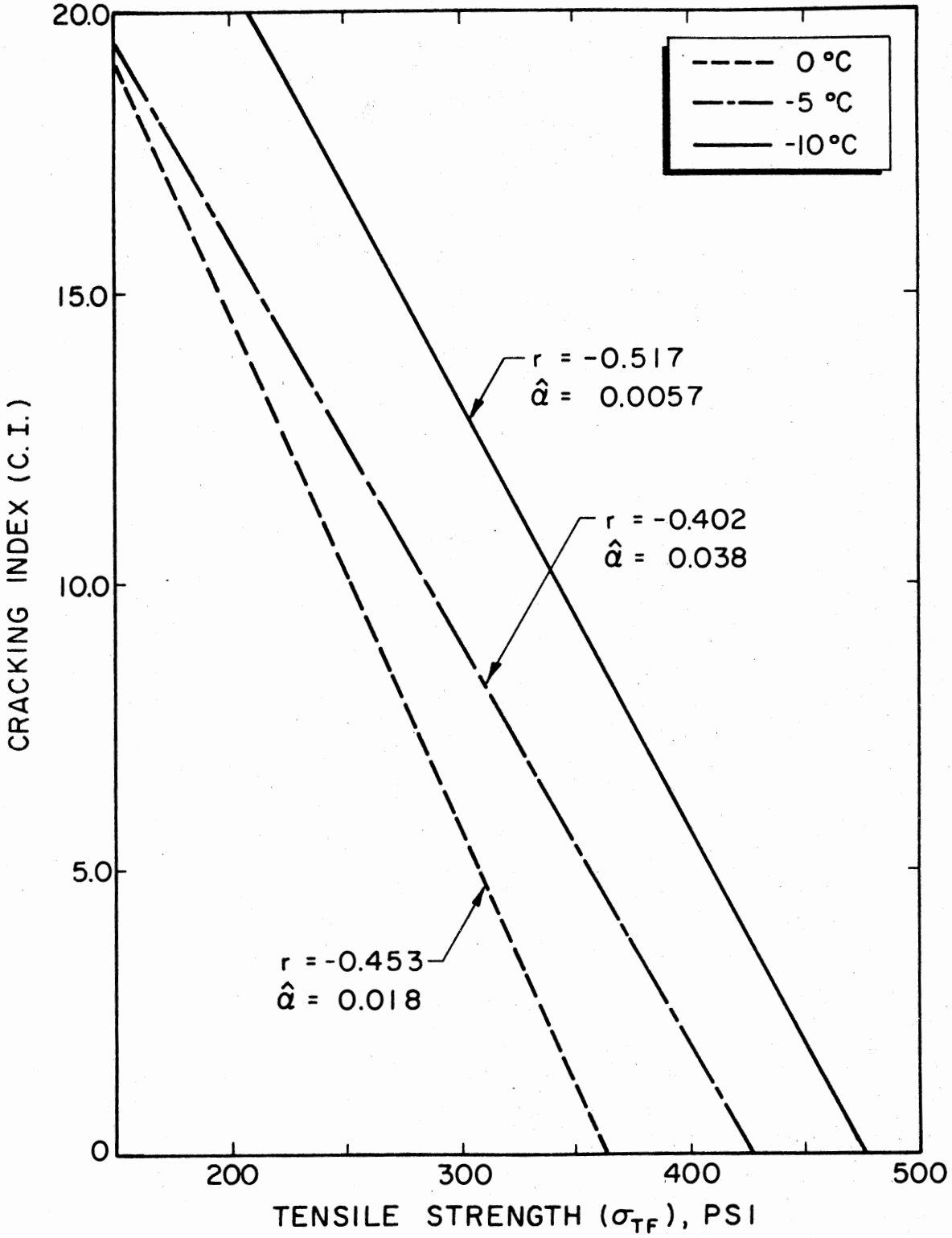

Figure 29. Relationship Between Tensile Strength of Non-Wheelpath Specimens and Cracking Index

TABLE III

AVERAGE TENSILE STRAIN AT FAILURE OF FIELD CORE SPECIMENS

Site No.	Average Tensile Strain At Failure (ε_{TF}), 10^{-3} in./in.					
	Wheelpath			Non-Wheelpath		
	-10° C	-5° C	0°C	-10° C	-5° C	0°C
1	3.014	0.934	2.671	2.287	1.674	1.718
2	2.573	1.357	2.219	1.897	1.445	1.646
3	3.215	2.109	2.236	1.765	1.561	2.066
4	0.934	0.969	1.474	0.467	0.872	0.744
5	3.947	4.934	5.542	3.711	5.101	5.348
6	0.930	1.683	2.288	0.564	1.740	1.758
7	1.683	2.961	2.707	1.903	2.454	2.594
8	5.498	4.965	6.393	4.113	3.933	6.617
9	4.228	4.780	3.558	3.947	3.871	4.728

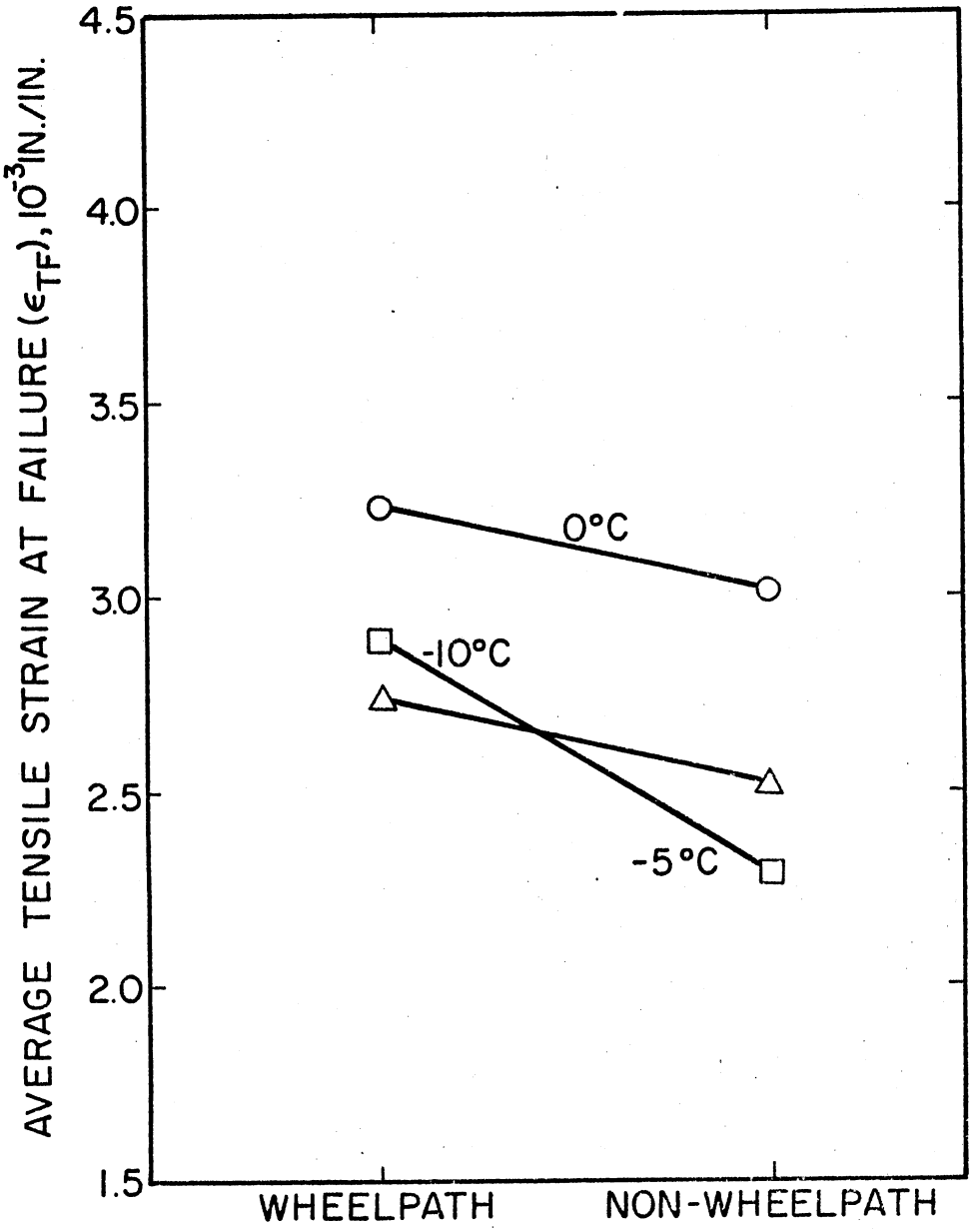

Figure 30. Average Tensile Strain at Failure of Wheelpath and Non-Wheelpath Specimens at Various Low Temperatures

Again, tensile strains at failure significantly differed between test sites ($\hat{\alpha}$ = 0.0001). It is interesting to note that, generally, a strong relation was observed between the tensile strength and strain at failure. For instance, Site 9, with a cracking index of zero, exhibited the highest average tensile strength and strain at failure. Also, Site 4, with a cracking index of 24.5, showed the lowest average tensile strength and strain values.

Results of the correlation analysis indicated a strong relationship between the tensile strains at failure and the observed degree of cracking (Figures 31 and 32). The coefficients of determination associated with this relation were markedly higher than those for the tensile strength values. The occurrence of transverse cracking was found to increase as the tensile failure strain decreased. This suggests that the resistance to cracking at any low temperature may be a function of the strain capability of the asphalt concrete mixture at this temperature. It also appears that a permissible or a "standard" failure strain for a given geographic region could be established by further testing. Such a value could be used in future mix design procedures in which asphalt viscosity, asphalt content and/or aggregate gradation are modified to meet the failure-strain design criteria.

Ultimate Failure Stiffness: Table IV and Figure 33 show the average failure stiffness values for the various test sites. The analysis of variance did not show evidence of location differences in the failure stiffness values ($\hat{\alpha}$ = 0.1183). However, a strong evidence of temperature differences was indicated ($\hat{\alpha}$ = 0.005). In general,

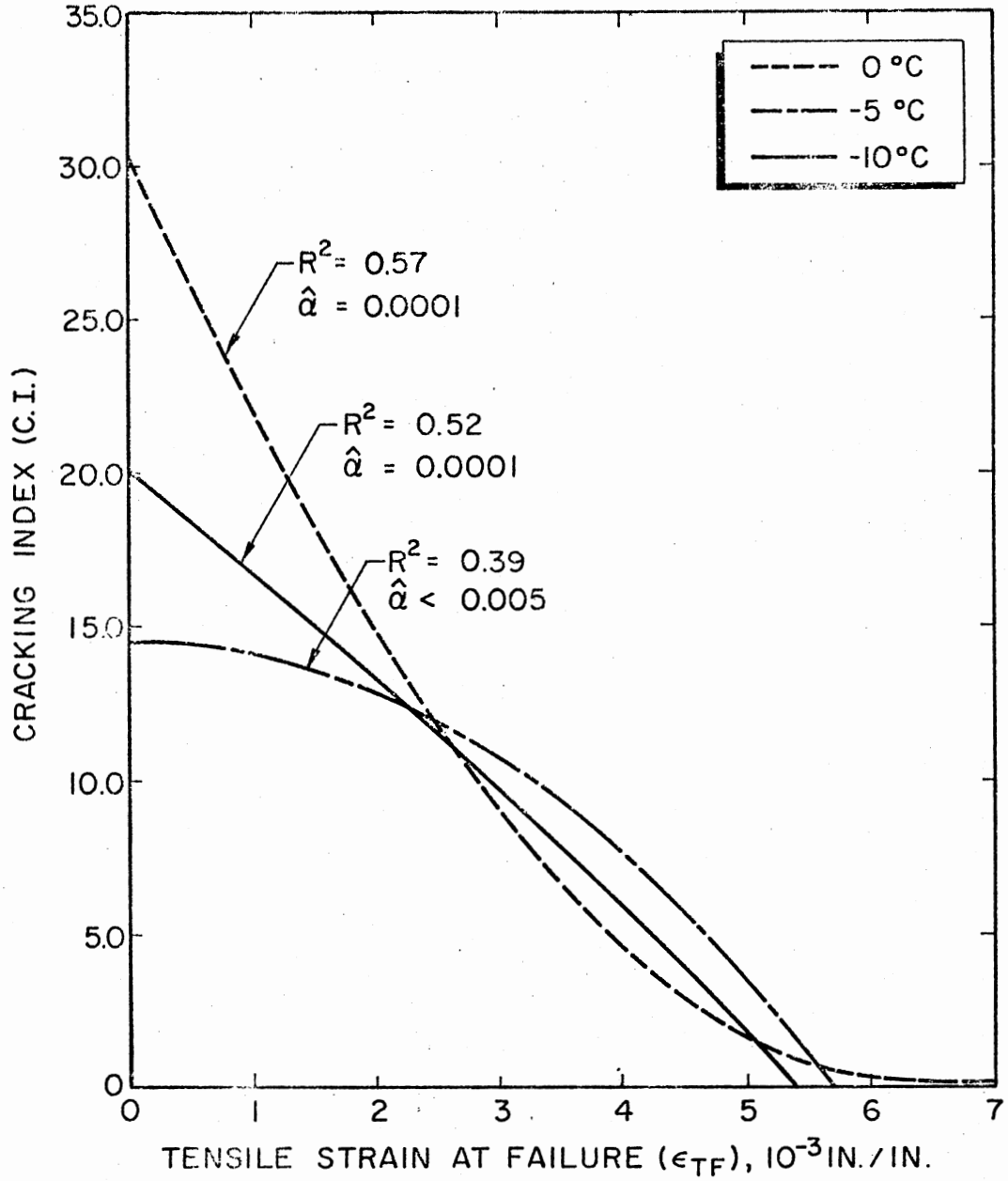

Figure 31. Relationship Between Tensile Failure Strain of Wheelpath Specimens and Cracking Index

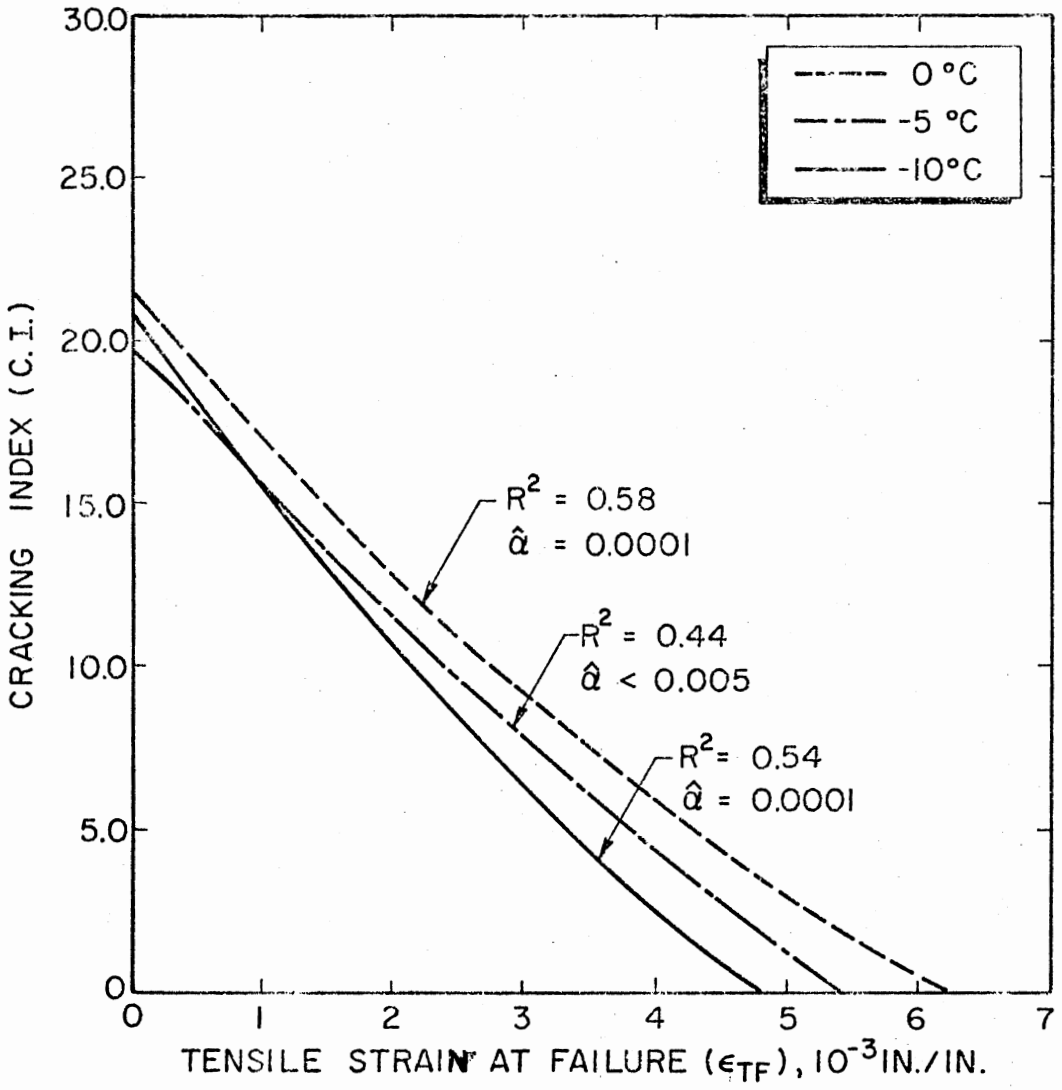

Figure 32. Relationship Between Tensile Failure Strain of Non-Wheelpath Specimens and Cracking Index

TABLE IV

AVERAGE ULTIMATE FAILURE STIFFNESS OF FIELD CORE SPECIMENS

Site No.	Average Ultimate Failure Stiffness (S_{TF}), 10^3 psi					
	Wheelpath			Non-Wheelpath		
	-10°C	-5°C	0°C	-10°C	-5°C	0°C
1	117.434	324.441	94.25	149.479	152.384	131.879
2	123.057	212.991	111.721	141.142	190.511	140.622
3	107.408	193.038	100.947	208.728	231.690	115.209
4	229.236	322.280	193.252	322.280	487.935	294.129
5	81.242	70.672	59.150	70.672	64.651	55.981
6	474.945	327.221	131.938	745.495	276.461	142.975
7	305.623	100.072	96.364	251.124	120.022	105.582
8	76.064	74.925	48.127	94.551	92.319	46.135
9	85.988	69.811	64.657	98.485	68.459	56.553

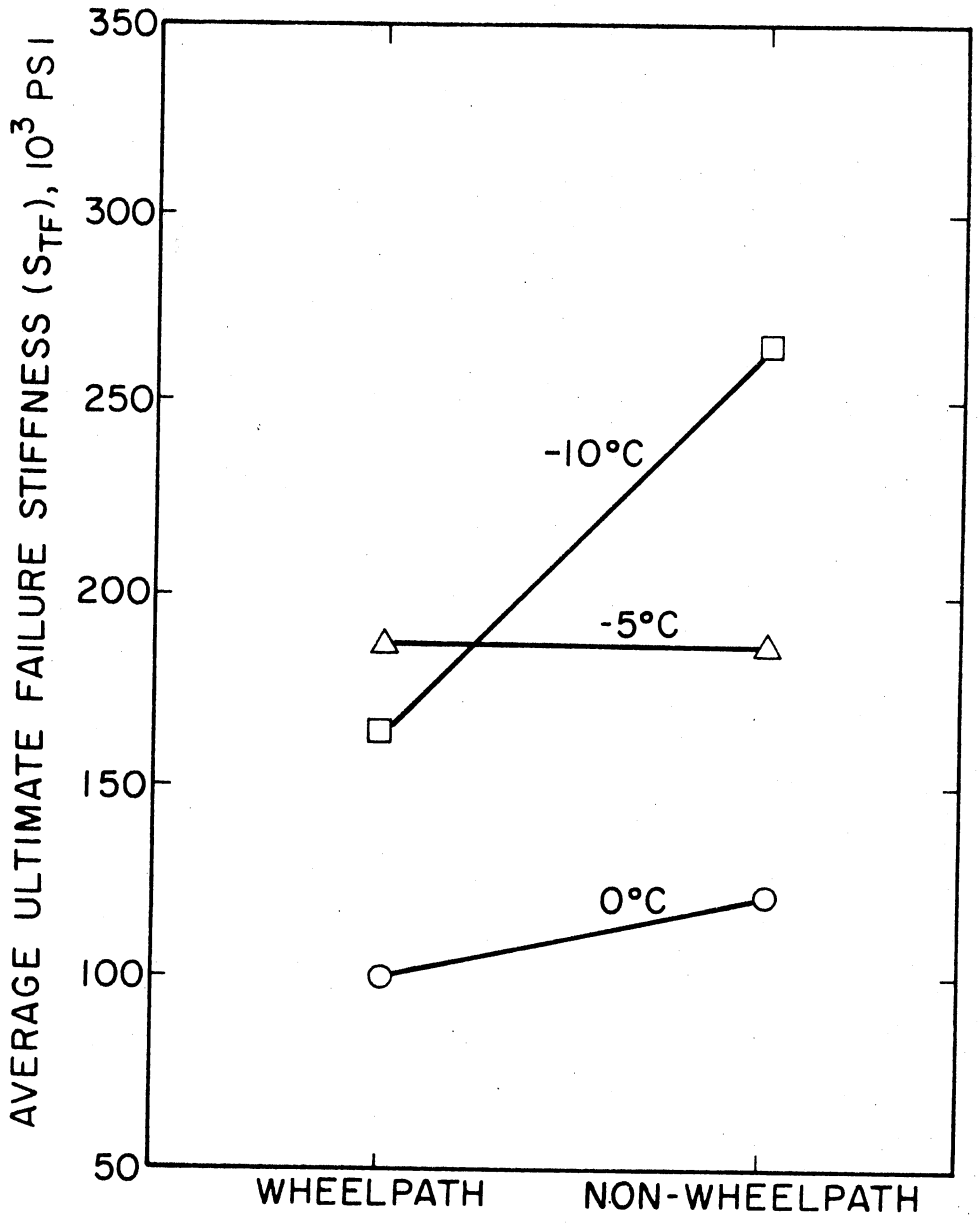

Figure 33. Average Ultimate Failure Stiffness of Wheelpath and Non-Wheelpath Specimens at Various Low Temperatures

higher average failure stiffness values were observed at lower temperatures. These results emphasized the earlier findings and indicated that the test sites were significantly different with respect to their ultimate failure stiffness responses.

Results of the correlation analysis are shown in Figure 34. The degree of cracking or cracking index was proportional to the ultimate failure stiffness at all test temperatures and test sites with a high degree of cracking generally exhibited the higher failure stiffness values. However, it should be noted that the determined correlation coefficients were relatively small. The best correlation between test results and degree of cracking was that of $0^{o}C$.

Stiffness Moduli of Recovered Asphalt Cements and Asphalt Mixtures

McLeod's method (23) was employed to calculate the stiffness moduli of recovered asphalt cements. At first, it was felt that a minimum service temperature of $-10^{o}C$ could be assumed for the stiffness calculations. This temperature was chosen in order to study the relationship between the calculated stiffness values and the tensile properties of the mixtures at the same temperature. However, a study of the climatological data (71) over a 73-year period revealed that the lowest minimum air temperature recorded in Oklahoma was $-17^{o}F$ ($-27.22^{o}C$). Based on temperature data reported in another research study (27), the temperature at a pavement depth of 2 in. was about 7^{o} to 8^{o} higher than the air temperature. The temperature at a pavement depth of 2 in. was specified by McLeod to ensure that a substantial thickness of the asphalt structure was being subjected to the contraction stresses and strains developed at the critical low temperature. Consequently,

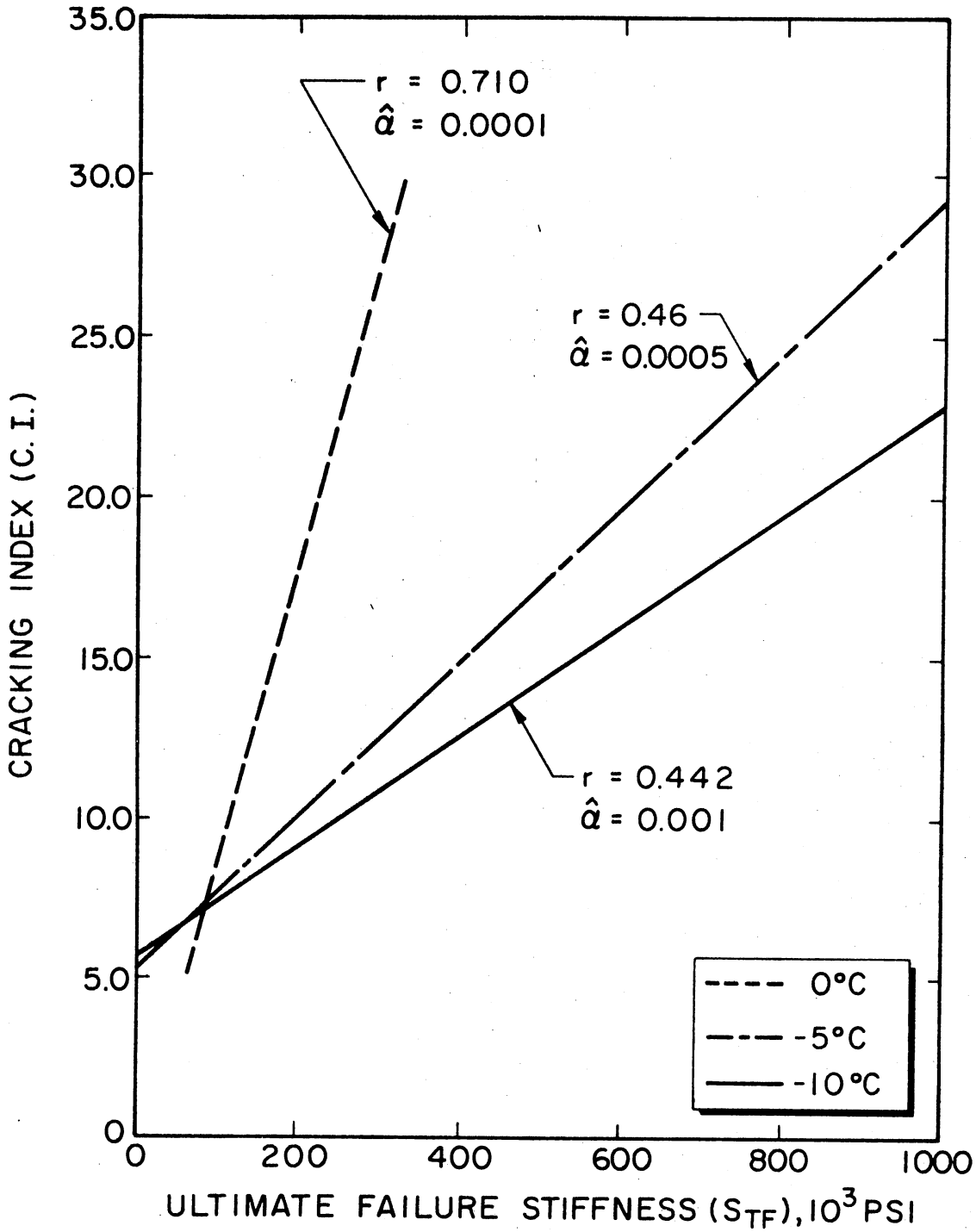

Figure 34. Relationship Between Ultimate Failure Stiffness and Cracking Index

modulus of stiffness values were calculated at a temperature of $-10^{o}F$. These values are listed in Appendix C.

The average stiffness modulus and the rheological properties of the recovered asphalt cements are given in Table V. Also, the average stiffness moduli of field asphalt mixtures are shown in Table VI along with the composition data of individual test specimens from the respective sites.

Correlation studies indicated that the low-temperature stiffness moduli of the recovered asphalt cements could be correlated with the observed degree of cracking (Figure 35). Pavement sections with a high degree of cracking were, generally, those having the stiffer asphalt cements in the surface layer. Only Site 7 showed an exception to this trend. The cracking index of this section was 20.0, but the stiffness modulus was relatively low (2916 psi). It is possible that the high cracking frequency of this site was associated with a subgrade problem or other related factors. If the data of this site is disregarded, the coefficient of determination goes up to 0.82. This is a considerably high value considering the variables that underlie this generalized relationship.

A similar relationship was found for the stiffness moduli of the field mixtures (Figure 36). However, the coefficients of determination associated with this relationship were relatively smaller than that of the previous one. This can be attributed to the variation in the other mix properties of the surfacing at the individual test sites, i.e., variation in asphalt content, specific gravity and percent density. Again, if the stiffness moduli of the Site 7 mixtures are disregarded, the coefficients of determination increase to 0.31 and 0.32 for the

TABLE V

RHEOLOGICAL PROPERTIES AND STIFFNESS MODULI OF RECOVERED ASPHALT CEMENTS

Site No.	Ring & Ball Softening Point, F°	Penetration at 77°F	Absolute Viscosity at 140°F (Poise)	Kinematic Viscosity at 275°F (C. St.)	Stiffness Modulus at -10°F, psi
1	167.72	26.00	651,700.0+	5,408.67	3738
2	160.52	32.00	65,327.0	3,063.00	3558
3	136.04	44.00	22,311.0	1,214.33	4876
4	173.04	18.00	218,360.0	2,353.33	14226
5	124.52	57.00	3,606.0	546.33	2703
6	139.55	41.50	20,630.0	1,146.50	3665
7	128.57	58.50	3,853.0	536.50	2916
8	126.32	59.33	4,058.3	639.00	2416
9	123.26	62.00	2,610.7	502.00	2688

TABLE VI

COMPOSITION AND STIFFNESS MODULI OF FIELD SPECIMENS

Site No.	Asphalt Content, %	Bulk Sp. Gravity		Per Cent Density		Volume Conc. of Agg., ($\bar{C}_v$)		Stiffness Mod., psi	
		WP*	NWP**	WP	NWP	WP	NWP	WP	NWP
1	5.619	2.368	2.327	94.845	93.992	0.8416	0.8358	451,470	415,086
2	5.920	2.325	2.327	93.803	93.211	0.8268	0.8212	329,766	306,309
3	5.605	2.414	2.380	97.236	96.989	0.8604	0.8595	703,958	696,339
4	5.884	2.177	2.172	91.854	90.871	0.8185	0.8097	737,773	664,394
5	5.475	2.471	2.405	98.827	96.178	0.8631	0.8856	516,405	453,347
6	4.867	2.412	2.396	97.031	96.047	0.8745	0.8703	793,486	721,770
7	5.834	2.411	2.376	98.368	96.467	0.8569	0.8516	480,532	436,460
8	5.508	2.466	2.420	97.873	96.630	0.8612	0.8567	463,585	425,840
9	5.573	2.420	2.393	98.257	96.710	0.8627	0.8562	510,891	454,556

* Wheelpath Specimens

** Non-Wheelpath Specimens

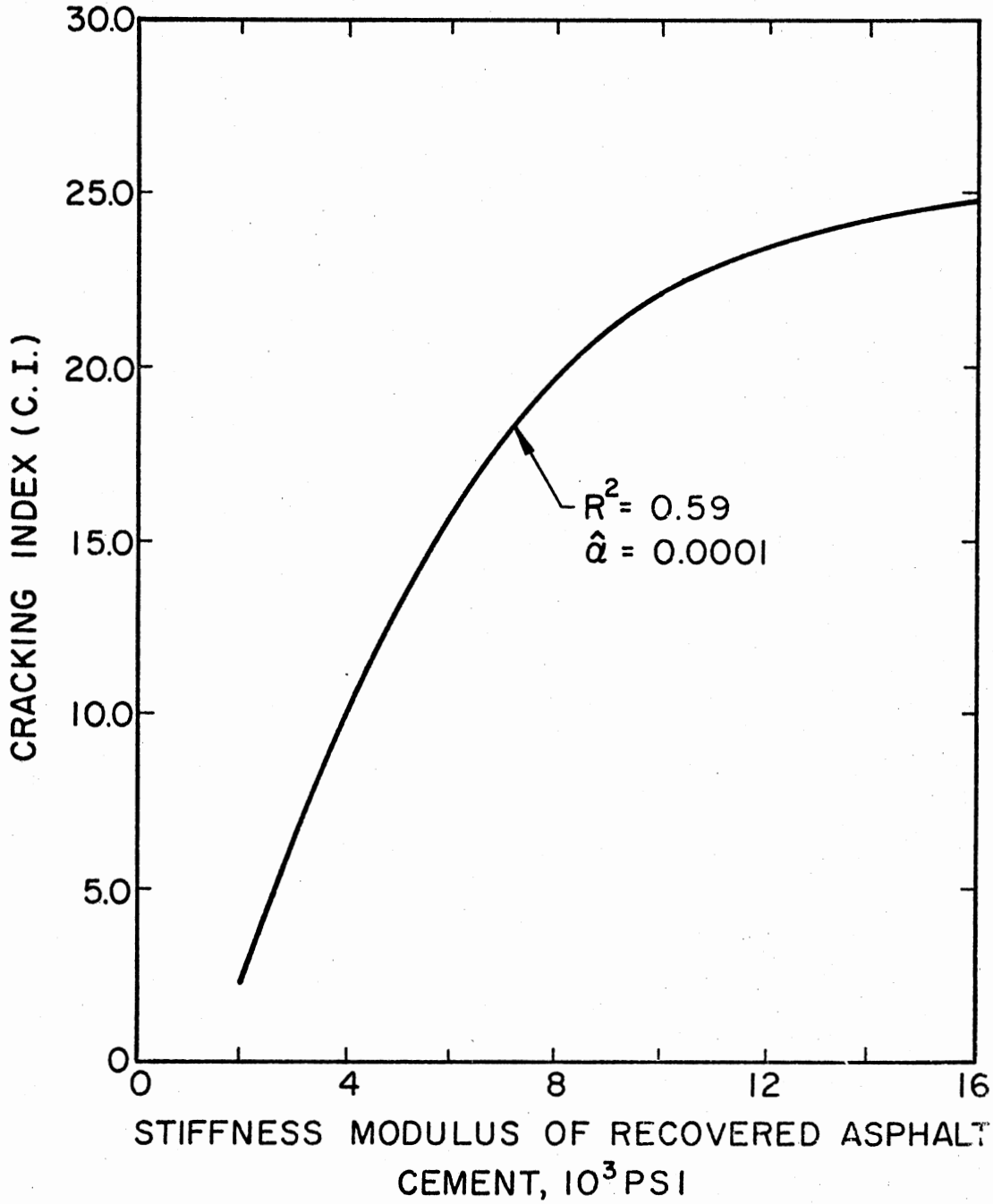

Figure 35. Relationship Between Stiffness Moduli of Recovered Asphalt Cements and Cracking Index

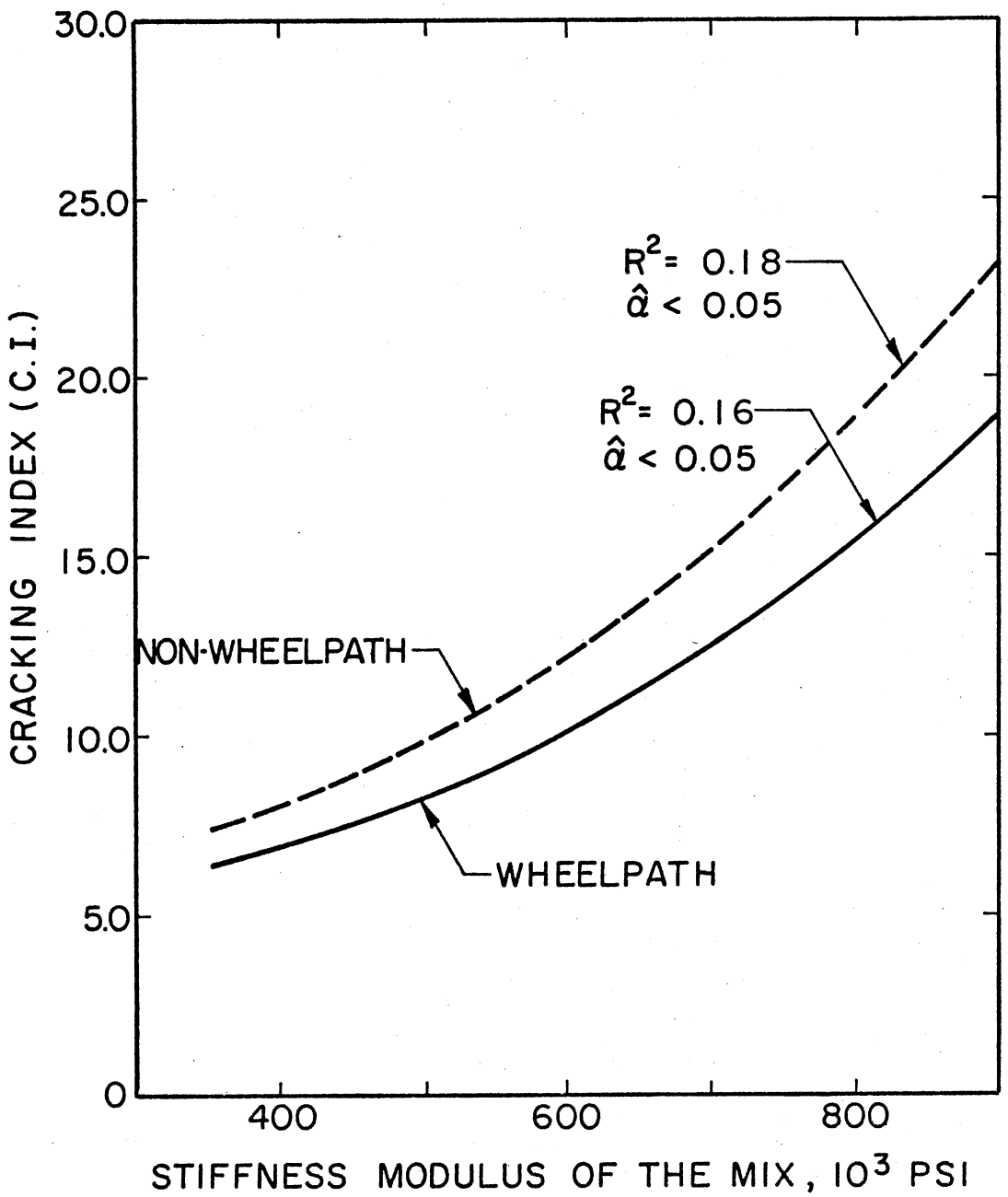

Figure 36. Relationship Between Stiffness Moduli of Field Mixtures and the Cracking Index

wheelpath and non-wheelpath stiffness moduli versus cracking index relationships, respectively.

Laboratory Mixtures

Tensile Properties at Various Temperatures

A factorial experiment was designed to investigate the effect of asphalt grade and asphalt content on the tensile properties of fresh asphalt concrete mixtures at different temperature levels. Results of the tensile splitting tests were analysed by the corresponding (SAS) computer program. The findings of this analysis are discussed in the following paragraphs under the three tensile properties studied.

Tensile Strength: The average tensile strength values are given in Table VII. Also, Figure 37 illustrates the effect of temperature, asphalt grade and asphalt content on the average tensile strength values. Based on these data, it seems that the temperature had a remarkable effect on the tensile strength or the stresses developed at failure. These stresses markedly increased as temperature decreased. Analysis of variance substantiated this finding and the observed significance level of the main temperature effect was 0.0001 indicating a strong evidence of temperature differences in the tensile strength values.

At each temperature level, higher average tensile strengths were associated with the stiffer asphalt cements. For instance, mixtures prepared with the 91-penetration asphalt cement showed the highest tensile strength values at all temperatures. Also, tensile strengths of the 124-penetration mixes were higher than those of the 160-penetration mixes at all temperatures. The observed significance level associated

TABLE VII

AVERAGE TENSILE STRENGTH OF LABORATORY SPECIMENS (psi)

Asphalt Pen. Grade	91 pen.			124 pen.			160 pen.		
Asphalt Content, %	4.5	5.0	5.5	4.5	5.0	5.5	4.5	5.0	5.5
a. Temp. = +20°C	58.433	71.833	64.433	49.467	60.867	46.933	24.139	28.889	29.001
b. Temp. = 0°C	242.467	239.190	235.587	218.783	215.146	186.693	187.054	153.673	132.409
c. Temp. = -10°C	381.777	390.913	388.434	357.314	344.123	291.794	320.294	319.424	289.716

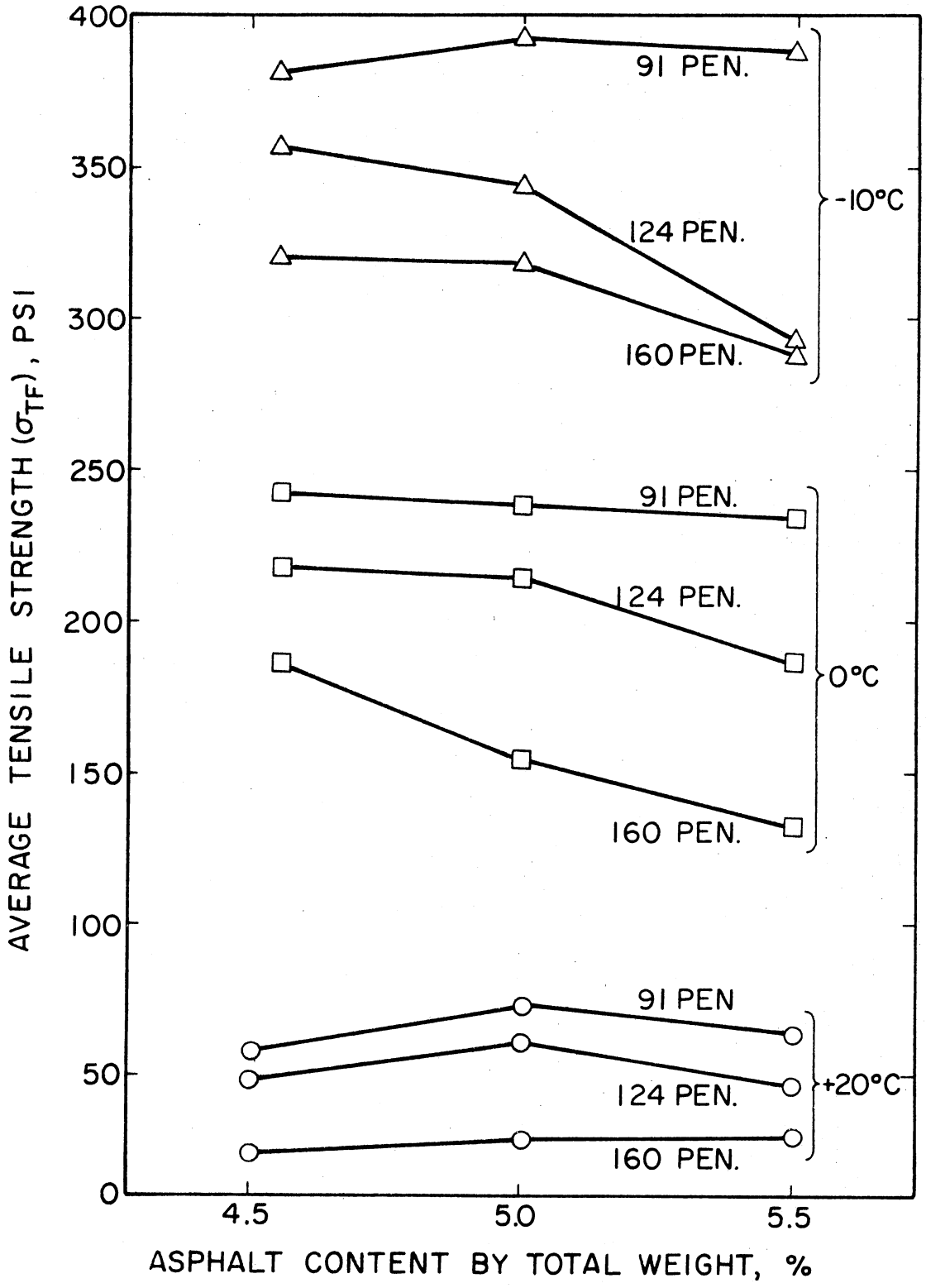

Figure 37. Average Tensile Strength Versus the Asphalt Content of the Mix

with the asphalt grade effect was 0.0001. However, it should be noted that the rate of increase in the tensile strength was dependent on the temperature, e.g., the increase in tensile strength values of the 91-penetration asphalt mixtures was noticeably higher at -10°C than that at 0° and 20°C. The analysis of variance confirmed this finding and indicated a significant interaction between the temperature and the asphalt grade factors. The observed significance level of this interaction was 0.001.

Asphalt content had a significant effect on the observed tensile strengths. The observed significance level was 0.001. However, this effect was apparently dependent on the levels of the other two factors as may be indicated in Figure 37. For instance, the maximum tensile strength values at 20°C of the 91 and 124-penetration mixture groups were achieved at 5.0 percent asphalt content, while those of the 160-penetration asphalt mixtures were attained at 5.5 percent asphalt content. With the exception of the 91-penetration asphalt mixtures at -10°C, average tensile strength values generally decreased as asphalt content increased. The amount of decrease was considerably greater at 5.5 percent asphalt content for the 124 and 160-penetration mixes than that of the 91-penetration mix. It appears that, as asphalt content increases, stiffness of the mixture decreases and relatively lower tensile stresses can be developed.

Tensile strength results generally showed that higher tensile strengths (stresses at failure) were associated with stiffer (lower penetration or higher viscosity) asphalt cements. As previously indicated, mixtures with high tensile strengths may be more resistant to deformation and cracking if they exhibit similarly high strains at

failure.

Tensile Strain at Failure: Table VIII shows the average tensile strain at failure of the different asphalt mixtures. The effects of temperature, asphalt grade and asphalt content on the average tensile failure strain are illustrated in Figure 38.

The analysis of variance indicated a strong evidence of temperature effect on the tensile strains at failure. The observed significance level was 0.0001. The average tensile strains at failure of all mixtures at 20°C were much higher than those at 0° and -10°C, respectively. This finding primarily reflected the elastic response of the asphalt mixture at relatively low temperatures. This elastic behavior would generally reduce the ability of the asphalt paving mixture to absorb the contraction strains developed at low temperatures. However, no significant differences were observed between the average tensile strains at 0° and -10°C, respectively.

The analysis of variance did not show evidence of asphalt grade differences in the tensile strain values and the observed significance level was 0.756. A significant interaction was found between the temperature and the asphalt grade effects and the observed significance level was 0.025. Apparently, this interaction affected the trend between the asphalt grade and the average tensile strains at failure, particularly at 0° and -10°C (figure 38).

Again, the effect of asphalt content on the measured tensile strain values was dependent upon the temperature. Analysis of variance indicated a strong interaction between the two effects ($\hat{\alpha} = 0.001$). Figure 38 shows that the average tensile strains at 20° and 0°C considerably increased as the asphalt content of the mixture increased from 5.0 to

TABLE VIII

AVERAGE TENSILE STRAIN AT FAILURE OF LABORATORY SPECIMENS (10^{-3} in./in.)

Asphalt Pen. Grade	91 pen.			124 pen.			160 pen.		
Asphalt Content, %	4.5	5.0	5.5	4.5	5.0	5.5	4.5	5.0	5.5
a. Temp. = +20°C	10.497	8.175	8.332	9.659	7.685	8.017	9.341	8.358	8.617
b. Temp. = 0°C	3.028	3.039	3.617	3.399	4.057	4.119	3.579	3.627	4.248
c. Temp. = -10°C	4.231	4.524	4.481	4.179	4.023	3.620	3.852	4.213	3.623

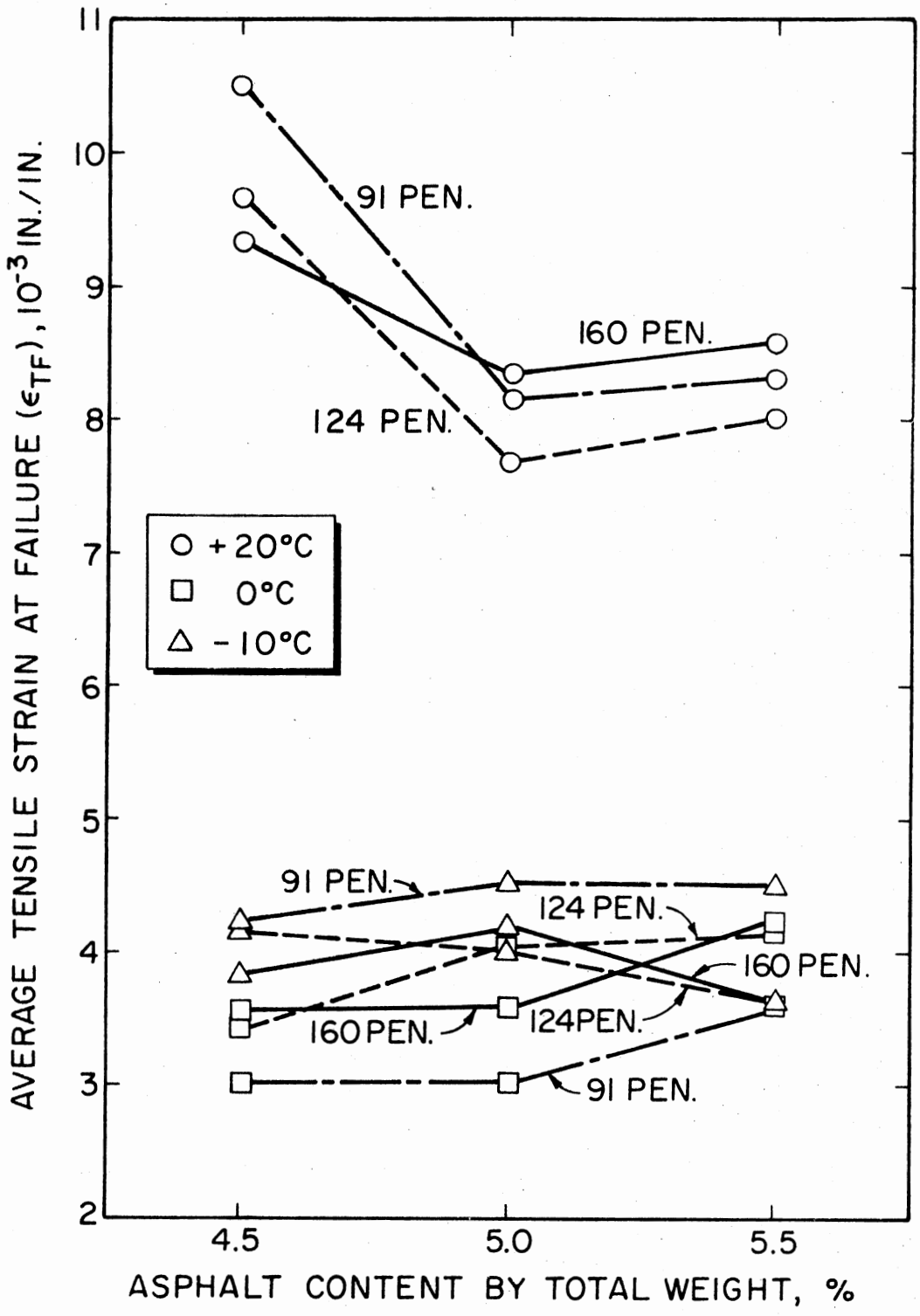

Figure 38. Average Tensile Strain at Failure Versus the Asphalt Content of the Mix

5.5 percent by weight. On the other hand, maximum tensile strains at 20°C were associated with 4.5 percent asphalt content. Also, no particular asphalt percent could be reported as the optimum content for maximum tensile strains at -10°C.

The previous discussion indicates that the tensile strain results alone did not show a great amount of information concerning the behavior of the laboratory asphalt mixtures. It seems that the strong interactions between the effects of some factors, as discussed above, tend to mask the relationship between these factors and the measured tensile strains at failure. Additional work may be required to further investigate the exact effects of asphalt grade and asphalt content on the failure tensile strains measured by the tensile-splitting test. However, it was hoped that the parameter of ultimate failure stiffness, a parameter that combined both the tensile strength and the failure tensile strain responses, would be a better indicator of the ability of a particular paving mixture to resist cracking at low temperatures.

Ultimate Failure Stiffness: The average ultimate failure stiffness values are given in Table IX. These values are also represented in Figure 39 to show the effect of temperature, asphalt grade and asphalt content on the failure stiffness. Analysis of variance showed that temperature had a significant effect on the measured failure stiffness values. The observed significance level associated with this effect was 0.0001. As temperature decreased, failure stiffnesses considerably increased. Figure 39 shows that the rate of increase was a function of both asphalt grade and asphalt content.

The results also indicated that high stiffness values were associated with low-penetration asphalt cements. At all temperature levels,

TABLE IX

AVERAGE ULTIMATE FAILURE STIFFNESS VALUES OF LABORATORY SPECIMENS (10^3 psi)

Asphalt Pen. Grade	91 pen.			124 pen.			160 pen.		
Asphalt Content, %	4.5	5.0	5.5	4.5	5.0	5.0	4.5	5.0	5.5
a. Temp. = +20°C	5.685	8.809	7.739	5.181	8.014	5.859	2.647	3.464	3.378
b. Temp. = 0°C	81.177	80.759	65.142	67.556	53.064	45.663	52.469	42.568	31.868
c. Temp. = -10°C	90.313	86.497	86.852	85.761	85.576	81.029	83.155	75.871	80.217

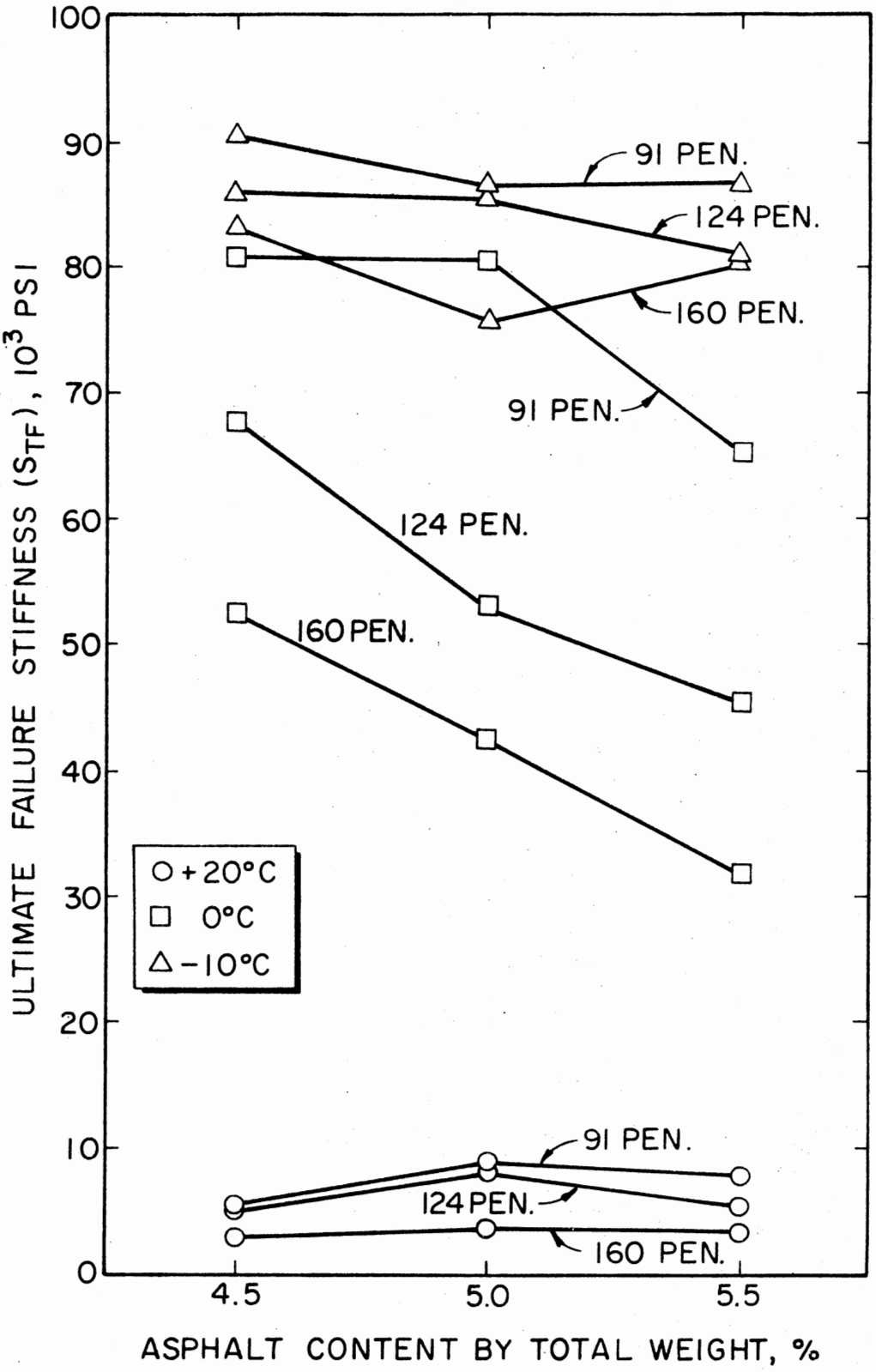

Figure 39. Average Ultimate Failure Stiffness Versus the Asphalt Content of the Mix

failure stiffness significantly decreased as softer asphalt grades were incorporated in the mix. The observed significance level was 0.0001 as indicated by the analysis of variance. Again, a significant interaction between temperature and asphalt grade was observed. This means that the effect of employing different asphalt grades on the failure stiffness values was not the same at each temperature level. For instance, the reduction in failure stiffness values with the use of soft asphalt grades (124 and 160-penetration asphalts) was more pronounced at 0^{o} and $-10^{o}C$ than at $20^{o}C$. As previously discussed, transverse cracking was attributed, in part, to the low-temperature response of the stiff asphalt in the surfacing mixture. Considering the remarkable decrease in failure stiffness at low temperatures associated with the soft asphalt grades, it appears that transverse cracking in Oklahoma could be either eliminated or reduced by using relatively softer grades in surface course mixtures.

Asphalt content showed a significant effect on the failure stiffness values. The observed significance level was 0.008. However, this effect varied considerably between the three temperature levels. At $20^{o}C$, mixtures with 5.0 percent asphalt showed the highest ultimate failure stiffness values. At 0^{o} and $-10^{o}C$, failure stiffnesses gradually decreased, with the exception of the 160-penetration asphalt mixtures at $-10^{o}C$, as asphalt content increased. This indicates that asphalt mixtures with relatively high asphalt contents may have greater ability to resist transverse cracking at low temperatures.

Stiffness Moduli of Fresh Asphalt Cements and Mixtures

The stiffness moduli of the laboratory asphalt cements and mixtures

were determined at various low temperatures ranging from 0^{o} to $-40^{o}C$. For comparison purposes, a mix containing 5.0 percent asphalt by weight was employed to estimate the stiffness moduli of the various asphalt concrete mixtures. Tables X and XI summarize the average stiffness moduli of the asphalt cements and asphalt mixtures, respectively. Also, Figures 40 and 41 provide plots of these values versus the corresponding service temperatures.

The stiffness moduli of 26 asphalt cement samples secured from various sources in Oklahoma were calculated at $-10^{o}F$ ($-23.3^{o}C$). Table XII shows the calculated stiffness values along with the corresponding penetration values of these asphalt samples. The rheological properties of these samples are given in Table XIX in Appendix B.

Data obtained from this analysis clearly indicate the significant effect of service temperature on the performance of asphalt cements and mixtures. As can be seen in Figures 40 and 41, stiffness moduli of all asphalt binders and mixtures vastly increased as service temperature decreased from 0^{o} to $-30^{o}C$. The stiffness modulus at a given temperature is apparently a function of the asphalt grade. For example, values given in Table X show that the stiffness values for the 91-penetration asphalt cement are significantly greater than those of the 124 and 160-penetration grades. Also, as temperature decreases from 0^{o} to $-30^{o}C$, the stiffness modulus of the 91-penetration asphalt cement increases at a rate twice that of the 124-penetration grade and four times that of the 160-penetration grade. Below $-30^{o}C$, the stiffness modulus of the 160-penetration asphalt cement slightly increases while the stiffness moduli of the other two grades show a rather great increase. These findings point out the sensitivity of asphalt cements

TABLE X

AVERAGE STIFFNESS MODULI OF LABORATORY ASPHALT CEMENTS

Asphalt Penetration at 25°C	Stiffness Modulus at Different Temperatures, Kg/cm^2				
	0°C	-10°C	-20°C	-30°C	-40°C
91	0.15	2.00	32.00	300.00	1500.00
124	0.08	0.92	10.00	150.00	800.00
160	0.04	0.50	3.50	74.00	110.00

TABLE XI

AVERAGE STIFFNESS MODULI OF LABORATORY ASPHALT MIXTURES

Asphalt Penetration at 25°C	Volume Conc. of Agg. Mix (C_v)	Stiffness Modulus at Different Temperatures, Kg/cm^2				
		0°C	-10°C	-20°C	-30°C	-40°C
91	0.859	200	1441	10,400	44,492	116,680
124	0.861	125	856	4,872	30,041	84,370
160	0.860	70	524	2,235	18,638	26,015

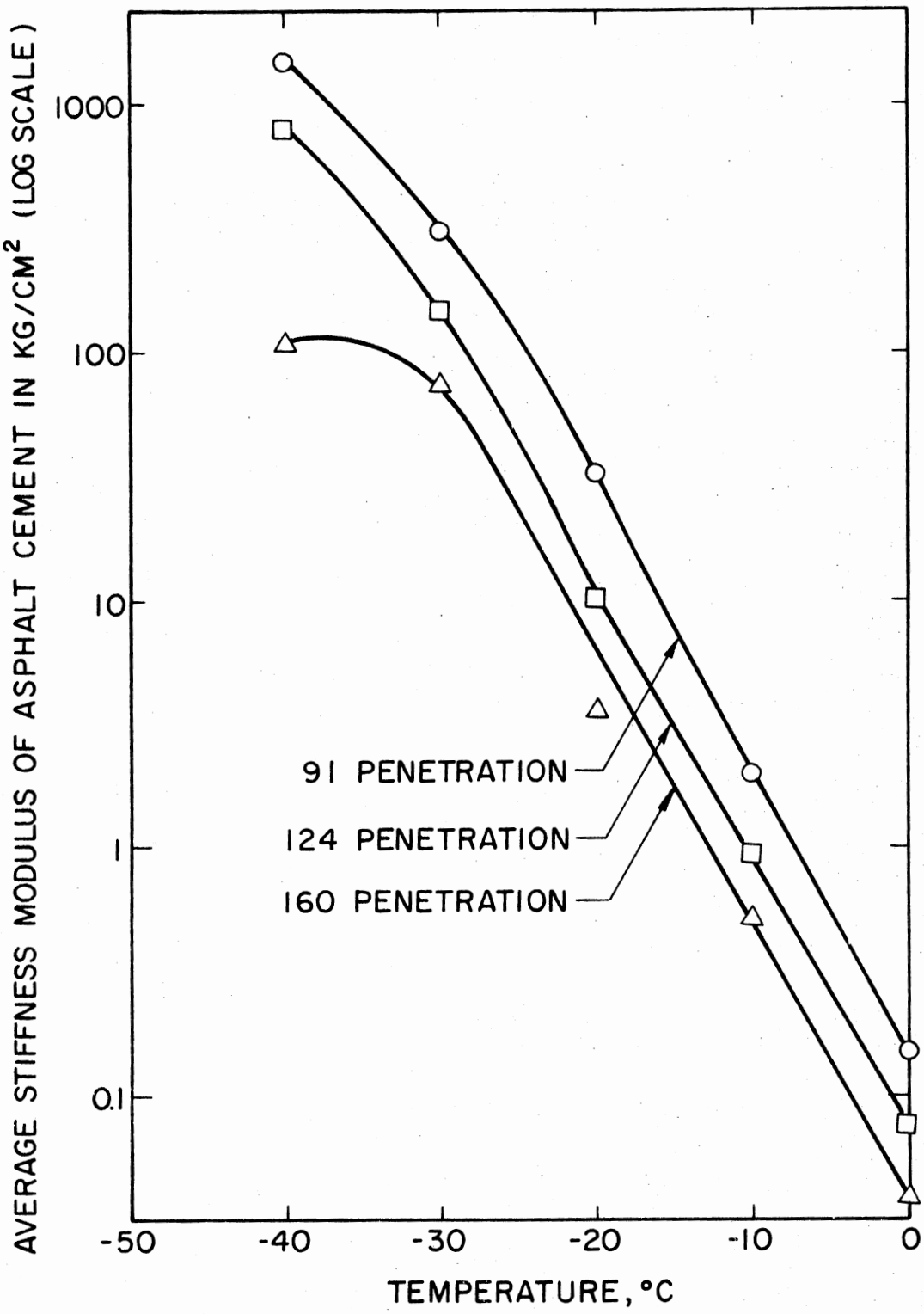

Figure 40. Stiffness Moduli of Laboratory Asphalt Cements Versus Service Temperature

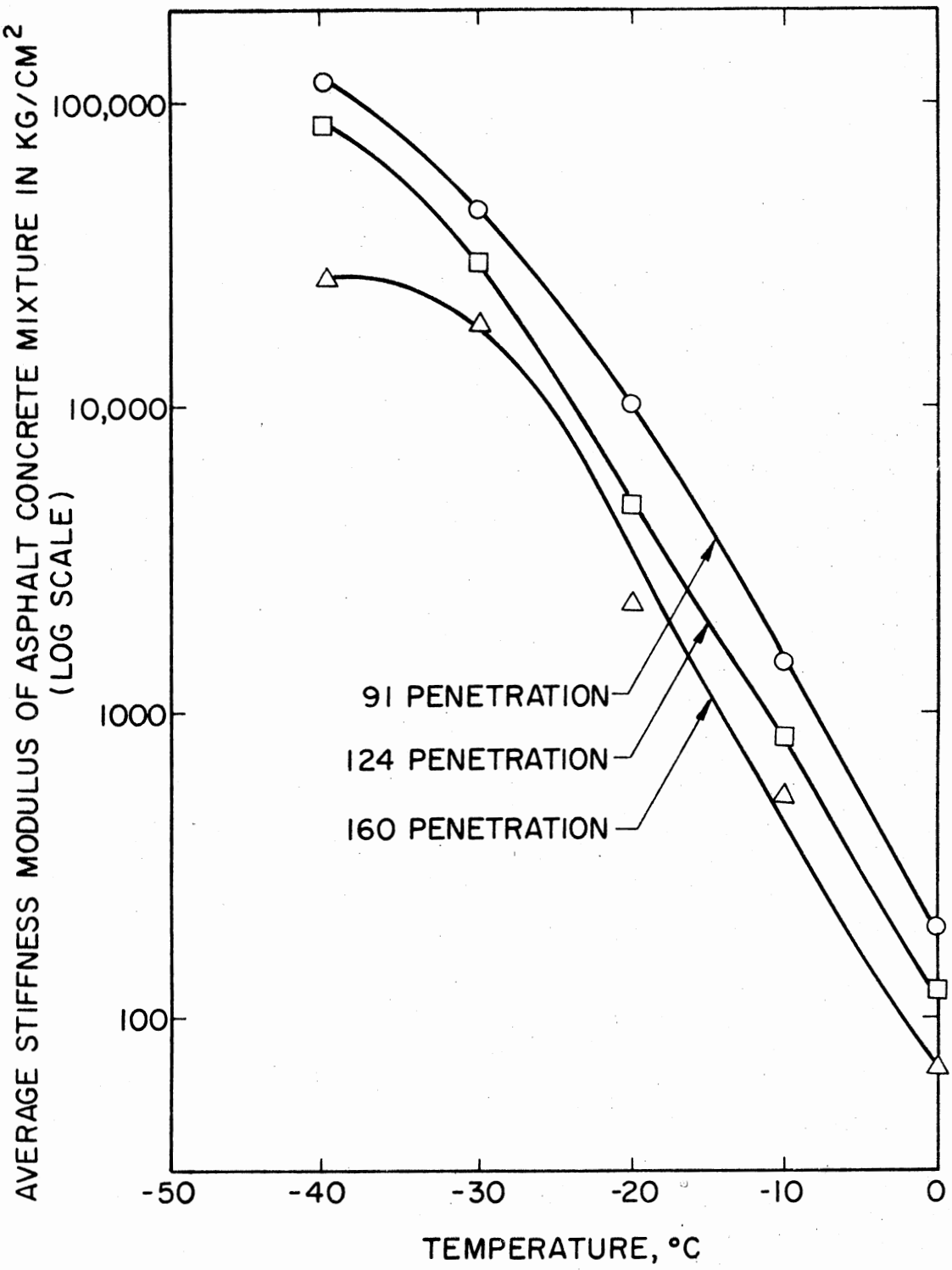

Figure 41. Stiffness Moduli of Laboratory Asphalt Concrete Mixtures Versus Service Temperature

to low-temperature changes and show that low-penetration (high viscosity) asphalt cement grades will generally exhibit significantly higher stiffness moduli at these low temperatures.

As reported earlier for the field samples, a satisfactory correlation between the stiffness moduli of field paving mixtures and the observed degree of cracking was found. Previous studies indicated that the ability of a particular paving mix to resist cracking may be predicted from the stiffness modulus of the mix at the expected minimum service temperature. Therefore, the stiffness values of the various asphalt mixtures employed in this study were compared to the limiting stiffness values shown in the literature for the same conditions of temperature and rate of loading (Table I).

From Figure 41 the stiffness modulus of the first mixture group employing the 91-penetration asphalt is approximately 17,783 kg/cm^2 (253,000 psi) at -23.3°C (-10°F). Compared with McLeod's design guide shown in Table I, this value is considerably above the maximum safe limit specified to avoid transverse pavement cracking at this temperature. Consequently, this mixture is considered to be much too stiff to eliminate transverse cracking at temperatures lower than -10°F.

As indicated before, McLeod's design guide was based on a dense well-graded mix (C_v = 0.88). Using Figure 9 in a reverse sense, McLeod's mix design guide can be translated into an asphalt cement selection guide. This selection guide indicates the maximum safe stiffness modulus of an asphalt cement at a particular low temperature. According to this procedure, an asphalt cement stiffness modulus of 23 kg/cm^2 (327 psi) could be interpreted as the maximum safe stiffness of an asphalt binder at a temperature of -23.3.°C (-10°F). Comparing

this value to the stiffness moduli shown in Table XII, it appears that none of the 26 asphalt cement samples satisfies the safe-stiffness design criteria at -23.3°C (-10°F).

From Figure 41 the stiffness moduli at -25° and -40°F (-31.7° and -40°C) of the second mixture group (124-penetration asphalt mixtures) are approximately 37,154 and 84,370 kg/cm^2 (528,448 and 1,200,000 psi), respectively. Again, these values are higher than the maximum safe stiffness moduli recommended to eliminate transverse cracking at these temperatures. On the other hand, the stiffness moduli of the third mixture group prepared with the 160-penetration asphalt cement is considerably lower than those suggested by McLeod. Apparently, surface course mixtures with this grade of asphalt could eliminate cracking in pavements subjected to temperatures as low as-40°F (-40°C).

As previously discussed, a minimum temperature of -10°F (-23.3°C) could be expected to occur at a pavement depth of 2.0 in. in Oklahoma. Based on the previous analysis, the 85-100 penetration asphalt cement commonly used in paving mixtures in Oklahoma seems to be too hard to avoid transverse cracking at this temperature. This analysis also indicated that transverse cracking at -10°F could be eliminated if the 120-150 asphalt penetration grade is used.

It should be pointed out that results achieved with relatively soft grades of asphalt cement were found very satisfactory and transverse cracking was practically eliminated without sacrificing pavement stability at high summer temperatures in Canada (23). Only a slight modification was required in the Canadian laboratory mix design procedures to achieve higher densities. This modification was suggested

TABLE XII

STIFFNESS MODULI OF DIFFERENT 85-100 PENETRATION GRADE ASPHALT CEMENT SAMPLES

Sample No.	Penetration at 25°C	Stiffness Modulus at -23.33°C, kg/cm^2	Sample No.	Penetration at 25°C	Stiffness Modulus at -23.33°C kg/cm^2
1	92	62.504	14	93	67.496
2	92	81.417	15	89	87.182
3	86	86.690	16	88	68.761
4	86	99.978	17	96	70.027
5	92	68.761	18	87	91.401
6	89	78.605	19	90	85.424
7	87	84.370	20	90	62.504
8	87	99.978	21	90	85.003
9	100	66.652	22	95	54.981
10	92	62.715	23	93	54.981
11	89	78.464	24	94	79.448
12	87	83.315	25	99	72.839
13	89	81.276	26	85	64.262

to reduce the tendency of these paving mixtures to densify much more rapidly under traffic. If high temperature stability requirements cannot be met with higher penetration asphalt cements and standard O.D.O.T. surface mixture gradation, a less desirable asphalt, i.e., an asphalt having a higher stiffness modulus, will have to be selected and some cracking tolerated.

CHAPTER VII

CONCLUSIONS AND RECOMMENDATIONS

Conclusions

The major conclusions drawn from this study may be summarized as follows:

1. Examination of recently developed transverse cracks revealed that, in most cases, the cracks had originated at the pavement surface. Thus, the major cause of these transverse cracks appears to be cold-temperature contraction of the asphalt concrete surface layer. This contraction of the surface is restrained by the underlying layers. However, some of these transverse cracks extended through the pavement matrix and may have originated at the pavement-subgrade interface due to thermal stresses, traffic stresses, or various problems in the subgrade material.

2. The tensile splitting test appears to be a practical method for evaluating the tensile properties of asphalt concrete mixtures and warrants inclusion as a routine test in future design procedures that take into account the mixture properties and behavior at low as well as high temperatures.

3. Temperature had a highly significant effect on the measured tensile properties of both field core samples and laboratory asphalt mixtures. As temperature decreased, tensile strengths (tensile

stresses at failure) and failure stiffnesses remarkably increased and tensile strains at failure decreased. This is primarily due to the increase in stiffness of the asphalt binder.

4. A satisfactory correlation was found between the tensile splitting test results of the field core samples and the observed degree of pavement cracking. The occurrence of transverse cracking was found to increase as the failure strains decreased and the failure stiffness increased.

5. Stiffness moduli of recovered asphalts, determined at the lowest minimum temperature in Oklahoma, were significantly correlated with the cracking indices of the pavement test sites. The stiffer or harder the asphalt cement in a pavement the greater was the degree of transverse cracking.

6. Lower tensile strength (tensile stress at failure) and ultimate failure stiffness values were observed for laboratory asphalt mixtures when softer asphalt grades were incorporated in the mix. However, no clear trend was found between average tensile strains and asphalt viscosity or penetration.

7. Increasing the asphalt content of the mix reduced failure stiffness and tensile strength in most cases. Again, tensile strains at failure did not significantly differ as asphalt content increased.

8. Based on the limiting stiffness concept, the 85-100 penetration asphalt commonly used for paving operations in Oklahoma is considered too hard a grade to avoid transverse cracking at the minimum service temperature to be expected in Oklahoma.

Recommendations

The following recommendations are pertinent to the results and the observations obtained from this research investigation:

1. Future research should be directed toward studying the effects of temperature cycles, traffic load stresses and subgrade properties on transverse cracking initiation and propagation.

2. The tensile splitting test should be utilized in further comprehensive testing of cracked and uncracked pavement sections to develop "safe" or "critical" strength, strain and/or failure stiffness values. The ability to resist transverse cracking of a particular paving mixture, which is satisfactory in all other respects, could then be predicted by comparing its tensile splitting test results with the developed design limits.

3. Current asphalt cement specifications are primarily concerned with the rheological properties at moderate and high temperatures (penetration at $77^{o}F$, viscosity at 140^{o} and $275^{o}F$ and softening point). For a wide range of design situations, the viscosity or some other consistency measurement at low temperatures should be included in future specifications.

4. The effect of using an asphalt cement with a lower stiffness modulus, either a 120-150 penetration asphalt or a 85-100 penetration asphalt with improved low-temperature sensitivity, and the corresponding modifications required in current mix design procedures should be investigated with regard to high-temperature stability problems. Based on the results of other research studies, the low-temperature sensitivity of asphalt binders could be improved by ad-

ditives such as synthetic polymers, natural rubber and asbestos fibers.

5. A more comprehensive and objective crack surveying technique for the Oklahoma highway network is needed. This technique should also include a measure of pavement serviceability.

6. Future research investigation is required to determine the most practical, efficient and economical method of treating existing cracked pavements.

BIBLIOGRAPHY

(1) Haas, R. C. G. et al. "Low Temperature Pavement Cracking in Canada: The Problem and Its Treatment." Proceedings of the Canadian Good Roads Association, 1970.

(2) Zube, E. "Cracking of Asphalt Concrete Pavements Associated With Absorptive Aggregates." Proceedings of the Association of the Asphalt Paving Technologists, Vol. 35 (1966), p. 329.

(3) Anderson, K. O., B. P. Shields, and J. M. Dacyszyn. "Cracking of Asphalt Pavements Due to Thermal Effects." Proceedings of the Association of Asphalt Paving Technologists, Vol. 35 (1966), p. 247.

(4) Marker, V. "Introduction to Non-Traffic Load Associated Cracking of Asphalt Pavements." Proceedings of the Association of Asphalt Paving Technologists, Vol. 35 (1966), p. 239.

(5) Kelly, J. E. "Cracking of Asphalt Concrete Pavements Associated With Volume Changes in Underlying Materials and Base Courses." Proceedings of the Association of Asphalt Paving Technologists, Vol. 35 (1966), p. 290.

(6) Campen, W. H. Prepared discussion, Proceedings of the Association of Asphalt Paving Technologists, Vol. 35 (1966), p. 309.

(7) Serafin, P. J. Prepared discussion, Proceedings of the Association of Asphalt Paving Technologists, Vol. 35 (1966), p. 314.

(8) Fromm, H. J. Prepared discussion, Proceedings of the Association of Asphalt Paving Technologists, Vol. 35 (1966), p. 324.

(9) Culley, R. W. "Temperature Cracking of Flexible Pavements in Saskatchewan." Saskatchewan Department of Highways, technical report, June, 1966.

(10) Deme, I. "Ste. Anne Test Road--Two Years Progress Report of Pavement Cracking." Manitoba Department of Transportation, Internal Report 69-1, 1969.

(11) Mcleod, N. W. "Reduction in Transverse Pavement Cracking by Use of Softer Asphalt Cements." The Highway Research Board Western Meeting, Denver, Colorado, August, 1968.

(12) Kingham, R. I. Prepared discussion, Proceedings of the Association of Asphalt Paving Technologists, Vol. 35 (1966), p. 329.

(13) Haas, R. C. G. "A Method for Designing Asphalt Pavements to Minimize Low-Temperature Shrinkage Cracking." The Asphalt Institute, Research Report 73-1 (RR-73-1), January, 1973.

(14) Anderson, K. O. and R. C. G. Haas. "Use of the Stiffness Concept to Characterize Bituminous Materials." Proceedings of the Canadian Technical Asphalt Association, 1970.

(15) Manke, P. G. and M. S. Nour El-Din. "A Preliminary Study of the Use of the Stiffness Concept in Minimizing Low-Temperature Transverse Cracking." Oklahoma State University, Research Project 72-03-3, Unpublished Interim Report III, March, 1976.

(16) "A User's Guide to the Statistical Analysis System." Department of Statistics, North Carolina State University, August, 1972.

(17) Rader, L. F. "Investigation of the Physical Properties of Asphaltic Mixtures at Low Temperatures." Proceedings of the Association of Asphalt Paving Technologists, Vol. 6 (January, 1935), pp. 49-61.

(18) "Road Research Needs in Canada." Canadian Good Roads Association, Technical Publication No. 27, May, 1965.

(19) "Symposium: Non-Traffic Load Associated Cracking of Asphalt Pavements." Proceedings of the Association of Asphalt Paving Technologists, Vol. 35 (1966), pp. 239-357.

(20) Tuckett, G. M., G. M. Jones, and G. Littlefield. "The Effects of Mixture Variables on Thermally Induced Stresses in Asphaltic Concrete." Proceedings of the Association of Asphalt Paving Technologists, Vol. 39 (1970), pp. 703-744.

(21) Burgess, R. A., O. Kopvillem, and F. D. Young. "Ste. Anne Test Road--Relationships Between Predicted Fracture Temperatures and Low-Temperature Field Performance." Proceedings of the Association of Asphalt Paving Technologists, Vol. 40 (1971), pp. 148-226.

(22) Fromm, H. J. and W. A. Phang. "A Study of Transverse Cracking of Bituminous Pavements." Proceedings of the Association of Asphalt Paving Technologists, Vol. 41 (1972), pp. 383-423.

(23) Mcleod, N. W. "A 4-Year Survey of Low Temperature Transverse Pavement Cracking on Three Ontario Test Roads." Proceedings of the Association of Asphalt Paving Technologists, Vol. 41 (1972), pp. 424-493.

(24) Christison, J. T., D. W. Murray, and K. D. Anderson. "Stress Prediction and Low-Temperature Fracture Susceptibility of Asphaltic Concrete Pavements." Proceedings of the Association of Asphalt Paving Technologists, Vol. 41 (1972), pp. 494-523.

(25) Hamilton, A. B. "Freezing Shrinkage in Compacted Clays." Canadian Geotechnical Journal, Vol. 3, No. 1 (February, 1966), pp. 1-17.

(26) Deme, I. and D. Fisher. "Ste. Anne Test Road--Instrumentation." Proceedings of the Canadian Technical Asphalt Association, 1968.

(27) Young, F. D., I. Deme, R. A. Burgess, and O. Kopvillem. "Ste. Anne Test Road--Construction Summary and Performance After Two Years Service." Proceedings of the Canadian Technical Asphalt Association, 1969.

(28) Van Cauwenberghe, R. A. and I. Deme. "Ste. Anne Test Road--Three Years Progress Report of Rutting and Wear." Manitoba Department of Transportation, Research Report 70-1, July, 1970.

(29) Shields, B. P., K. O. Anderson, and J. M. Dacyszyn. "An Investigation of Low-Temperature Cracking of Flexible Pavements." Proceedings of the Canadian Good Roads Association, 1969.

(30) Haas, R. C. G. and T. H. Topper. "Thermal Fracture Phenomena in Bituminous Surfaces." Highway Research Board, Special Report 101, 1969, pp. 136-153.

(31) Culley, R. W. "Relationships Between Hardening of Asphalt Cements and Transverse Cracking of Pavements in Saskatchewan." Proceedings of the Association of Asphalt Paving Technologists, Vol. 38 (1969), p. 629.

(32) Mcleod, N. W. "Transverse Pavement Cracking Related to Hardness of the Asphalt Cement." Proceedings of the Canadian Technical Asphalt Association, 1968.

(33) Haas, R. C. G. "Thermal Shrinkage Cracking of Some Ontario Pavements." Department of Highways of Ontario, Report RR 161, May, 1970.

(34) Van der Poel, C. "A General System Describing the Viscoelastic Properties of Bitumens and Its Relation to Routine Test Data." Journal of Applied Chemistry, Vol. 4 (May, 1954), pp. 221-236.

(35) Heukelom, W. "Observations on the Rheology and Fracture of Bitumens and Asphalt Mixes." Proceedings of the Association of Asphalt Paving Technologists, Vol. 35 (1966), pp. 358-399.

(36) Mcleod, N. W. Prepared discussion on Ste. Anne Test Road. Proceedings of the Canadian Technical Asphalt Association, 1969.

(37) Annual Book of ASTM Standards. Part 15. Philadelphia: American Society of Testing and Materials, 1975.

(38) Pfeiffer, J. P. and P. M. Van Doormaal. "The Rheological Properties of Asphaltic Bitumen." Journal of the Institute of Petroleum Technology, Vol. 22 (1936), p. 414.

(39) Heukelom, W. "A Bitumen Test Data Chart for Showing the Effect of Temperature on the Mechanical Behavior of Asphalt Bitumens." Journal of the Institute of Petroleum Technology, Vol. 55 (November, 1969), pp. 404-417.

(40) Heukelom, W. and A. J. G. Klomp. "Road Design and Dynamic Loading." Proceedings of the Association of Asphalt Paving Technologists, Vol. 33 (February, 1964), pp. 92-125.

(41) Van Draat, W. E. F. and P. Sommer. "Ein Gerat zur Bestimmung der Dynamischen Elastizitattsmoduln von Asphalt." Stresse und Autobahn, Vol. 35 (1966).

(42) Anderson, K. O. and W. P. Hahn. "Design and Evaluation of Asphalt Concrete with Respect to Thermal Cracking." Proceedings of the Association of Asphalt Paving Technologists, Vol. 37 (1968), pp. 1-31.

(43) Christianson, R. H. A. "Analysis of the Tensile Splitting Test for Low Temperature Tensile Properties of Asphaltic Concrete." (Unpub. M.S. thesis, The University of Alberta, 1970.)

(44) Tons, E. and E. M. Krokosky. "Tensile Properties of Dense Graded Bituminous Concrete." Proceedings of the Association of Asphalt Paving Technologists, Vol. 32 (1963), pp. 497-529.

(45) Phang, W. A. "On Transverse Cracking of Asphalt Pavements." Unpublished paper, Department of Highways of Ontario. Presented to Pavement Design and Evaluation Committee, Canadian Good Roads Association, September, 1968.

(46) Fromm, H. J. and W. A. Phang. "Temperature Susceptibility Control in Asphalt Cement Specifications." Department of Highways of Ontario, Report IR 35, November, 1970.

(47) Lefebvre, J. A. "A Modified Penetration Index for Canadian Asphalts." Proceedings of the Association of Asphalt Paving Technologists, Vol. 39 (1970), pp. 443-480.

(48) Hajek, J. J. and R. C. G. Haas. "Predicting Low-Temperature Cracking Frequency of Asphalt Concrete Pavements." Highway Research Board, Research Record No. 407, 1972, pp. 39-54.

(49) Hills, J. F. and D. Brien. "The Fracture of Bitumens and Asphalt Mixes by Temperature Induced Stresses." Proceedings of the Association of Asphalt Paving Technologists, Vol. 35 (1966), pp. 293-309.

(50) Haas, R. C. G. and W. A. Phang. "Case Studies of Pavement Shrinkage Cracking as Feedback for a Design Subsystem." Highway Research Board, Research Record No. 313, 1970, pp. 32-43.

(51) Humphreys, J. S. and C. J. Martin. "Determination of Transient Thermal Stresses in a Slab with Temperature-Dependent Viscoelastic Properties." Transactions of the Society of Rheology, Vol. 7 (1963), pp. 155-170.

(52) Monismith, C. L., G. A. Secor, and K. R. Secor. "Temperature-Induced Stresses and Deformation in Asphalt Concrete." Proceedings of the Association of Asphalt Paving Technologists, Vol. 34 (1965), pp. 248-285.

(53) Christison, J. T. and K. O. Anderson. "The Response of Asphalt Pavements to Low-Temperature Climatic Environments." Paper prepared for Third International Conference on the Structural Design of Asphalt Pavements, London, September, 1972.

(54) Shahin, M. Y. and B. F. McCullough. "Stiffness History of Asphalt Concrete Surfaces in Roads." Highway Research Board, Research Record No. 466, 1973, pp. 96-112.

(55) Thompson, P. D. "Merits of Adding Natural Rubber to Bituminous Road Surfacing Materials." Highway Research Board, Research Record No. 273, 1969, pp. 87-98.

(56) Fabb, T. R. J. "The Influence of Mix Composition, Binder Properties and Cooling Rate on Asphalt Cracking at Low Temperatures." Proceedings of the Association of Asphalt Paving Technologists, Vol. 43 (1974), pp. 285-331.

(57) Hignell, E. T., J. J. Hajek, and R. C. G. Haas. "Modification of Temperature Susceptibilities of Asphalt Paving Mixtures." Proceedings of the Association of Asphalt Paving Technologists, Vol. 41 (1972), pp. 524-561.

(58) Wolters, R. O. "Sealing Cracks in Bituminous Pavements." Minnesota Department of Highways, Investigation No. 185, Final Report, 1973.

(59) Burington, R. S. and D. C. May, Jr. Handbook of Probability and Statistics with Tables. Second ed. New York: McGraw-Hill Book Company, 1970.

(60) Manke, P. G. and S. Oteng-Seifah. "Characteristics of Rutting on High Quality Bituminous Highway Pavements." Interim Report II, Research Project 72-03-3, Oklahoma State University, December, 1975.

(61) Steel, R. G. D. and J. H. Torrie. Principles and Procedures of Statistics. New York: McGraw-Hill Book Company, 1960.

(62) "Standard Specifications for Highway Construction." Oklahoma State Highway Commission, Oklahoma Department of Transportation, 1976.

(63) Mitchell, N. B. "The Indirect Tension Test for Concrete." Materials Research and Standards, Vol. 1 (October, 1961), pp. 780-787.

(64) Wright, P. J. F. "Comments on an Indirect Tensile Test on Concrete Cylinders." Magazine of Concrete Research, Vol. 7 (October, 1955), pp. 87-96.

(65) Thompson, M. R. "Split-Tensile Strength of Lime-Stabilized Soils." Highway Research Board, Highway Research Record No. 92, 1965.

(66) Hudson, W. R. and T. W. Kennedy. "An Indirect Tensile Test for Stabilized Materials." Research Report 98-1. Center for Highway Research, The University of Texas at Austin, January, 1968.

(67) "Test Procedures for Characterizing Dynamic Stress-Strain Properties of Pavement Materials." Transportation Research Board, Special Report 162, 1975.

(68) Hadley, W. O., W. R. Hudson, and T. W. Kennedy. "A Method of Estimating Tensile Properties of Materials Tested in Indirect Tension." Research Report 98-7, Center for Highway Research, The University of Texas at Austin, July, 1970.

(69) Anagnos, J. N. and T. W. Kennedy. "Practical Method of Conducting the Indirect Tensile Test." Research Report 98-10. Center for Highway Research, The University of Texas at Austin, August, 1972.

(70) Manke, P. G. "Asphalt Mix Design Procedures." Laboratory manual for CIVEN 5653, School of Civil Engineering, Oklahoma State University, 1970.

(71) "Climatic Atlas of the United States." U. S. Department of Commerce, Environmental Sciences Service Administration, Environmental Data Service, June, 1968.

APPENDIX A

TEST SITE INFORMATION

TABLE XIII

TEST SITE INFORMATION

Test Site Number	Highway Number	Location	County	Construction Project Number	Date Completed	Overlay Date
1	US 177	4.0 miles south of US 66	Lincoln	S 251 (9) S	1951*	1972
2	US 177	8.0 miles south of US 66	Lincoln	S 251 (10) S	1951*	1972
3	US 177	4.5 miles south of US 62	Pottawatomie	S 251 (6) (7)	1951*	1971
4	US 177	6.5 miles south of US 62	Pottawatomie	S 251 (6) (7)	1951*	1971
5	IS 35	4.0 miles north of Cimmaron River Bridge	Payne	I-35-4 (19) 165	1961	....**
6	IS 35	4.0 miles north of Perry	Noble	I-35-4 (29) 187	1963	1971
7	IS 40	1.0 mile east of Oklahoma-Pottawatomie county line	Pottawatomie	I-40-5 (49) 193	1965	1972
8	IS 35	5.5 miles north of Cimmaron River bridge	Payne	I-35-4 (19) 165	1961	....**
9	IS 40	2.5 miles east of Oklahoma-Pottawatomie county line	Pottawatomie	I-40-5 (49) 193	1965	1972

* These projects were completed before 1951.

** These projects have had no overlays.

TABLE XIV

TRANSVERSE CRACKING DATA

Test Site Number	No. of Cracks in the chosen 500 ft length				Cracking Index*
	Multiple	Full	Half	Part	
1	--	1	11	52	6.5
2	--	10	1	3	10.5
3	1	7	15	14	15.5
4	1	9	29	27	24.5
5	--	--	4	7	2.0
6	--	4	10	29	9.0
7	--	19	2	--	20.0
8	--	--	--	--	0.0
9	--	--	1	3	0.5

* see equation (2.1)

APPENDIX B

PROPERTIES OF LABORATORY MATERIALS AND MIXTURES

TABLE XV

SUMMARY OF SIEVE ANALYSIS TEST RESULTS

Sieve Size or Number	Per Cent Passing by Weight, %			
	1/2-in. Crushed Limestone	Limestone Screenings	Coarse Sand	Fine Sand
1/2-in.	100.0	100.0	100.0	100.0
3/8-in.	82.0	100.0	99.0	100.0
4	9.0	96.0	92.0	100.0
10	1.0	58.0	71.0	99.0
40	1.0	28.0	18.0	70.0
80	1.0	21.0	3.0	16.0
200	1.0	14.6	0.8	6.3

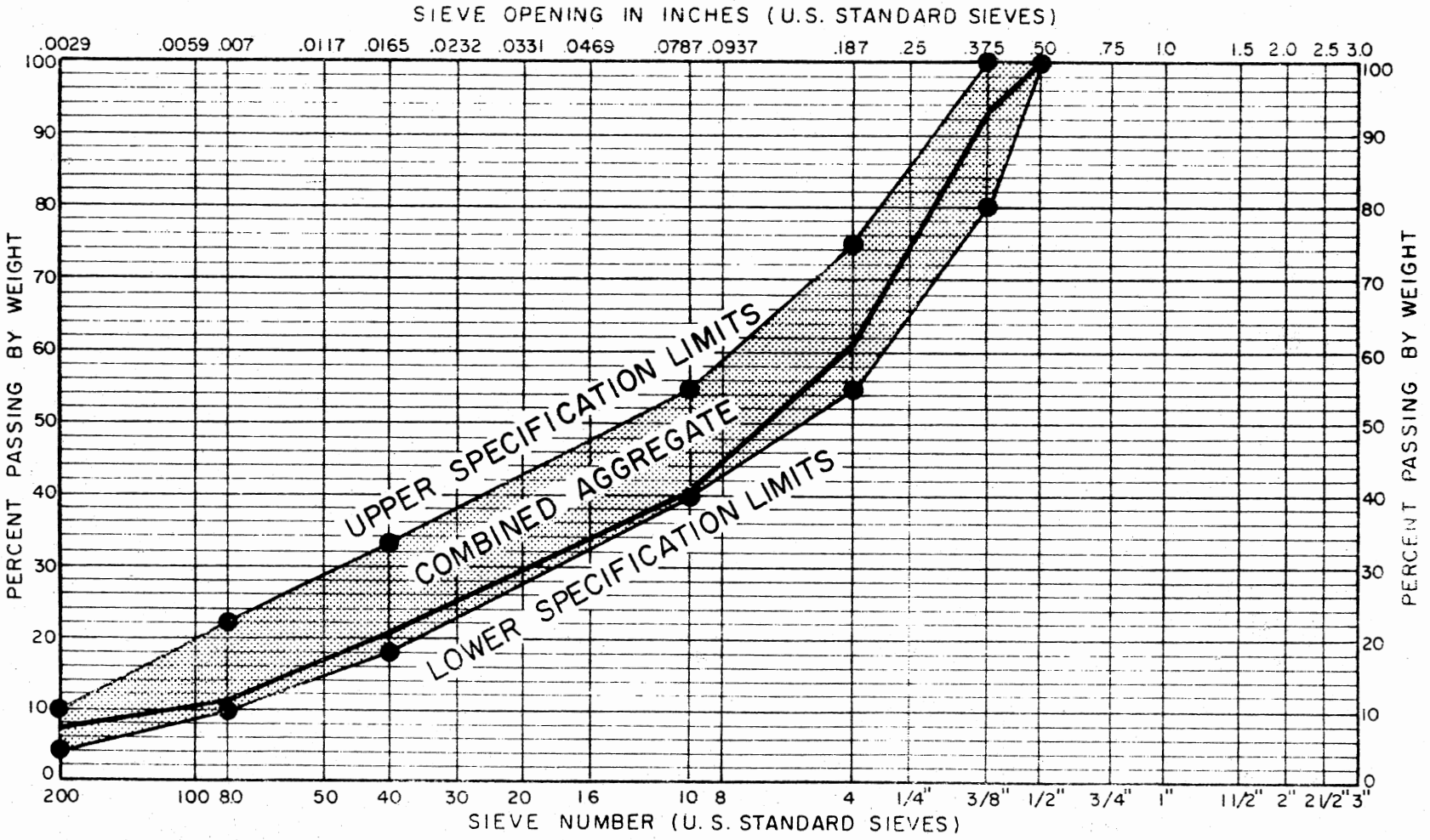

Figure 42. Combined Aggregate and Specification Limits Grading Curves

TABLE XVI

SUMMARY OF SPECIFIC GRAVITY AND WATER ABSORPTION TEST RESULTS

Aggregate	Per Cent by Weight	Bulk Specific Gravity	Apparent Specific Gravity	Percent Absorption, %
1/2-in. crushed Limestone	40	2.741	2.871	1.656
Limestone screenings	40	2.716	2.867	1.941
Coarse sand	10	2.605	2.662	0.820
Fine sand	10	2.576	2.669	1.376
Combined Aggregate	100	2.700	2.828	1.658

TABLE XVII

RHEOLOGICAL PROPERTIES OF LABORATORY ASPHALT CEMENTS

Sample Number	1	2	3
Specific gravity, 77°F/77°F	1.004	0.999	0.997
Penetration 200 gm, 60 sec, 39.2°F	26.000	34.000	44.000
Penetration 100 gm, 5 sec, 77°F	91.000	124.000	160.000
Absolute Viscosity 140°F, 300 mm Hg vacuum poise	1485.000	939.300	652.300
Kinematic Viscosity 275°F C. Stokes	3876.000	325.000	268.800
Ring and Ball Softening point, F°	112.060	107.240	102.740

TABLE XVIII

PROPERTIES OF COMPACTED ASPHALT MIXTURES

Asphalt Penetration	Asphalt Content by Weight, %	Bulk Specific Gravity	Maximum Specific Gravity	Per Cent Density	Hveem Stability, lb
91	4.5	2.423	2.588	93.62	50.6
	5.0	2.458	2.574	95.49	47.6
	5.5	2.474	2.554	96.87	45.9
124	4.5	2.420	2.580	93.80	55.5
	5.0	2.454	2.564	95.71	50.3
	5.5	2.455	2.536	96.81	47.7
160	4.5	2.420	2.574	94.02	50.3
	5.0	2.451	2.563	95.63	48.4
	5.5	2.453	2.541	96.54	47.0

TABLE XIX

RHEOLOGICAL PROPERTIES OF THE 85-100 PENETRATION GRADE ASPHALT CEMENT SAMPLES

Sample No.	Specific Gravity, 77°F/77°F	Penetration 200 gm, 60 sec, 39.2°F	Penetration 100 gm, 5 sec, 77°F	Absolute Viscosity 140°F, 300 mm Hg Vacuum Poise	Kinematic Viscosity 275°F C. Stokes	Ring and Ball Softening Point, F°
1	0.9966	33	92	1572.6	435.2	116.33
2	0.9959	28	92	1200.8	369.0	115.61
3	1.0053	30	86	1572.6	362.6	113.63
4	1.0039	29	86	1503.8	350.0	112.46
5	0.9961	38	92	1503.5	429.3	114.89
6	0.9912	35	89	1591.6	412.0	117.50
7	1.0030	31	87	1487.7	365.4	113.81
8	1.0010	28	87	1176.1	327.4	114.35
9	0.9993	35	100	1210.3	346.5	112.64
10	0.9948	36	92	1584.0	434.9	115.61
11	0.9969	30	89	1596.9	432.1	114.80
12	0.9951	29	87	1198.7	370.1	114.26
13	1.0002	37	89	1580.7	408.5	117.86
14	0.9949	34	93	1771.0	424.1	117.41
15	0.9904	36	89	1576.7	394.9	116.42
16	0.9935	38	88	1983.5	435.0	118.04
17	0.9944	36	96	1447.2	406.7	113.18
18	0.9915	29	87	1663.6	400.7	116.51
19	0.9906	35	90	1354.5	374.6	114.26
20	0.9902	37	90	1690.2	462.8	116.87
21	1.0008	31	90	1168.7	330.4	110.84
22	0.9925	33	95	1449.3	413.5	114.62
23	0.9953	34	93	1606.8	430.9	114.98
24	0.9972	33	94	1335.5	382.2	113.95
25	0.9936	42	99	1308.9	371.9	115.93
26	0.9969	29	85	1661.5	446.0	114.80

APPENDIX C

TEST RESULTS OF FIELD CORE SAMPLES

TABLE XX

TENSILE STRENGTH OF FIELD CORE SPECIMENS

Site No.	Cracking Index (C.I.)	Tensile Strength (σ_{TF}), psi					
		Wheelpath			Non-Wheelpath		
		-10°C	-5°C	0°C	-10°C	-5°C	0°C
1	6.5	312.939	284.269	227.948	358.592	237.116	196.150
		362.353	249.923	262.603	333.986	230.698	161.587
		364.188	253.007	252.427	315.780	249.513	311.606
2	10.5	280.040	251.460	243.917	228.622	237.051	192.725
		330.087	248.928	234.442	289.594	236.276	233.256
		312.547	300.321	222.093	239.838	269.560	220.597
3	15.5	339.319	274.211	232.295	332.154	276.490	232.720
		358.201	402.779	214.275	350.867	313.212	230.064
		336.258	341.900	206.568	337.640	335.878	219.215
4	24.5	317.802	242.423	242.305	272.488	205.825	224.537
		225.235	286.719	263.693	261.631	230.437	213.855
		257.944	228.152	250.791	265.178	270.576	217.207
5	2.0	344.094	366.225	361.390	365.535	307.073	302.699
		398.713	314.533	283.656	400.450	355.541	296.085
		357.904	360.338	326.134	389.638	321.963	298.288
6	9.0	315.660	402.056	295.582	467.017	317.900	234.000
		418.140	321.231	275.269	411.005	345.063	225.002
		447.524	292.754	300.755	377.726	324.578	294.428
7	20.0	421.006	268.550	225.086	347.256	254.799	292.823
		416.669	296.789	260.750	295.408	292.954	248.950
		381.255	294.087	259.208	394.877	285.650	274.492
8	0.0	391.738	341.072	282.954	351.177	314.181	305.601
		376.147	348.401	282.649	372.696	374.810	309.314
		469.947	370.788	350.675	375.964	383.749	299.389
9	0.5	371.542	341.870	255.476	358.862	254.299	271.687
		351.375	326.828	213.724	407.241	260.347	258.262
		343.796	327.574	221.826	387.078	264.172	270.842

TABLE XXI

TENSILE STRAIN AT FAILURE OF FIELD CORE SPECIMENS

Site No.	Cracking Index (C.I.)	Tensile Strain at Failure (ε_{TF}), 10^{-3} in/in					
		Wheelpath			Non-Wheelpath		
		-10°C	-5°C	0°C	-10°C	-5°C	0°C
1	6.5	2.696	0.607	2.171	2.463	1.982	1.374
		3.727	1.427	2.688	1.886	1.876	1.242
		2.620	0.767	3.153	2.511	1.163	2.538
2	10.5	1.903	0.899	1.809	2.273	2.141	1.034
		2.749	1.824	1.861	2.140	1.084	1.758
		3.066	1.348	2.987	1.279	1.110	2.146
3	15.5	3.406	2.960	2.946	1.956	0.878	1.744
		3.172	2.257	1.964	2.201	2.484	2.749
		3.066	1.110	1.798	1.137	1.322	1.706
4	24.5	0.317	1.348	0.827	0.555	1.876	0.801
		1.691	0.502	1.744	0.317	0.370	0.708
		0.793	1.057	1.850	0.529	0.370	0.724
5	2.0	3.642	5.603	4.942	3.330	4.942	5.233
		3.654	4.335	5.498	2.913	5.788	5.207
		4.546	4.863	6.185	4.889	4.572	5.603
6	9.0	1.985	0.529	1.758	0.635	3.344	1.577
		0.529	3.303	2.171	0.582	1.110	1.629
		0.275	1.216	2.934	0.476	0.767	2.068
7	20.0	1.005	3.463	2.016	3.065	1.731	2.611
		1.137	2.327	3.225	0.740	3.357	2.792
		2.907	3.093	2.881	1.903	2.273	2.378
8	0.0	4.440	4.097	7.506	5.498	3.080	6.502
		5.709	6.793	6.344	3.198	4.662	6.370
		6.344	4.006	5.328	3.642	4.058	6.978
9	0.5	5.203	5.328	3.829	4.329	4.287	4.839
		3.996	4.579	3.350	4.079	4.163	4.849
		3.486	4.433	3.496	3.434	3.163	4.495

TABLE XXII

ULTIMATE FAILURE STIFFNESS OF
FIELD CORE SPECIMENS

Site No.	Cracking Index (C.I.)	Ultimate Failure Stiffness (S_{TF}), 10^3 psi		
		-10°C	-5°C	0°C
1	6.5	116.075	468.318	104.997
		97.224	175.139	97.694
		139.003	329.866	80.059
		145.592	119.635	142.758
		177.087	122.973	130.102
		125.759	214.543	122.776
2	10.5	147.157	279.710	134.835
		120.075	136.474	125.976
		101.940	222.790	74.353
		100.582	110.720	186.388
		135.324	217.967	132.683
		187.520	242.847	102.795
3	15.5	99.624	92.639	78.851
		112.926	178.458	109.101
		109.673	308.018	114.888
		169.813	314.909	133.440
		159.413	126.092	83.690
		296.957	254.068	128.496
4	24.5	133.196	179.839	292.993
		325.276	571.153	151.200
		490.970	215.849	135.563
		825.334	109.715	280.321
		501.282	622.803	302.055
			731.286	300.010
5	2.0	94.479	65.362	73.126
		70.519	72.557	51.593
		78.729	74.098	52.730
		109.770	62.135	57.844
		137.470	61.427	56.863
		79.697	70.421	53.237
6	9.0	159.030	553.707	100.730
		790.859	97.230	156.579
		735.965	330.725	138.504
		706.631	95.076	148.410
		793.889	310.915	138.157
			423.393	142.358

TABLE XXII (Continued)

Site No.	Cracking Index (C.I.)	Ultimate Failure Stiffness (S_{TF}), 10^3 psi		
		-10°C	-5°C	0°C
7	20.0	419.117	77.558	69.801
		366.607	127.566	129.318
		131.144	95.092	89.973
		469.336	147.128	112.168
		155.219	87.273	89.170
		128.817	125.665	115.409
8	0.0	88.222	85.141	53.107
		65.887	85.046	44.557
		74.083	54.587	46.717
		103.236	102.004	43.798
		63.876	80.396	48.560
		116.541	94.557	46.047
9	0.5	71.409	64.165	66.721
		87.932	71.375	63.798
		98.622	73.894	63.451
		82.897	59.319	56.145
		99.838	62.538	53.261
		112.719	83.519	60.254

TABLE XXIII

STIFFNESS MODULI OF RECOVERED FIELD ASPHALT CEMENTS AND ASPHALT MIXTURES

Site No.	Cracking Index (C.I.)	Stiffness Modulus of the Recovered Asphalt Cement, psi	Stiffness Modulus of the Mix, 10^3 psi	
			Wheelpath	Non-Wheelpath
1	6.5	4030	470,584	485,738
		3058	430,049	396,544
		4125	479,323	362,975
			425,924	
2	10.5	2845	333,515	246,923
		2850	310,592	321,843
		4980	345,192	352,038
				304,432
3	15.5	6502	714,512	741,089
		4673	682,849	736,542
		3454	714,512	611,386
4	24.5	12200	766,474	639,833
		14223	688,811	700,203
		16255	758,054	674,096
				643,443
5	2.0	2845	515,461	428,464
		2703	518,854	404,739
		2560	514,899	526,837
6	9.0	3501	851,528	675,737
		3829	636,874	819,761
			892,057	669,812
7	20.0	2845	482,821	426,221
		2987	478,079	469,292
			480,695	413,867
8	0.0	2705	470,711	401,747
		2002	464,026	466,058
		2540	456,019	409,714
9	0.5	2845	514,266	509,170
		1950	514,245	399,942
		3275	504,162	

VITA

Magdy Salah Noureldin

Candidate for the Degree of

Doctor of Philosophy

Thesis: A STUDY OF TRANSVERSE CRACKING IN OKLAHOMA FLEXIBLE HIGHWAY PAVEMENTS

Major Field: Civil Engineering

Biographical:

Personal Data: Born in Cairo, Egypt, April 8, 1947, the son of Mr. and Mrs. S. Noureldin; married Wafia Bahgat Eteiba, August, 1976.

Education: Graduated from Nokrashi Model High School, Cairo, Egypt, in July, 1964; received the Bachelor of Science degree in Civil Engineering from Ain Shams University, Cairo, Egypt, in June, 1969; received the Master of Science degree in Civil Engineering from Ain Shams University, Cairo, Egypt, in July, 1973; enrolled in the doctoral program in the School of Civil Engineering, Oklahoma State University, in 1974; completed requirements for the Doctor of Philosophy degree in May, 1977.

Professional Experience: Graduate teaching assistant, Faculty of Engineering, Ain Shams University, Cairo, Egypt, 1969-1973; Designer, Transportation Planning Consultants, Cairo, Egypt, 1970-1974; part-time graduate research assistant, Remote Sensing Research Project, Academy of Scientific Research and Technology, Cairo, Egypt, 1971-1973; Assistant Lecturer, Faculty of Engineering, Ain Shams University, Cairo, Egypt, 1973-1974; graduate research assistant, School of Civil Engineering, Oklahoma State University, 1974-1976.

Professional Organizations: Member, Egyptian Society of Engineers, Cairo, Egypt; Associate Member, American Society of Civil Engineers; Transportation Research Board; Member, Chi Epsilon.